

The First Report of a Working Group on  
Atmospheric Dispersion

**A Model for Short and Medium Range  
Dispersion of Radionuclides Released  
to the Atmosphere**

R.H. Clarke

Chairman of the Working Group

**National  
Radiological  
Protection  
Board**

Harwell, Didcot, Oxon OX11 0RQ  
September 1979

© NATIONAL RADIOLOGICAL PROTECTION BOARD – 1979

The National Radiological Protection Board was established by the Radiological Protection Act 1970 and is responsible for carrying out research and development and providing information advice and services to those with responsibilities for radiological protection.

Any questions relating to this report should be addressed to the Publications Officer, National Radiological Protection Board, Harwell, Didcot, Oxfordshire, England.

Further copies of this report are available from Her Majesty's Stationery Office.

The first report of a Working Group on Atmospheric Dispersion

A MODEL FOR SHORT AND MEDIUM RANGE DISPERSION  
OF RADIONUCLIDES RELEASED TO THE ATMOSPHERE

R H Clarke

Chairman of the Working Group

ABSTRACT

This report is the first of a series which will give practical guidance on the estimation of the dispersion of radioactive releases to the atmosphere. It represents the conclusions of a Working Group established to review recent developments in atmospheric dispersion modelling and to propose models for use within the UK. This first report deals with the estimation of dispersion in the short and medium range, that is from about 100 m to a few tens of kilometres from the source, and is based upon a Gaussian plume model. A scheme is presented for categorising atmospheric conditions and values of the associated dispersion parameters are given. Typical results are presented for releases in specific meteorological conditions and a scheme is included to allow for durations of release of up to 24 hours. Consideration has also been given to predicting longer term average concentrations, typically annual averages, and results are presented which facilitate site specific calculations. The results of the models are extended to 100 km from the source, but the increasing uncertainty with which results may be predicted beyond a few tens of kilometres from the source is emphasised.

The three technical appendices provide some of the rationale behind the decisions made in adopting the various models in the proposed dispersion scheme. These appendices have been contributed by individual members of the Working Group.

National Radiological Protection Board  
Harwell  
Didcot  
Oxon OX11 0RQ

September 1979

On sale through the  
Stationery Office  
£5.00

ISBN 0 85951 117 0

## CONTENTS

	<u>Page No.</u>
1. INTRODUCTION	1
2. THE GAUSSIAN PLUME DIFFUSION MODEL	2
2.1 Basic formulation	2
2.2 The choice of wind speed	3
2.3 Reflections from the ground and inversion layers	4
2.4 Continuous releases and annual average concentrations	5
3. THE CHOICE OF METEOROLOGICAL DISPERSION CATEGORY	7
4. CHOICE OF DISPERSION PARAMETERS	8
4.1 Boundary layer depth and wind speed	8
4.2 The vertical cloud standard deviation ( $\sigma_z$ )	9
4.3 The horizontal cloud standard deviation ( $\sigma_y$ )	10
4.4 The sector angle ( $\alpha$ ) for meteorological data in continuous releases	11
4.5 The stability category distribution for different wind directions ( $f_{ij}$ )	11
5. ACCURACY OF THE PREDICTIONS OF THE SUGGESTED MODEL	11
6. THE CONDITIONS FOR APPLICABILITY OF THE PROPOSED SCHEME	11
7. REPRESENTATIVE RESULTS FOR DISPERSION FROM SINGLE SOURCES	12
7.1 Short release results	12
7.2 Effects of prolonging the release duration	13
7.3 Results for prolonged or annual average conditions	13
8. CONCLUSIONS	15
9. ACKNOWLEDGEMENTS	15
10. REFERENCES	15
11. SYMBOLS USED	17
TABLES (see list on pp ii)	18
FIGURES (see list on pp ii)	20
APPENDIX A Diffusion in the lower layers of the atmosphere	60
APPENDIX B The determination of the crosswind spread	66
APPENDIX C Accuracy of the prediction of ensemble means and the spread about the mean	72

Contents (contd)

Page No.

TABLES

1.	Values for use in calculating wind speed at source height	18
2.	Typical values of wind speed and depth of mixing layer for use when measured values are not available	19
3.	Coefficients given by Hosker to derive the vertical standard deviation of the plume for the various stability categories	19

FIGURES

1.	Virtual source model to represent the reflections from the ground and the top of the mixing layer.	20
2.	The nomogram of Smith for the determination of the stability parameter P.	21
3.	Incoming solar radiation at Cambridge.	22
4.	A nomogram for estimating the depth of the boundary layer in day time in the absence of marked advective effects of basic changes in weather conditions.	23
5.	The vertical dispersion parameter, $\sigma_z$ , as a function of distance in neutral atmospheric stability and for a ground roughness length of 0.1 m.	24
6.	Ratio of vertical dispersion standard deviation, $\sigma_z$ , for any value of stability parameter, to that in neutral conditions as a function of downwind distance.	25
7.	Ratio of vertical dispersion standard deviation, $\sigma_z$ , at any ground roughness length to that at 0.1 m.	26
8.	Vertical standard deviation, $\sigma_z$ , as function of distance for each Pasquill stability category and a ground roughness length of 0.3 m.	27
9.	A comparison of the Hosker fit and Smith's data for the vertical standard deviation in each weather category and a ground roughness length of 0.1 m.	28
10.	The horizontal standard deviation due to turbulence, $\sigma_{yt}$ , as a function of distance in each Pasquill category.	29
11.	Frequency of occurrence of the Pasquill stability categories over Great Britain.	30
12.	Horizontal standard deviation, $\sigma_y$ , for a release of 30 min duration in each Pasquill stability category.	31

List of Figures (contd)

13.	On-axis ground level time integrated concentrations as a function of effective release height for a short (30 min) release of unit activity in Category A conditions.	32
14.	As Figure 13 - in Category B conditions.	33
15.	As Figure 13 - in Category C conditions.	34
16.	As Figure 13 - in Category D conditions.	35
17.	As Figure 13 - in Category E conditions.	36
18.	As Figure 13 - in Category F conditions.	37
19.	As Figure 13 - in Category G conditions.	38
20.	Modifying factor for the on-axis ground level concentration as a function of release duration in Category A conditions.	39
21.	As Figure 20 - in Category B conditions.	40
22.	As Figure 20 - in Category C conditions.	41
23.	As Figure 20 - in Category D conditions.	42
24.	As Figure 20 - in Category E conditions.	43
25.	As Figure 20 - in Category F conditions.	44
26.	As Figure 20 - in Category G conditions.	45
27.	On-axis ground level time integrated concentrations for unit releases as a function of effective height of release for uniform horizontal dispersion into a sector of angular width $\pi/6$ ( $30^\circ$ ) in Category A conditions.	46
28.	As Figure 27 - in Category B conditions.	47
29.	As Figure 27 - in Category C conditions.	48
30.	As Figure 27 - in Category D conditions.	49
31.	As Figure 27 - in Category E conditions.	50
32.	As Figure 27 - in Category F conditions.	51
33.	As Figure 27 - in Category G conditions.	52
34.	Continuous release results for ground level concentration as a function of distance and stack height for unit release. A uniform windrose is assumed and the frequency distribution of Pasquill categories corresponds to the 50% 'D' contour of the UK Pasquill stability map (see Figure 11).	53
35.	As Figure 34 - with the frequency distribution of Pasquill categories corresponding to the 55% 'D' contour.	54

List of Figures (contd)

36.	As Figure 34 - with the frequency distribution of Pasquill categories corresponding to the 60% 'D' contour.	55
37.	As Figure 34 - with the frequency distribution of Pasquill categories corresponding to the 65% 'D' contour.	56
38.	As Figure 34 - with the frequency distribution of Pasquill categories corresponding to the 70% 'D' contour.	57
39.	As Figure 34 - with the frequency distribution of Pasquill categories corresponding to the 75% 'D' contour.	58
40.	As Figure 34 - with the frequency distribution of Pasquill categories corresponding to the 80% 'D' contour.	59

As from 1 April 1978 NRPB adopted the International System of Units (SI). The relationship between the new SI units which are used in this report and the previous units are shown in the table below.

Quantity	New named unit and symbol	In other SI units	Old special unit and symbol	Conversion factor
Exposure	-	$C\ kg^{-1}$	röntgen (R)	$1\ C\ kg^{-1} \sim 3876\ R$
Absorbed dose	gray (Gy)	$J\ kg^{-1}$	rad (rad)	$1\ Gy = 100\ rad$
Dose equivalent	sievert (Sv)	$J\ kg^{-1}$	rem (rem)	$1\ Sv = 100\ rem$
Activity	becquerel (Bq)	$s^{-1}$	curie (Ci)	$1\ Bq \sim 2.7 \times 10^{-11}\ Ci$



## FOREWORD

In December 1977 a meeting of representatives of Government Departments, utilities and research organisations was held to discuss methods of calculation of atmospheric dispersion for radioactive releases. Those present agreed on the need for a review of recent developments in atmospheric dispersion modelling and an Expert Working Group was established in order to facilitate the review.

The members of the Working Group which has proposed the model reported here were as follows.

Dr R H Clarke (Chairman)	National Radiological Protection Board
Dr H M ApSimon	Nuclear Power Section, Imperial College of Science and Technology, London
Dr C D Barker	Central Electricity Generating Board, Research Department, Berkeley Nuclear Laboratories, Berkeley
Dr B E A Fisher	Central Electricity Generating Board, Research Department, Central Electricity Research Laboratory, Leatherhead
Ms L S Fryer	United Kingdom Atomic Energy Authority, Safety and Reliability Directorate, Risley
Dr A W C Keddle	Department of Industry, Warren Springs Laboratory, Stevenage
Dr D J Moore	Central Electricity Generating Board, Research Department, Central Electricity Research Laboratory, Leatherhead
Dr F B Smith	Ministry of Defence, Meteorological Office, Bracknell
Dr J A Jones (Secretary)	National Radiological Protection Board

The main text of this report describes the proposed model; representative results are presented which have been obtained by applying the model to a range of situations of interest in the UK. In addition there are three technical appendices which provide some of the rationale behind the decisions made in the proposed model. These appendices have been contributed by individual members of the Working Group and are attributed to the responsible member.

This report is the first of a series which will give practical guidance on the estimation of the dispersion of radioactive releases in the atmosphere. Topics under consideration by the Working Group for future reports include building entrainment, plume depletion and long-range dispersion, ie, dispersion up to several thousand kilometres from the source in both normal operation and accident situations.

## 1. INTRODUCTION

Any material discharged into the atmosphere is carried along by the wind and dispersed by the action of turbulent diffusion. In the vertical direction the dispersion deepens the plume until the turbulent boundary layer is uniformly filled. The boundary layer is of variable depth, being typically some tens to hundreds of metres deep at night and from hundreds to one or two thousand metres deep during the day. The depth is usually determined by the thermal and dynamic energy available to maintain the turbulence (see Appendix A). On other occasions it is limited by the presence of an "external" synoptically-induced inversion, ie, a sharp rise in temperature over several tens of metres which suppresses vertical motions. Horizontally the dispersion process is unlimited, and is effected by turbulence which draws its energy not only from the same sources as does the vertical turbulence, but also from the disturbing influences of large clouds, meteorological depressions and anticyclones, and the effects of mountains, slopes, cities, etc. In the remainder of this report the variations in the intensity of turbulence are reflected in what is called the stability of the atmosphere.

The problem of predicting the distribution of airborne material released from a source is commonly approached by solving the diffusion-transport equation. There is a range of models which have been developed to solve the equation depending upon the simplifying assumptions made and boundary conditions imposed. In this report consideration has been confined to those models for short and medium range dispersion (ie, less than 100 km from the source) which are available and fairly widely used within the UK. Recent reports have compared the predictions from some of these models for a range of meteorological conditions<sup>(1,2)</sup> and with a limited amount of experimental data<sup>(3-6)</sup>.

On the basis of these comparisons, the model proposed for use in calculation of the dispersion of radioactive releases is the Gaussian Plume Diffusion Model. Other models exist which are considered to represent better the physical processes of turbulent diffusion in the atmosphere; for example, closure models of which eddy-diffusivity models<sup>(7)</sup> are the simplest examples, but these have only a limited application in the "real time" estimation of the dispersion of radioactive material. Their main value lies in increasing the knowledge of the physical processes involved and in providing data on the most likely behaviour of the plume, which supplements and illuminates experimentally-determined data. These models, being more complex, generally require more computer time to obtain results and have not at present been developed so that the user may easily relate the values of parameters required by these computer models to readily measurable meteorological quantities. Moreover, the results obtained by Barker<sup>(1)</sup> and Jones<sup>(2)</sup> do not provide evidence that the results of the more complex calculations on their own give either a sufficiently different result, or a greater confidence in the

predictions of downwind concentrations, to warrant the additional complexity and cost to users. This is not too surprising since, in the development of parameters for use in Gaussian plume models, results have been incorporated from more complex calculations.

There is work currently being undertaken which may enable the more complex transport models to be related to easily measured meteorological parameters<sup>(8)</sup>. However, it is likely that it will be several years before such a scheme has been developed, validated and expressed in a readily usable form. In addition meteorological data are available for a large number of sites in this country, expressed in terms of a diffusion typing scheme applicable to the Gaussian plume model. On the basis of such evidence the use of the Gaussian diffusion model appears warranted, taking account of recent models developed for obtaining the basic parameters used.

The models included here apply simply to the atmospheric diffusion of a neutrally buoyant plume over land from an isolated stack for distances not greater than 100 km from the source, provided that meteorological and topographical conditions have remained constant during the travel time. The models have been chosen to be compatible with models which will deal with dry and wet deposition, plume rise and entrainment of the effluents into the plume wake behind buildings. These topics will be considered in subsequent reports by the Working Group. The present report describes the basic model on atmospheric dispersion. This model enables calculations to be performed for a range of atmospheric stabilities, with allowance for the influence of the duration of release and the frictional drag of the underlying surface. Graphical results are included for short releases, defined as being of approximately half-an-hour's duration, together with modifying factors which enable the release duration to be extended for various times up to 24 hours. In addition, graphical data are presented to facilitate the calculation of dilution for continuous releases. For these results typical values of parameters have been chosen so that the results represent the broad range of releases of interest in the nuclear industry.

## 2. THE GAUSSIAN PLUME DIFFUSION MODEL

### 2.1 Basic formulation

The model assumes that the dispersion of material is described by a Gaussian distribution characterised by standard deviations,  $\sigma_y$  and  $\sigma_z$  in the horizontal and vertical directions respectively. The basic equation using a Gaussian plume model for an elevated release is as follows:

$$C(x, y, z) = \frac{Q}{2\pi u_{10} \sigma_z \sigma_y} \exp\left[-\frac{1}{2} \left( \frac{y^2}{\sigma_y^2} + \frac{(z-h)^2}{\sigma_z^2} \right) \right] \dots\dots\dots(1)$$

where C = the air concentration (Bq m<sup>-3</sup>) or its time integral (Bq s m<sup>-3</sup>)

- Q = release rate ( $\text{Bq s}^{-1}$ ) or total amount released (Bq)
- $u_{10}$  = wind speed at 10 m above the ground ( $\text{m s}^{-1}$ )
- $\sigma_z$  = standard deviation of the vertical Gaussian distribution (m)
- $\sigma_y$  = standard deviation of the horizontal Gaussian distribution (m)
- $\left. \begin{matrix} x \\ y \\ z \end{matrix} \right\} = \text{rectilinear co-ordinates} \left\{ \begin{matrix} \text{along the wind direction (m)} \\ \text{cross-wind (m)} \\ \text{above ground (m)} \end{matrix} \right.$
- h = effective release height (m)

The origin of the co-ordinate system is at ground level beneath the discharge point. In the derivation of equation (1) it is assumed that diffusion in the x-direction, ie, in the direction of the wind, can be ignored since for releases which last a finite time the diffusive component is of negligible importance. Moreover, it is the time integrated concentration which is of primary interest. The choice of wind speed in equation (1) will now be discussed in more detail.

## 2.2 The choice of wind speed

The velocity of the wind in the boundary layer increases with increasing height above the ground because the effect of the drag or frictional forces at the surface of the earth diminishes with height; the initial rapid increase in wind speed with height gives way to a much slower increase within a few tens of metres of the ground and eventually the wind velocity attains the geostrophic or free stream value. For many practical purposes it has been convenient to describe the profile by a power law<sup>(6)</sup>:

$$u(z) = u_{10} (z/10)^n \dots\dots\dots(2)$$

where  $u(z)$  is the wind speed at height  $z$  and  $u_{10}$  is the wind speed at the reference height of 10 metres. The shape of the profile depends on  $n$  which is a function of surface roughness (ie, the physical features, whether natural or man-made, on the surface of the earth) and, to some extent, atmospheric stability. In general,  $n$  will increase with increasing surface roughness and values of  $n$  which have been taken from Smith<sup>(9)</sup> are given in Table 1 for neutral conditions. It is seen in Table 1 that the dependence of  $n$  upon atmospheric stability which has been discussed by Keddie<sup>(6)</sup> and Touma<sup>(10)</sup> has been ignored in the present work.

In dispersion calculations the expression in equation (2) is commonly used to calculate the wind speed at the height of the plume centre-line, or the mean wind speed through the depth of the plume given the value of the wind speed at 10 metres. However, while the wind speed ( $u$ ) increases, the lateral spread of the plume ( $\sigma_y$ ) decreases with increasing height of the source above the ground. In the Gaussian dispersion model (equation (1)) the denominator contains the product of wind speed  $u$  and lateral spread ( $\sigma_y$ ). For simplification, the  $\sigma_y$  values which have been

derived for use with equation (1) correspond with the use of the 10 m wind speed. Therefore, when evaluating the concentration from equation (1) the 10 metre wind speed,  $u_{10}$ , should be used. This procedure will give rise to an error in the exponential term  $\exp(-y^2/2\sigma_y^2)$  for off-axis concentrations well above the ground for highly elevated sources, but the error is acceptably small in all cases. Equation (2) can be used to correct any measured wind speed from the height of the instruments to the reference height.

### 2.3 Reflections from the ground and inversion layers

When material is discharged from an elevated source the plume will spread vertically until the lower part eventually reaches the ground. There is then a bar to downwards diffusion. The actual vertical distribution of activity is well represented by assuming that the plume is reflected and effectively dispersed back up into the air as shown in Figure 1. This can be considered as a virtual source at a distance  $h$  below the ground. In this situation the air concentration at  $(x, y, z)$  is given by:

$$C(x, y, z) = \frac{Q}{2\pi u_{10} \sigma_z \sigma_y} \exp\left[\frac{-y^2}{2\sigma_y^2}\right] \left( \exp\left[-\frac{(z-h)^2}{2\sigma_z^2}\right] + \exp\left[-\frac{(z+h)^2}{2\sigma_z^2}\right] \right) \dots\dots\dots(3)$$

Inversion conditions, which are positive temperature gradients in the lower levels of the atmosphere, occur at varying heights; where an inversion exists the dispersed material would be trapped between this inversion and the ground (see Figure 1). Reflections will occur, in this case, both at the ground and at the top of the mixing layer which is the inversion. In the absence of reflection the Gaussian plume would spread in a vertical plane to a size determined solely by  $\sigma_z$  at the distance of interest. The effect of introducing multiple reflections is that the airborne concentration at the point of interest must be obtained by summation of the contributions from many virtual sources. The number of contributions depends on the relative values of  $\sigma_z$  and the depth of the mixing layer. The vertical heights of the virtual sources can be represented as

$$z = \pm 2mH \pm h \quad (m = 0, 1, 2, 3\dots)$$

where  $H$  is the depth of the mixing layer. The concentration from this series of virtual sources decreases as  $m$  increases and, in general, sufficient accuracy is obtained if the series is truncated after the  $m = 1$  term. The concentration distribution can then be expressed as

$$C(x, y, z) = \frac{Q}{2\pi u_{10} \sigma_z \sigma_y} \exp\left[\frac{-y^2}{2\sigma_y^2}\right] F(h, z, A) \dots\dots\dots(4)$$

where

$$F(h, z, A) = \exp\left[\frac{-(z-h)^2}{2\sigma_z^2}\right] + \exp\left[\frac{-(z+h)^2}{2\sigma_z^2}\right] + \exp\left[\frac{-(2A+z+h)^2}{2\sigma_z^2}\right] \\ + \exp\left[\frac{-(2A+z-h)^2}{2\sigma_z^2}\right] + \exp\left[\frac{-(2A-z+h)^2}{2\sigma_z^2}\right] + \exp\left[\frac{-(2A-z-h)^2}{2\sigma_z^2}\right] \dots\dots\dots(5)$$

Although experimental evidence shows that the vertical distribution of dispersed materials will be non-Gaussian, these formulations enable the Gaussian model to predict measured ground level concentrations.

When the value of the vertical dispersion coefficient  $\sigma_z$  becomes greater than the depth of the boundary layer, the vertical concentration distribution effectively becomes uniformly distributed throughout the mixing layer. The concentration is then given by

$$C(x, y, z) = \frac{Q}{\sqrt{2\pi} u_{10} A \sigma_y} \exp\left[\frac{-y^2}{2\sigma_y^2}\right] \dots\dots\dots(6)$$

The concentration given by equation (4) may be shown<sup>(11)</sup> to be within a few percent of that given by equation (6) for any height above ground (z) and any stack height (h) when  $\sigma_z = A$ . Equation (6) will be essentially exact at all downwind distances beyond that for which  $\sigma_z = A$ . Consequently equation (4) should be used to estimate air concentrations at distances where  $\sigma_z < A$ ; equation (6) should be used at larger distances.

#### 2.4 Continuous releases and annual average concentrations

Thus far the equations for the Gaussian model of atmospheric dispersion relate to the situation where the duration of the release is such that the resulting distribution of activity may be considered to be in the form of a plume. The equations apply while the meteorological and topographical conditions remain steady and methods will be explained in the following sections which enable values of the relevant parameters to be assessed. However, there is a need to calculate the average concentration distribution around a source for releases over extended periods, typically months to years. In such situations a different approach may be adopted. The main feature that changes is that the horizontal dispersion of the plume is not now satisfactorily described by the Gaussian model with standard deviation  $\sigma_y$ .

The choice of model here is influenced by the availability of Meteorological Office data for observation sites around the United Kingdom, which is expressed in terms of the frequency distributions both of wind directions and of a meteorological stability classification in those directions. The principle adopted is to evaluate the distribution of activity in sectors defined by the meteorological data available. In this case the horizontal distribution of the activity can be assumed to be constant over a sector of angular width  $\alpha$ . A typical value for the sector width would be  $\pi/12$  ( $30^\circ$ ) for Meteorological Office data. The concentration distribution  $C_{ij}(r, z)$  in such a sector,  $i$ , is then given for each particular meteorological condition,  $j$ ;

- a) for distances such that  $\sigma_{zj}$  is less than the boundary layer depth ( $A_j$ ) in the condition of interest

$$C_{ij}(r, z) = \frac{Q}{\sqrt{2\pi} r \alpha u_{sj} \sigma_{zj}} F_j(h, z, A_j) \dots\dots\dots(7)$$

- b) for greater distances, when  $\sigma_{zj} \gg A_j$

$$C_{ij}(r, z) = \frac{Q}{r \alpha u_{sj} A_j} \dots\dots\dots(8)$$

where  $r$  is the distance from the source (m); and  $u_{sj}$  is now the wind speed at the effective source height, or for sources with effective source heights of less than 10 m, it is the 10 m wind speed, in the meteorological condition  $j$ .

The wind speed at the effective source height is calculated using equation (2) and the values of  $n$  are given in Table 1. The use of the wind speed at any particular specified height in this formula represents an approximation to obtaining concentrations in the vertical direction. As discussed above in Section 2.2 the wind speed is a function of height above the ground, but in the continuous release case the variation in  $u$  cannot be compensated by the reduction in  $\sigma_y$  with source height as was the case with the plume, since  $\sigma_y$  does not appear in equations (7) and (8). However, using the wind speed at source height in this model gives an acceptable prediction for the ground level concentration.

The average concentration in the  $i$ th sector may then be obtained by summing the concentration obtained for each set of meteorological conditions weighted by the fractional occurrence of those conditions, ie,

$$C_i(r, z) = \sum_j f_{ij} C_{ij}(r, z) \dots\dots\dots(9)$$

where  $f_{ij}$  is the frequency of the meteorological condition  $j$  within the  $i$ th sector. The source term  $Q$  to be used in equation (7) is the release rate, assumed constant, over the period of interest which may typically be one year. The time-integrated concentration over the same period will be found by using the total release.

The width of the sector ( $\alpha$ ) is determined by the number of sectors in which the meteorological data,  $f_{ij}$  and  $u_j$ , are available.

The formulations presented here are applicable to long-term average concentrations where the frequency distribution of meteorological conditions has some statistical validity. However there will be occasions where releases last for periods of time which are of insufficient duration to allow such treatment. Such releases may be evaluated using equations (4) and (6) for each period in which the wind direction and meteorological conditions can be assumed constant. Further consideration of the effects of fluctuations in wind direction for prolonged release durations is given in Section 4.3.

### 3. THE CHOICE OF METEOROLOGICAL DISPERSION CATEGORY

Perhaps the most widely known scheme for classifying the meteorological conditions into a grouping structure is that due to Pasquill<sup>(12)</sup>. Pasquill based his scheme on a range of experimental observations and suggested values for dispersion parameters to be used in the Gaussian plume model for six weather categories, which he designated A to F in order of increasing atmospheric stability. The procedure for classifying a given set of meteorological conditions suggested by Pasquill was qualitative and since that time there have been many attempts to produce a more quantitative approach. The problem is twofold; firstly an attempt must be made to categorise any given combination of heat fluxes, wind speeds, cloud cover, etc; then secondly, representative values of the dispersion parameters ( $\sigma_y$  and  $\sigma_z$ ) have to be ascribed to each weather category. Schemes of this type based on the Gaussian plume model are widely used; for example, Vogt and Geiss<sup>(13)</sup> have developed a typing scheme based upon measured lapse rates (vertical temperature profiles). A review of a range of these schemes has recently been produced by Gifford<sup>(14)</sup>.

In this report the diffusion typing scheme due to Smith<sup>(15,16)</sup> is used, which has been developed from the original Pasquill formulation<sup>(12)</sup>. The scheme proposed by Smith is now quantitative and attempts to take into account a number of factors, including the sensible heat flux in the lower layers of the atmosphere (ie, the amount of heat per unit horizontal area passing between the air and the underlying surface as a result of air-surface temperature differences, often caused by net solar heating of the surface during the day or radiative cooling at night), wind speed over a wide range and the effect of ground roughness (grass, woodlands, water, etc), and clearly distinguishes night-time conditions. Another important feature of the Smith scheme is its ready applicability and useful presentation, in nomogram form, of the essential variables.

A major change from the Pasquill scheme is the choice by Smith<sup>(15)</sup> to give a continuous index of atmospheric stability  $P$ , rather than the series of six discrete stability categories, and a description is given in Appendix A of the



derivation of this stability parameter P. In practical situations the value of the stability parameter can be deduced from the vertical sensible heat flux, and the 10 m wind speed using the nomogram shown in Figure 2. The left hand side of Figure 2 refers to daylight hours when there is incoming solar radiation and it is seen that the atmosphere cannot be more stable than neutral atmospheric conditions, with P lying between 3 and 4 and corresponding to Pasquill's category D. In fact, in Figure 2, Pasquill stability categories have been assigned to the broad ranges of P to which they apply.

Figure 2 further shows that stable conditions occur only at night and when there is low wind speed although, strictly, just after dawn and sunset there will be some error in this scheme before the correct heat balance in the atmosphere is established, but this is not considered to lead to significant errors here. It is also noticed that increasing wind speed tends to give more neutral conditions even with high solar radiation input. In nearly all cases information on the vertical sensible heat flux can be deduced from the amount of cloud cover, the time of day and time of year which indicate the incoming solar radiation. In the nomogram shown in Figure 3 data are given to estimate the incoming solar radiation, S, typical of the UK and the approximation may be made that the sensible heat flux, H, is given by the following equation:

$$H = 0.4 (S-100) \dots\dots\dots(10)$$

where H and S are in  $W m^{-2}$ .

Values of stability index of 0.5, 1.5, 2.5, 3.6, 4.5 and 5.5 can be taken as equivalent to the Pasquill categories A to F respectively. Smith extended the range of the meteorological conditions considered, and a value of the stability parameter of 6.5 can be taken to correspond to very stable conditions, sometimes referred to as Category G. The values of dispersion parameters which correspond to these categories will now be considered.

#### 4. CHOICE OF DISPERSION PARAMETERS

##### 4.1 Boundary layer depth and wind speed

In most practical cases the depth of the boundary layer is unlikely to be available. However, Smith has produced a nomogram<sup>(17)</sup> which is given in Figure 4 and should be used whenever sufficient data are available. In those calculations for which no meteorological data are available, the typical values of wind speed and boundary layer depth have been compiled for use in Table 2. The wind speeds used are 10 m values and wind speeds at the source height of interest for use in calculations of long-term average concentration should be obtained from equation(2) and Table 1.

The data shown in Figure 4 are applicable only in daytime. At night when stable weather conditions arise, ie, where inversion conditions occur, it is also necessary to take account of multiple reflections within the inversion layer. Although the inversion layer may start at the air/ground interface, in Table 2 values of typical inversion heights are given for categories E, F and G so that equations (4), (5) and (7) may be used for short and continuous releases respectively.

#### 4.2 The vertical cloud standard deviation ( $\sigma_z$ )

The vertical cloud standard deviation ( $\sigma_z$ ) at a given distance from the source is a function of the atmospheric stability, downwind distance and ground roughness. The value of  $\sigma_z$  can be found using the following procedure:

- (a) Figure 5 tabulates  $\sigma_z$  as a function of distance in neutral stability conditions assuming a ground roughness length ( $z_0$ ) of 10 cm;
- (b) the value of  $\sigma_z$  applicable to any other stability conditions but for the same 10 cm ground roughness length is obtained using the ratio of  $\sigma_z$  in that stability to  $\sigma_z$  in neutral conditions given in Figure 6;
- (c) the value of  $\sigma_z$  may be modified for other ground roughness lengths using the ratio given in Figure 7 which is applicable for all atmospheric stability conditions.

In Figure 8, for convenience, values for  $\sigma_z$  have been obtained assuming a value of P for each of the six Pasquill categories A to F (P values of 0.5, 1.5, 2.5, 3.6, 4.5 and 5.5). In addition, results for a P value of 6.5 are shown which are appropriate to extremely stable conditions (category G). The values given in Figure 8 are for a roughness length of 30 cm, which has been quoted as a typical roughness length for rural country with small villages<sup>(15)</sup>, and this value would be appropriate to large areas of southern England. Specific values of  $z_0$  for different types of terrain are given in Table 1, which have been taken from Smith<sup>(9,15,16)</sup>.

An analytical formula for  $\sigma_z$  in each Pasquill category together with a correction for roughness lengths, other than for the 10 cm reference value of  $z_0$  used by Smith, has been derived by Hosker<sup>(18)</sup>. The formula and its parameter values are given in Table 3. A comparison between the values for  $\sigma_z$  at the roughness length of 10 cm as predicted by Hosker's formulation and the original graphical scheme of Smith is shown in Figure 9. The results indicate that the Hosker representation provides a good fit to the Smith values and therefore may be used if desired to avoid any difficulties which may arise in interpolation from the graphical results. The disadvantage of using the Hosker scheme is that only certain specific roughness lengths may be used.

#### 4.3 The horizontal cloud standard deviation ( $\sigma_y$ )

The dispersion of the plume in the horizontal plane is the result of turbulence processes together with fluctuations in wind direction. These two components can be thought of as acting independently and in Appendix B a discussion is given of the horizontal dispersion processes which led to the formulation used here for  $\sigma_y$ . The values of  $\sigma_y$  given originally by Pasquill were essentially for very short (three minutes typically) releases, or short observation times from continuous releases. In the present work it is proposed that this very short three-minute release component is retained and applied to releases of much less than 30 minutes duration. The resulting predicted time integrated concentration represents an upper limit. For longer durations of release some account must be taken of the fluctuations in wind direction. This variation implies that as the time of release increases, although each short-term release behaves according to the turbulence of the atmosphere there is a spread of results over a range of directions. The final value of  $\sigma_y$  is that due to Moore<sup>(19)</sup> and is represented as

$$\sigma_y^2 = \sigma_{y_t}^2 + \sigma_{y_w}^2 \dots\dots\dots(11)$$

where  $\sigma_{y_t}$  is the turbulent diffusion or three minute term,  
 $\sigma_{y_w}$  is the component due to fluctuations in wind direction.

For this report, the values of  $\sigma_{y_t}$  given by Gifford<sup>(24)</sup>, shown in Figure 10 and based on the original work of Pasquill, have been used and a fuller discussion is given in Appendix B. The effects of wind direction fluctuations can be included by using one of the following forms -

$$\begin{aligned} \sigma_{y_w} &= \sigma_\theta x \\ \text{or} \quad \sigma_{y_w} &= 0.065 \sqrt{\frac{T}{u_{10}}} x \end{aligned} \dots\dots\dots(12)$$

where  $\sigma_\theta$  is the standard deviation of the horizontal wind directions when averaged over consecutive three minute periods and sampled over the release duration,

T is the release duration in hours.

The second equation should be used whenever the value of  $\sigma_\theta$  is not available.

This form for the horizontal distribution of a plume as represented in equations (4) and (6) may be used for any duration of release longer than about 30 minutes for which the weather category and wind direction remain unchanged.

#### 4.4 The sector angle ( $\alpha$ ) for meteorological data in continuous releases

The form for concentration distribution given by equations (7) and (8) may be used for the concentration averaged over a period long compared with the duration of a given weather category and wind direction. The angle  $\alpha$  in equation (7) should be equal to that for which the distribution of wind direction and weather categories is available from meteorological data;  $\alpha$  is measured in radians.

#### 4.5 The stability category distribution for different wind directions ( $f_{ij}$ )

The average concentration in a given direction from a discharge continuing over an extended period may be a sensitive function of the stability category distribution for winds blowing in the appropriate direction. Where possible this distribution should be obtained from measurements made at the site or at a local meteorological station and taken over a period of several years. Data on the frequency distributions of, and wind speeds in each category for a number of sites are available from the Meteorological Office. Where such data are not available the typical values for the stability category distributions over the UK derived by Smith<sup>(20)</sup> and shown in Figure 11 may be used. This option should only be used if no better data are available as it contains no information on the directional distribution of the stability categories.

### 5. ACCURACY OF THE PREDICTIONS OF THE SUGGESTED MODEL

For short duration releases the predicted concentration in the plume is likely to be within a factor of three of the actual concentration if measured values are used for all parameters and the correct stability category has been assigned. Further discussion on the probable accuracy of the predicted concentration is given in Appendix C. It must be emphasised that the suggested accuracy is not for a minute by minute prediction of concentration, but for its time integral over periods of at least half-an-hour. In general, predictions of the annual average concentration are likely to be more accurate and the work of Keddie<sup>(6)</sup> has shown agreement to within about  $\pm 50\%$  between measured pollution concentration and theoretical predictions for long-term averages from multiple sources.

The values of the parameters in the models have maximum reliability for dispersion over distances of up to a few tens of kilometres. In this report a maximum distance of 100 km has been used and it must be emphasised that when considering dispersion over distances approaching 100 km, predictions are likely to be increasingly less accurate than indicated by the factors discussed here.

### 6. THE CONDITIONS FOR APPLICABILITY OF THE PROPOSED SCHEME

The procedure proposed in this report for estimating dispersion is only applicable when the release point is sufficiently distant from surrounding buildings for the airflow at the release height to be relatively undisturbed. The effects of building entrainment will be considered separately in a later report, but the model

considered will be compatible with the dispersion scheme suggested here. In addition the proposed scheme assumes that the height of release used is the effective height so that account must be taken of the buoyancy and momentum of the plume before applying the models described here. Finally it is assumed that the released material undergoes no chemical or radioactive transformations and that it does not deposit upon the ground. Again subsequent reports will consider models for dry and wet deposition which are compatible with the basic dispersion model.

In fact, because of the diffusivity profile in the atmosphere, the vertical dispersion will be a function of the height of release, but for the purpose of this report the differences in predicted atmospheric concentrations may be ignored. The methods then presented are adequate for effective heights of release up to 200 m, for sources within the mixing layer.

## 7. REPRESENTATIVE RESULTS FOR DISPERSION FROM SINGLE SOURCES

In the following section typical results are presented for on-axis, downwind, ground-level, time-integrated concentrations for unit release (or standing concentration per unit-release rate) from a range of stack heights. The results have been calculated for four sets of circumstances which should cover a wide range of conditions of interest. In performing the calculations representative wind speeds have been used for each atmospheric stability category. In any more realistic calculations the actual distribution of wind speeds applicable to the site of interest should be used. The first set of results gives downwind concentrations for short-term releases in conditions representing each of the seven weather categories, A to G. The second set of results indicates how the downwind concentrations in each category change as the duration of the release increases. The third and fourth sets of results are presented to facilitate calculations of annual average concentrations for continuous release situations.

### 7.1 Short release results

In Section 4.3 it was pointed out that the original Pasquill or Gifford expressions for  $\sigma_y$  (Figure 10) referred to releases lasting only a few minutes, typically three-minute release or sampling times. The duration of release, which perhaps is more useful as a minimum for use in the nuclear industry, is probably more likely to be 30 minutes. The first set of results have therefore been generated for 30-minute releases using the equations described above. Equations (11) and (12) have been used to generate  $\sigma_y$  as a function of distance in the various weather categories and the results are shown in Figure 12. It is noted that the variation of  $\sigma_y$  with weather category is no longer monotonically decreasing with increasing atmospheric stability, because of the influence of the wind speed in equation (12).

The resulting ground level concentrations are shown in Figures 13-19 for releases in weather categories A ( $P = 0.5$ ), B ( $P = 1.5$ ), C ( $P = 2.5$ ), D ( $P = 3.6$ ), E ( $P = 4.5$ ), F ( $P = 5.5$ ) and G ( $P = 6.5$ ), where  $P$  is Smith's stability parameter. Effective heights of release of up to 200 m have been considered except in categories F and G and the depth of the mixing layer has been taken from the values in Table 2. The depth of the mixing layer is 100 m in categories F and G so that the maximum stack height used is also 100 m. A ground roughness length of 30 cm has been used as being typical of southern England<sup>(15)</sup>. Wind speed values for each category were also taken from Table 2. The change in slope of the dispersion curve with distance, which is most noticeable in the unstable categories (A and B), is due to the plume dispersing to fill the mixing layer. Beyond the point at which this happens there is less dispersion with distance than at shorter distances.

### 7.2 Effects of prolonging the release duration

In Figures 20-26 results are given for the modifying factors for on-axis concentrations, which should be used to correct the short release (30 min) results of Section 7.1 when, for the same release, the duration is extended in time. The modifying factors effectively represent the ratio of the  $\sigma_y$  values for a 30 min release and each longer release period respectively. Results are presented for releases lasting 1, 2, 4, 6, 9 and 12 h in all weather categories. As will be recalled from Figure 2, only near neutral conditions can persist for longer periods and therefore results are presented additionally for 24 h in category D conditions. The calculations are presented for all downwind distances from 100 m to 100 km and may be used simply as multiplying factors with the relevant concentrations for the 30 min releases given in Figures 13-19.

For example, suppose there is a release of one unit of activity in category F conditions from a 30 m stack. Figure 18 shows that at the point of maximum concentration, 1300 m downwind, for a 30 min duration of release, the time integrated concentration is  $1.9 \times 10^{-5}$ . For the same unit release over 4 h, Figure 25 shows that the modifying factor is 0.38 for category F conditions and a downwind distance of 1300 m, leading to a time integrated concentration of  $0.72 \times 10^{-5}$ .

Figures 13 to 26 enable calculations to be performed for a wide range of conditions of interest for situations where the meteorological conditions remain constant.

### 7.3 Results for prolonged or annual average concentrations

The procedure for calculating dispersion following prolonged releases or for obtaining annual average concentrations has been outlined in Section 2.4. The method proposed is basically to obtain the frequency distributions of wind directions and the frequency distribution of weather categories in each of these directions, which may then be used with dispersion curves for each sector. To facilitate these calculations, results are presented for unit releases uniformly dispersed horizontally through a  $30^\circ$  sector. This sector size has been chosen

since much site specific meteorological data is obtained in  $30^\circ$  sectors. The vertical dispersion follows the weather category chosen and since the results are to be applied for long-term average concentrations, as suggested in Section 2.4, the wind speed used will vary as a function of the effective height of the release. The results are shown in Figures 27-33 for categories A to G and it will be noticed that the concentrations do not converge at long distances for different stack heights in the same weather category, because of the different wind speeds used.

The average concentrations in a sector can now be obtained by taking the total release over the period in question and multiplying by the probabilities of weather category and wind direction for that sector together with the dilution factors in Figures 27-33. The resulting concentrations are then summed over the various weather categories to give the average time integrated concentration at the point of interest.

The final set of results presented are again for continuous release conditions. In Figures 34-40 concentrations are produced as a function of distance for continuous releases assuming a uniform windrose, ie, dispersion around  $2\pi$ , and the distribution of weather categories are taken from the contours of Smith's Pasquill Stability Map (Figure 11). Thus Figure 34 corresponds to 50% category D conditions (other categories having the frequencies indicated in Figure 11) and Figure 40 corresponds to 80% category D.

These results may be used for releases at sites for which meteorological data is not available, the most appropriate set of dispersion curves being chosen from the location of the site of interest on Figure 11. If there is knowledge of the windrose, then the dilution factors from the appropriate figure may be weighted by the frequency distribution of wind directions. The approximation then is that the frequency of weather categories is independent of wind direction. This may be a reasonable assumption for many sites.

If, however, data are available for the frequency distributions of weather categories by direction for the site of interest, and those distributions of weather categories may be approximated by the standard combinations used in Figures 34-40, then the long-term average concentration may be calculated fairly easily. For each sector around the site, one of the Figures 34-40 will be most applicable. Knowing the fractional release into that sector for the period of interest, that source term can be used with the dilution factor from the most applicable combination of weather categories for Figures 34-40 which must be multiplied by the number of sectors. This factor must be used because Figures 34-40 assume a uniform distribution of the source term around  $2\pi$ , whereas if calculations are performed on a sector basis, the release into the sector is used to obtain the dilution factor.

## 8. CONCLUSIONS

In this report a method has been proposed for the calculation of the dispersion of nuclear effluents in the short and medium distance ranges from the source. No new models have been developed, but various features from existing models have been used to produce a new procedure for calculation of atmospheric dispersion. In proposing the procedure consideration has been given not only to the recent developments in calculations of meteorological dispersion, but also to the ease of applicability of the model and the availability of a scheme to classify any given set of meteorological conditions into parameters for use in the various models available. On the basis of these considerations a Gaussian plume model has been used and a methodology has been outlined for a diffusion category typing scheme.

Results from the resulting dispersion model have been obtained which allow estimation of the dilution factors for a range of release durations from the short term, here chosen to be 30 min, to annual average concentrations.

The model applies to dispersion of a non-depositing effluent from a stack where the influence of surrounding buildings may be ignored. The basic model proposed here has, however, been chosen so that in subsequent work it may be modified to allow for the effects of building entrainment, deposition from the plume and radioactive transformations.

## 9. ACKNOWLEDGEMENTS

I would like to thank all the members of the Working Group for their assistance in the preparation of this document.

Special thanks are due to Dr J A Jones who undertook all the calculational and computational work for the graphical results in this report, and who has also acted as Secretary to the Working Group.

## 10. REFERENCES

1. Barker, C D, A comparison of Gaussian and diffusivity models of atmospheric dispersion. Berkeley, Glos., CEEB Report RD/B/N4405 (1978).
2. Jones, J A, The radiological consequences of accidental release of radioactivity to the atmosphere. Sensitivity to the choice of atmospheric dispersion model. Harwell, NRPB-R88 (1979). (London, HMSO).
3. Barker, C D, A comparison of the Gaussian plume diffusion model with experimental data from Tilbury and Northfleet. Berkeley, Glos., CEEB Report RD/B/N4624 (1979).
4. Smith, F B, The character and importance of plume lateral spread affecting the concentration downwind of isolated sources of hazardous airborne material. IN Proc. WMO Symposium on Long Range Transport of Pollutants and its Relation to General Circulation, including Stratospheric and Tropospheric Exchange Processes, Sofia, October, 1979.
5. Nickola, P W, Hanford 67-series diffusion measurements. Richland, Wash., Battelle Pacific Northwest Laboratory, PNL-2433 (1977).
6. Keddie, A W C, Bowes, J S, Maughan, R A, Roberts, G H and Williams, F P, The measurement, assessment and prediction of air pollution in the Forth Valley of Scotland - Final Report. Warren Springs Laboratory, LR 279(AP) (1978).
7. Maul, P R, The mathematical modelling of the meso-scale transport of gaseous pollutants, Atmos. Environ., 11, 1191 (1977).
8. Smith, F B, Application of data from field programmes to estimation of K-profiles and vertical dispersion. IN Proc. Conference on Mathematical Modelling of Turbulent Diffusion in the Environment, Liverpool, September 1978.



9. Smith, F B, Meteorological Office, Private communication (1978).
10. Touma, J S, Dependence of the wind profile power law on stability for various locations. *J. Air Poll. Control Assoc.*, 22, 863 (1979).
11. Pasquill, F, The Gaussian plume model with limited vertical mixing. Washington DC, US Environmental Protection Agency, EPA-600/4-76-042 (1976).
12. Pasquill, F, The estimation of the dispersion of windborne material. *Met. Mag.*, 90, no. 1063, 33 (1961).
13. Vogt, K and Geiss, H, Tracer experiments on dispersion of plumes over terrain of major surface roughness. Jülich, Research Centre, Publication 1131 (1976).
14. Gifford, F A, Turbulent diffusion typing schemes - a review. *Nucl. Safety*, 17, 69 (1976).
15. Smith, F B, A scheme for estimating the vertical dispersion of a plume from a source near ground level. IN Proc. 3rd Meeting of an Expert Panel on Air Pollution Modelling. Paris, October 1972. Brussels, NATO-CCMS Report 14 (1973).
16. Pasquill, F, Atmospheric diffusion. Chichester, Ellis Horwood Ltd (1974).
17. Smith, F B and Carson, D J, Some thoughts on the specification of the boundary layer relevant to numerical modelling. *Bound. Layer Met.*, 12, 307 (1977).
18. Hosker, R P, Estimates of dry deposition and plume depletion over forests and grasslands. IN Proc. Symposium on Physical Behaviour of Radioactive Contaminants in the Atmosphere, Vienna, November 1973. Vienna, IAEA, p291 (1974).
19. Moore, D J, Calculation of ground level concentration for different sampling periods and source locations. IN *Atmospheric Pollution*. Amsterdam, Elsevier, p5160 (1976).
20. Smith, F B, Pasquill stability map of the United Kingdom. Meteorological Office, Private communication (1978).
21. Carson, D J, The development of a dry-inversion-capped convectively unstable boundary layer. *Q. J. R. Met. Soc.*, 99, 450 (1973).
22. Moore, D J, The distribution of surface concentrations of sulphur dioxide emitted from tall chimneys. *Philos. Trans. R. Soc. London, Ser. A*, 265, 245 (1969).
23. Moore, D J, Observed and calculated magnitudes and distances of maximum ground level concentration of gaseous effluent material downwind of a tall stack. *Adv. Geophys.*, 18B, 201 (1974).
24. Gifford, F A, Diffusion in the lower layers of the atmosphere, IN *Meteorology and Atomic Energy* (D Slade, ed). US Atomic Energy Commission, TID-24190, p65 (1968).
25. Hanna, S, Briggs, G, Deardorff, J, Egan, B, Gifford, F and Pasquill, F, AMS workshop on stability classification schemes and sigma curves - summary of recommendations. *Bull. Am. Met. Soc.*, 58, 1305 (1977).
26. Gifford, F A, Statistical properties of a fluctuating plume model. *Adv. Geophys.*, 6, 117 (1959).
27. Smith, F B and Hay, J S, The expansion of clusters of particles in the atmosphere. *Q.J.R. Met. Soc.*, 87, 82 (1961).
28. Hay, J S and Pasquill, F, Diffusion from a continuous source in relation to the spectrum and scale of turbulence. *Adv. Geophys.*, 6, 345 (1959).
29. Moore, D J, A simple boundary layer model for predicting time mean ground concentrations of material emitted from tall chimneys. *Proc. Inst. Mech. Eng.*, 182, 33 (1975).

11. SYMBOLS USED

A	Depth of mixing layer (m)	
$C(r,z)$	Air concentration for a continuous release at radius r ( $Bq\ m^{-3}$ )	
$C(x,y,z)$	Air concentration or its time integral for a short release ( $Bq\ m^{-3}$ or $Bq\ s\ m^{-3}$ )	
$f_{ij}$	Frequency distribution of wind direction and weather category in the <i>i</i> th sector and <i>j</i> th category.	
F	A term defined in equation (5) giving the vertical distribution of activity in the plume	
h	Effective release height (m)	
H	Vertical heat flux ( $W\ m^{-2}$ )	
i	Subscript denoting sector	
j	Subscript denoting category	
n	Index of the power law relating wind speed with height above ground	
P	Index of atmospheric stability	
Q	Release rate or total activity released ( $Bq\ s^{-1}$ or Bq)	
r	Distance from the release point for a continuous release (m)	
s	Incoming solar radiation ( $W\ m^{-2}$ )	
T	Release duration (h)	
$u_s$	Wind speed at the effective stack height ( $m\ s^{-1}$ )	
$u(z)$	Wind speed at height z ( $m\ s^{-1}$ )	
$u_{10}$	Wind speed at a height of 10 m ( $m\ s^{-1}$ )	
x	} Rectilinear co-ordinates	along the mean wind direction
y		horizontally at right angles to the
z		mean wind direction vertically
$z_0$	Ground roughness length (m)	
$\alpha$	Angular width of a sector (radians)	
$\sigma_y$	Standard deviation of the cross-wind Gaussian plume profile (m)	
$\sigma_{yt}$	Standard deviation of the cross-wind Gaussian plume profile due to turbulent diffusion (m)	
$\sigma_{yw}$	Standard deviation of the cross-wind Gaussian plume profile due to fluctuations in wind direction (m)	
$\sigma_z$	Standard deviation of the vertical Gaussian plume profile (m)	
$\sigma_\theta$	Standard deviation of the horizontal wind direction fluctuation (radians)	

Table 1

Values for use in calculating wind speed at  
source height

Terrain	$z_0$ (m)	$n^*$
Sea	$10^{-4}$	0.07
Sandy desert	$10^{-3}$	0.1
Short grass	0.005	0.13
Open grassland	0.02	0.15
Root crops	0.1	0.2
Agricultural areas	{ 0.2	0.24
	{ 0.3	0.255
Parkland	} 0.5	0.3
Open suburbia		
Cities, woodlands	1.0	0.39

\*  $n$  values obtained assuming the relationship  $u(z) = u_{10} \left(\frac{z}{10}\right)^n$

Under near-neutral stability conditions the power-law form of the wind speed profile can be compared with the more accurate log-law form of the profile. The exponent  $n$  may then be related to  $z_0$  by equating the wind speeds in the two forms at 5 m and 50 m above ground (or, more strictly, above the so-called displacement height).

the log-law is 
$$u = \frac{u_*}{k} \ln \frac{z}{z_0}$$

Hence 
$$n = \log \left( \frac{\ln 50/z_0}{\ln 5/z_0} \right)$$

giving values for  $n$  in the table.

In unstable conditions the log-law profile may be modified to:

$$u(z) = \frac{u_*}{k} \left( \ln \frac{y-1}{y+1} + 2 \tan^{-1} y + \ln \frac{|L|}{2z_0} - \frac{\pi}{2} \right)$$

where  $y = \left(1 + 16 \frac{z}{L}\right)^{1/4}$ ,  $L$  is the Monin-Obukhov length (see Appendix A)  
provided  $z_0 \ll 1$  m,  $z \ll |L|$

While in stable conditions the form is

$$u(z) = \frac{u_*}{k} \left( \ln \frac{z}{z_0} + 5.2 \frac{(z - z_0)}{L} \right)$$

provided  $z \ll L$ .

Table 2

Typical values of wind speed and depth of mixing layer for use when measured values are not available

Stability category	Typical wind speed at 10 m (m/s)	Typical mixing layer depth (m)
A	1	1300
B	2	900
C	5	850
D	5	800
E	3	400
F	2	100
G	1	100

Table 3

Coefficients given by Hosker to derive the vertical standard deviation of the plume for the various stability categories

$$\text{Vertical standard deviation, } \sigma_z = \frac{a x^b}{1 + c x^d} F(z_0, x)$$

Stability category	a	b	c	d
A	0.112	1.06	$5.38 \times 10^{-4}$	0.815
B	0.130	0.950	$6.52 \times 10^{-4}$	0.750
C	0.112	0.920	$9.05 \times 10^{-4}$	0.718
D	0.098	0.889	$1.35 \times 10^{-3}$	0.688
E	0.0609	0.895	$1.96 \times 10^{-3}$	0.684
F	0.0638	0.783	$1.36 \times 10^{-3}$	0.672

Coefficients for the roughness correction factor

Roughness length (m)	f	g	h	j
0.01	1.56	0.0480	$6.25 \times 10^{-4}$	0.45
0.04	2.02	0.0269	$7.76 \times 10^{-4}$	0.37
0.1	2.72	0	0	0
0.4	5.16	-0.098	18.6	-0.225
1.0	7.37	-0.0957	$4.29 \times 10^3$	-0.60
4.0	11.7	-0.128	$4.59 \times 10^4$	-0.78

$$F(z_0, x) = \begin{cases} \ln(f x^g [1 + (h x^j)^{-1}]) & , z_0 \geq 0.1 \text{ m} \\ \ln(f x^g [1 + h x^j]^{-1}) & , z_0 < 0.1 \text{ m} \end{cases}$$

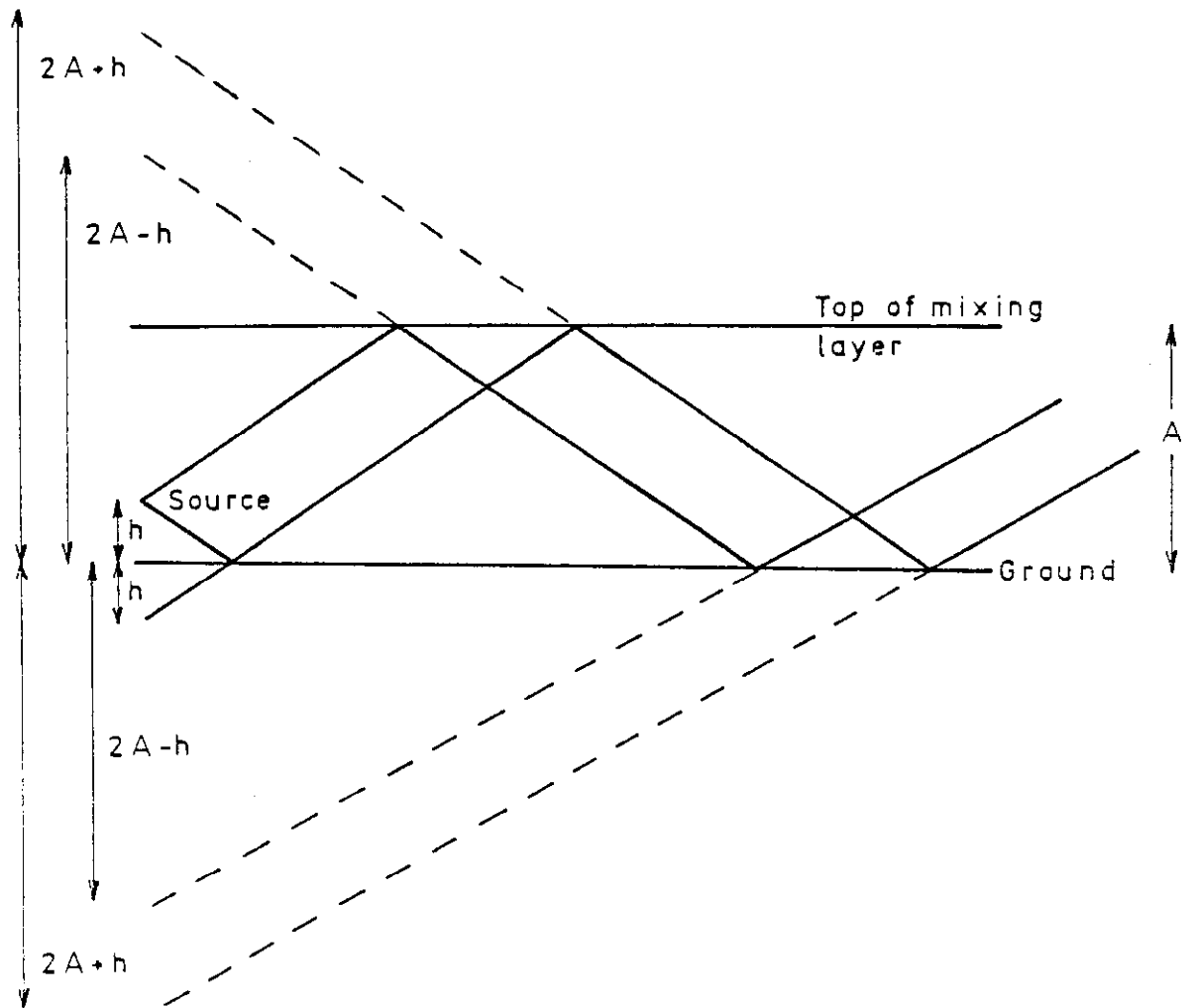


Figure 1. Virtual source model to represent the reflections from the ground and the top of the mixing layer

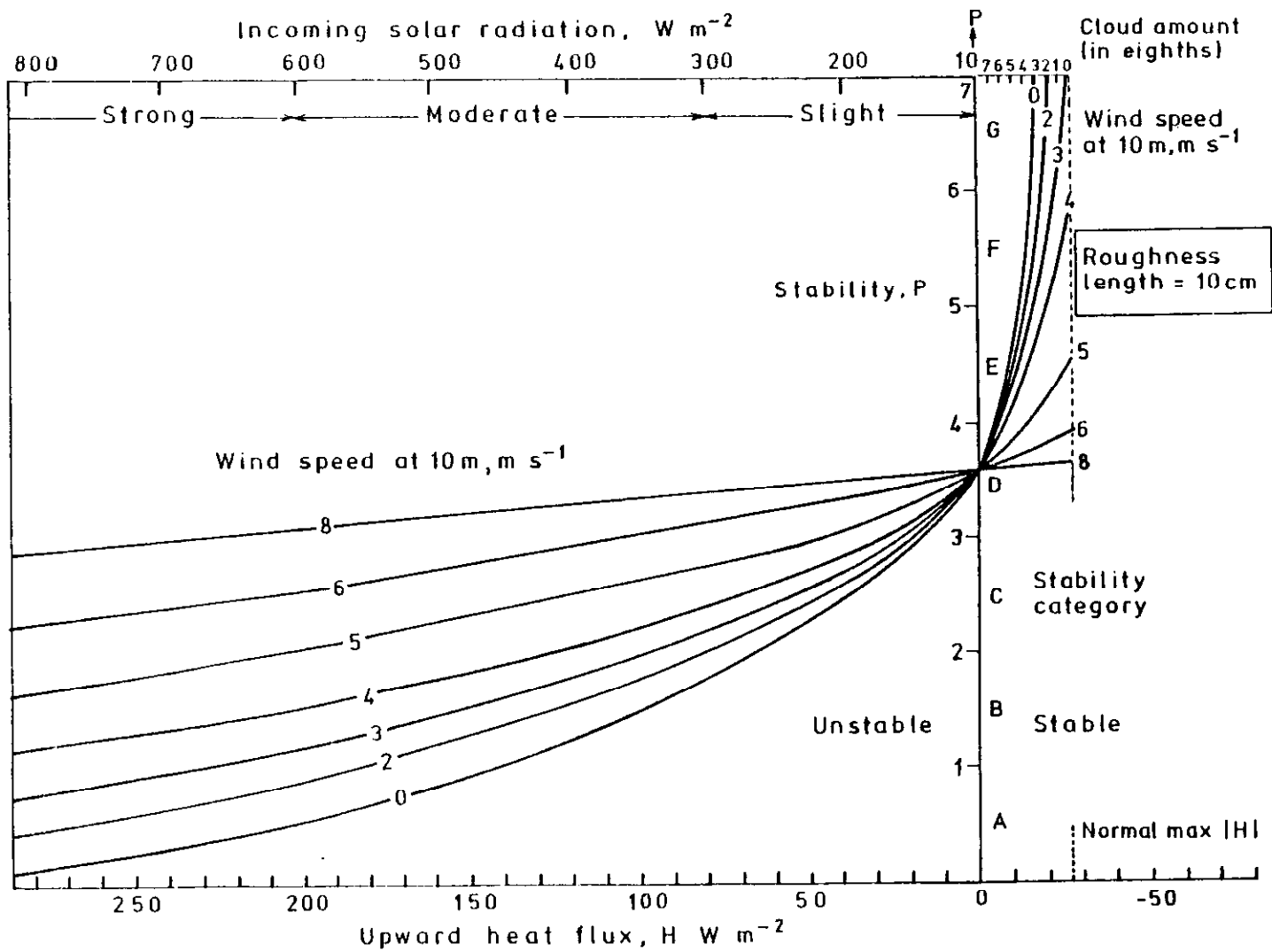
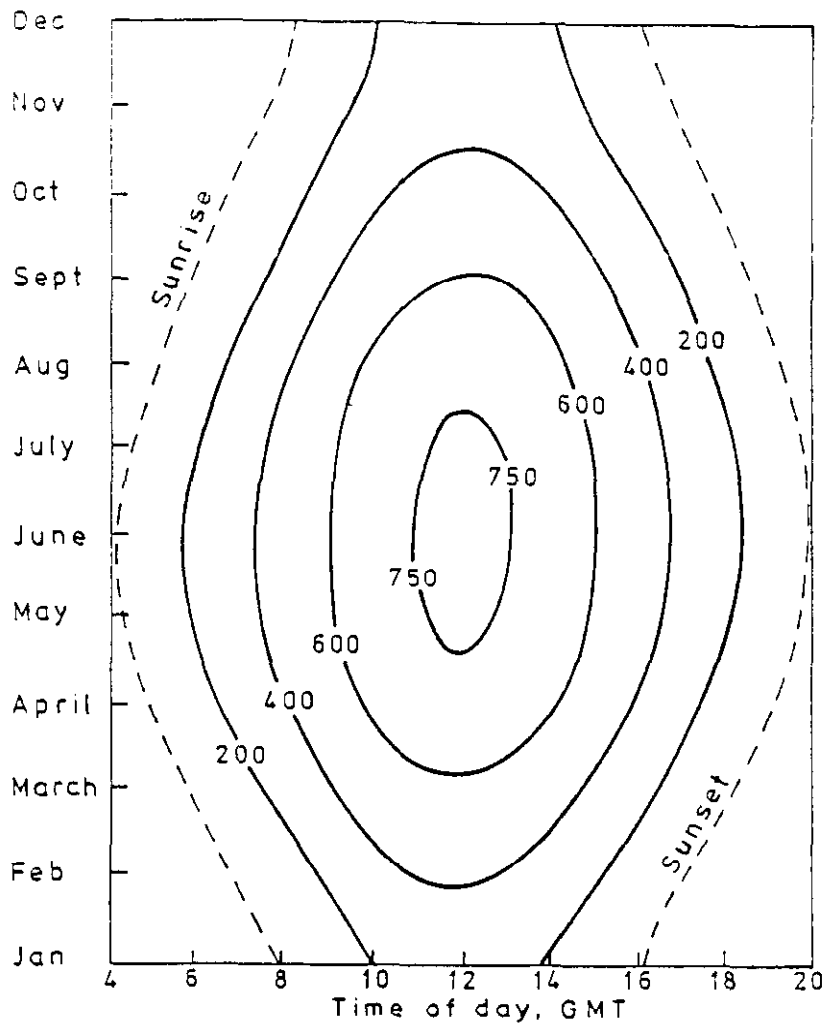


Figure 2. The nomogram of Smith for the determination of the stability parameter P <sup>(15)</sup>



Cloud amount	Multiply I.S.R. by:
0	1.07
1	0.89
2	0.81
3	0.76
4	0.72
5	0.67
6	0.59
7	0.45
8	0.23

Figure 3. Incoming solar radiation ( $\text{W m}^{-2}$ ) at Cambridge (0-1 eighths cloud)

(The incoming solar radiation ( $\text{W m}^{-2}$ ) reaching the ground on a cloudless day is expressed in the main figure in terms of time of day and month. For cloudy conditions multiply this amount by the factor appropriate to the cloud amount in eighths)

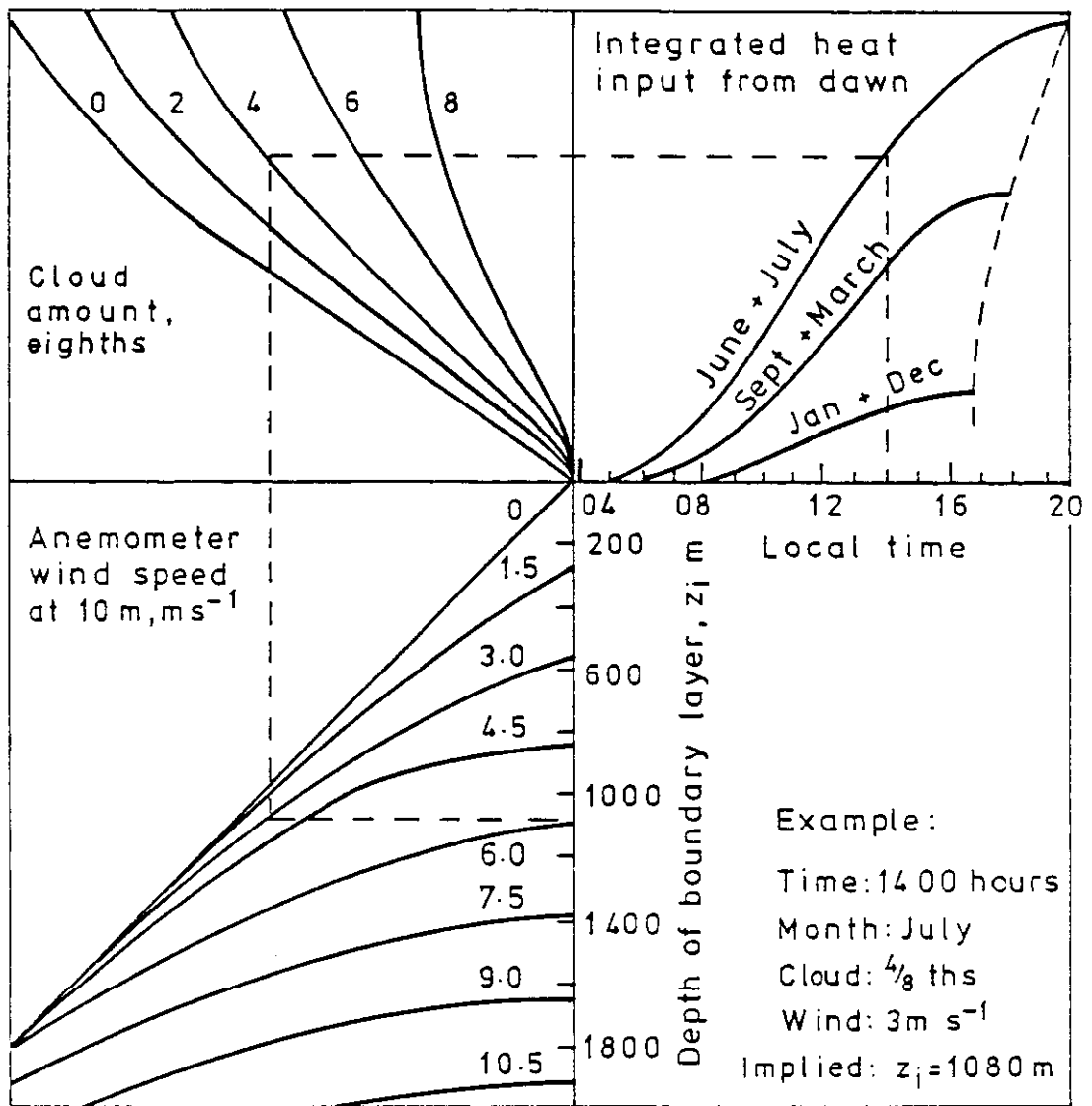


Figure 4. A nomogram for estimating the depth of the boundary layer in day time in the absence of marked advective effects or basic changes in weather conditions. The marked example shows how the diagram is to be used



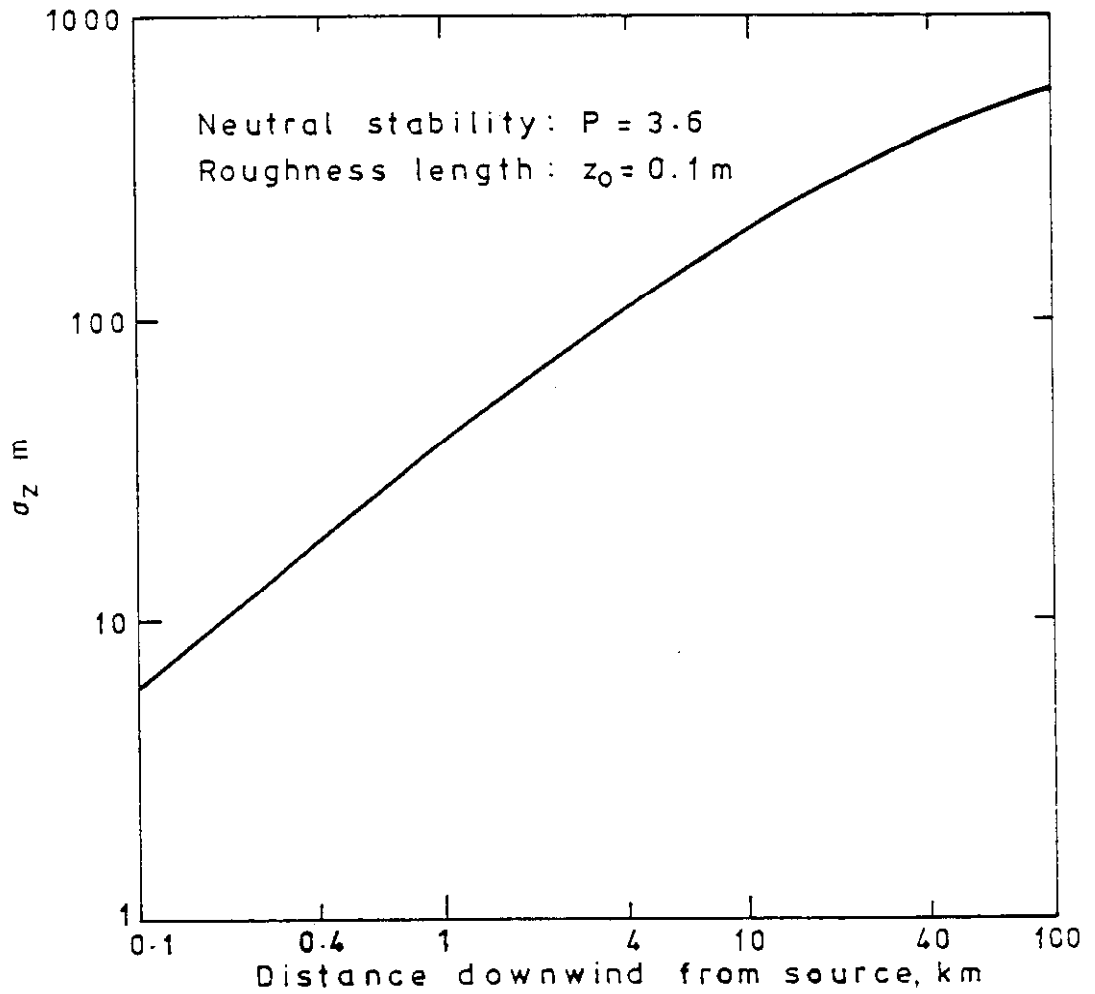


Figure 5. The vertical dispersion parameter  $\sigma_z$  as a function of distance in neutral atmospheric stability and for a ground roughness length of 0.1 m

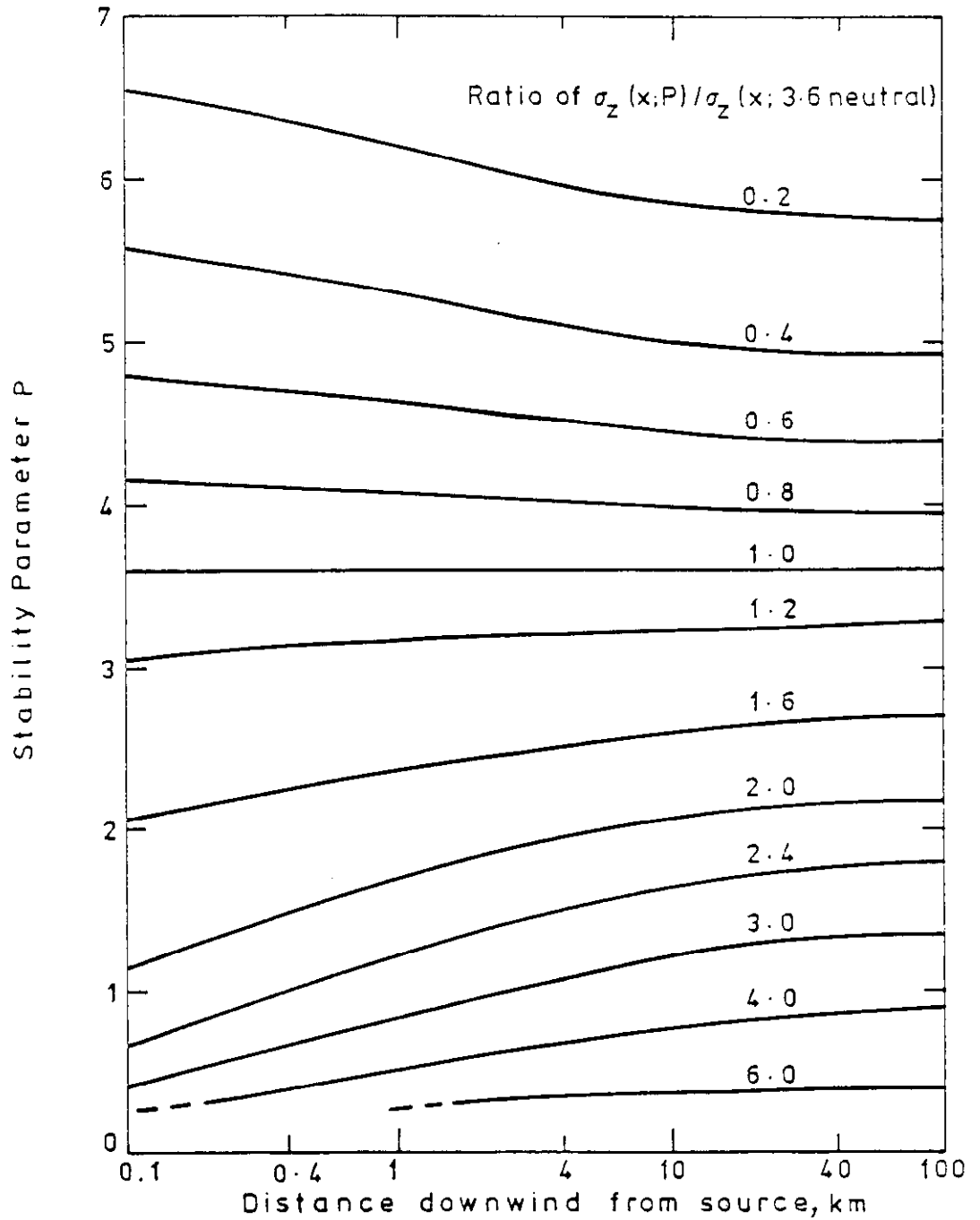


Figure 6. Ratio of vertical dispersion standard deviation,  $\sigma_z$ , for any value of stability parameter, to that in neutral conditions as a function of downwind distance

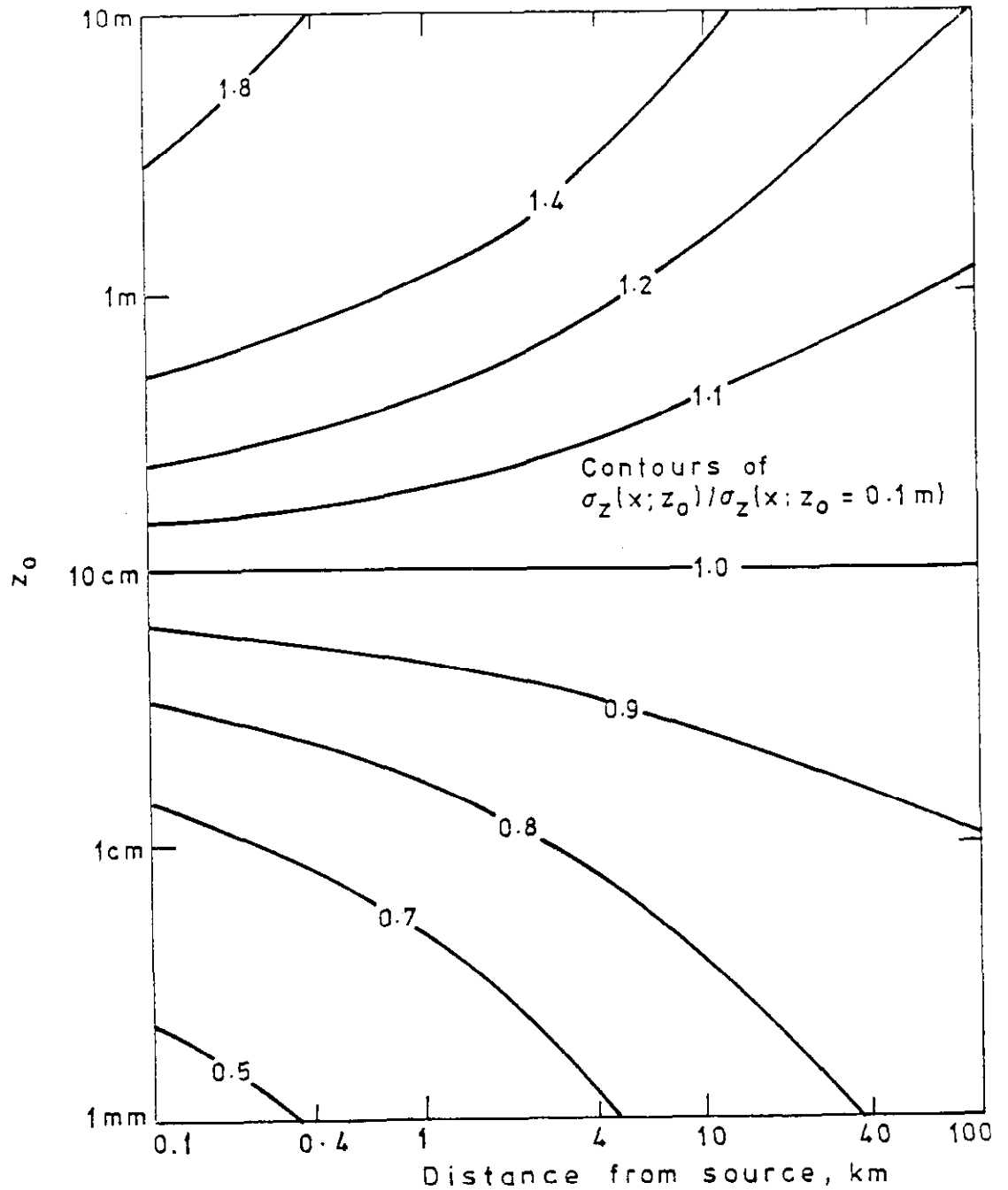


Figure 7. Ratio of vertical dispersion standard deviation,  $\sigma_z$ , at any ground roughness length to that at 0.1 m. The ratio is virtually independent of the atmospheric stability parameter

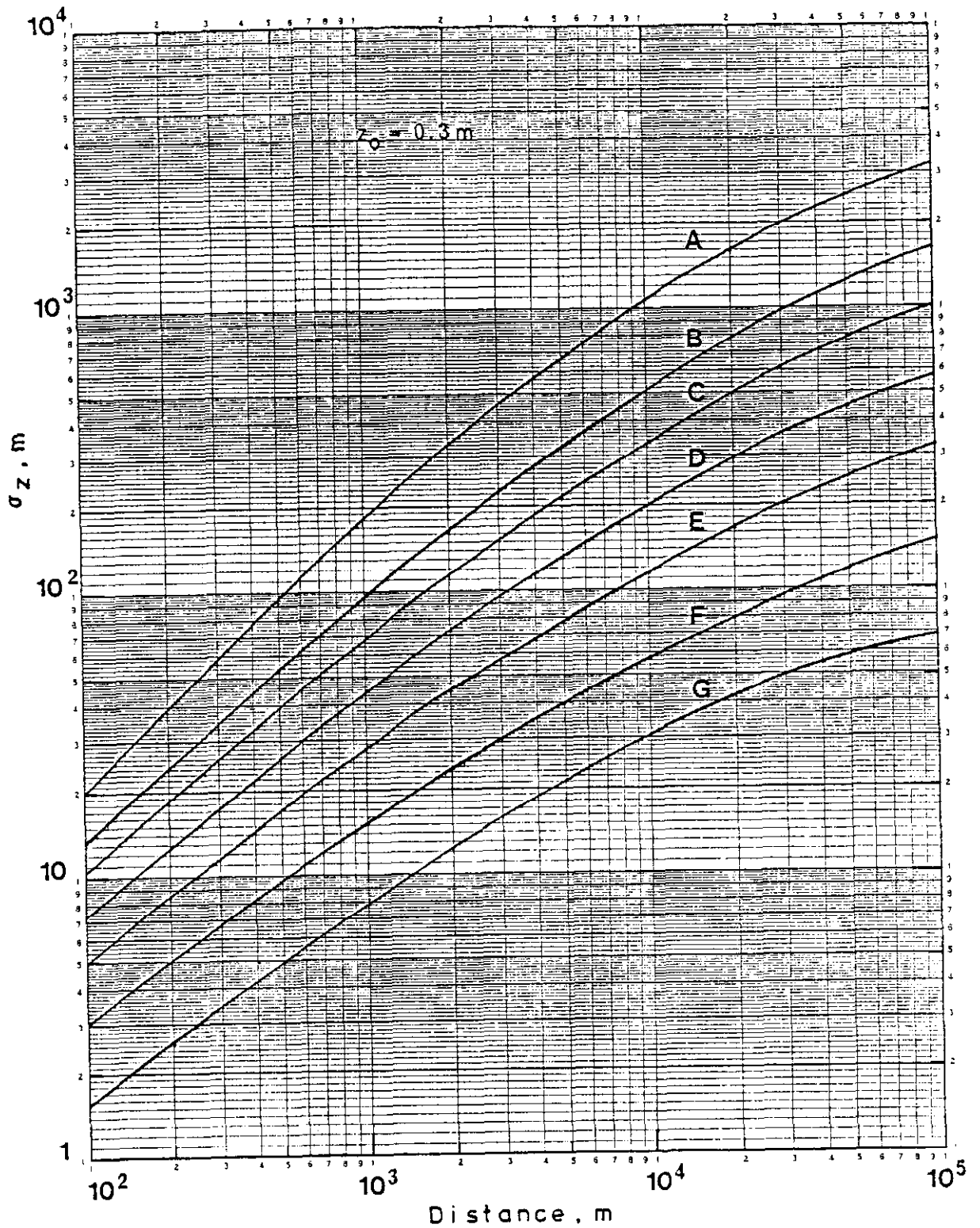


Figure 8. Vertical standard deviation,  $\sigma_z$ , as a function of distance for each Pasquill stability category and a ground roughness length of 0.3 m



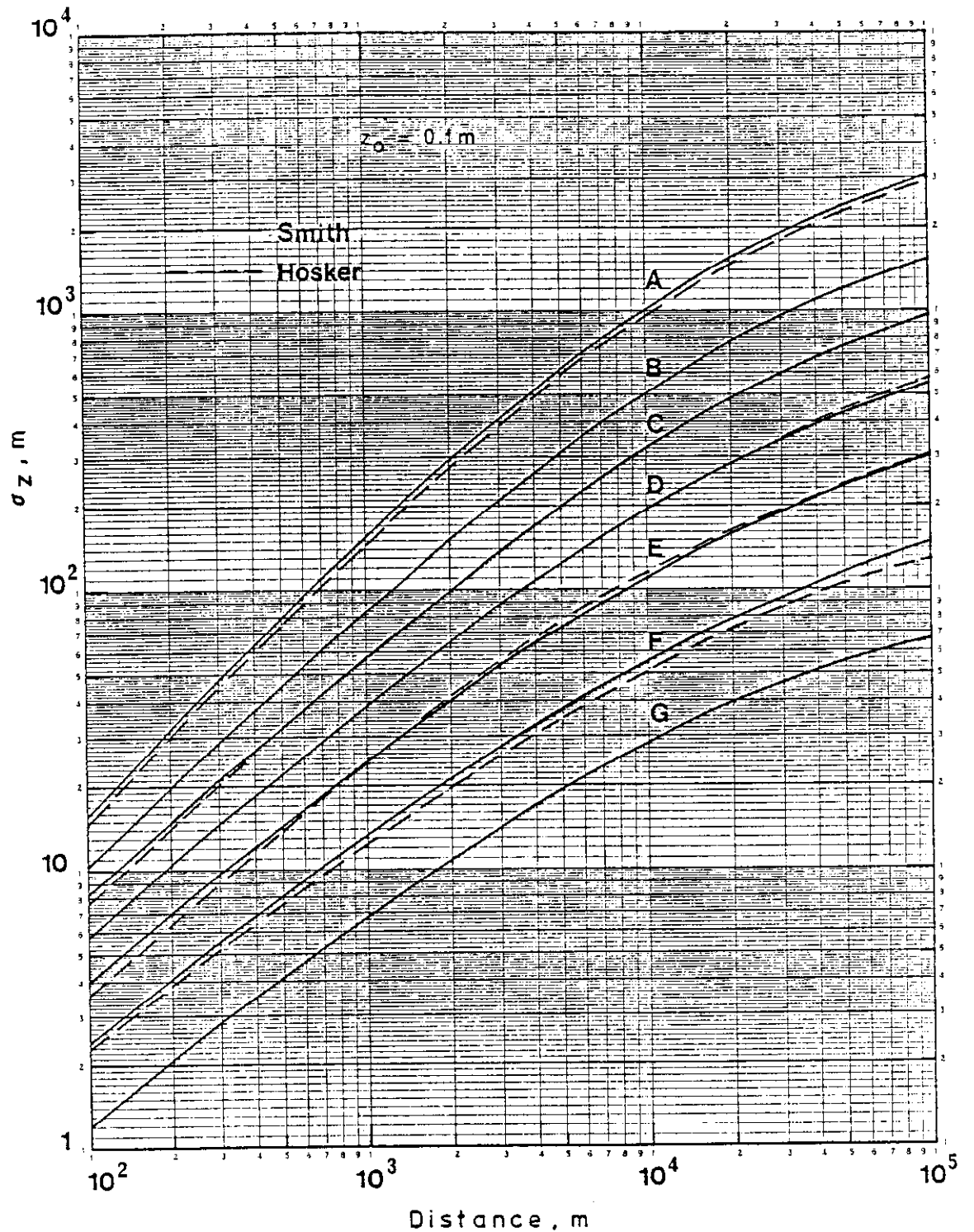


Figure 9. A comparison of the Hosker fit and Smith's data for the vertical standard deviation in each weather category and a ground roughness length of 0.1m

(The Hosker fit is not available for Category G; in Categories B, C and D, Smith and Hosker are indistinguishable)

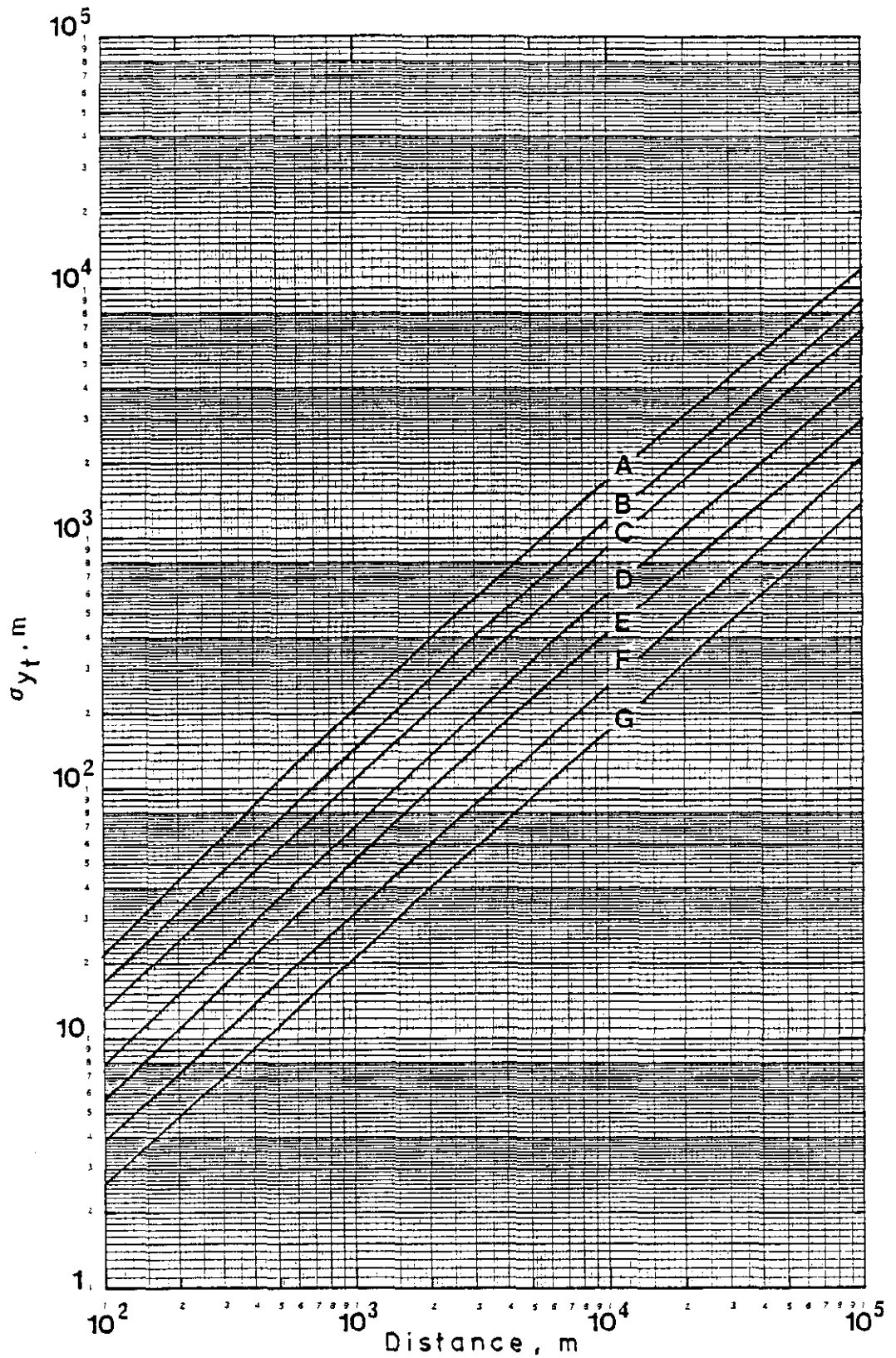


Figure 10. The horizontal standard deviation due to turbulence,  $\sigma_{yt}$ , as a function of distance in each Pasquill category

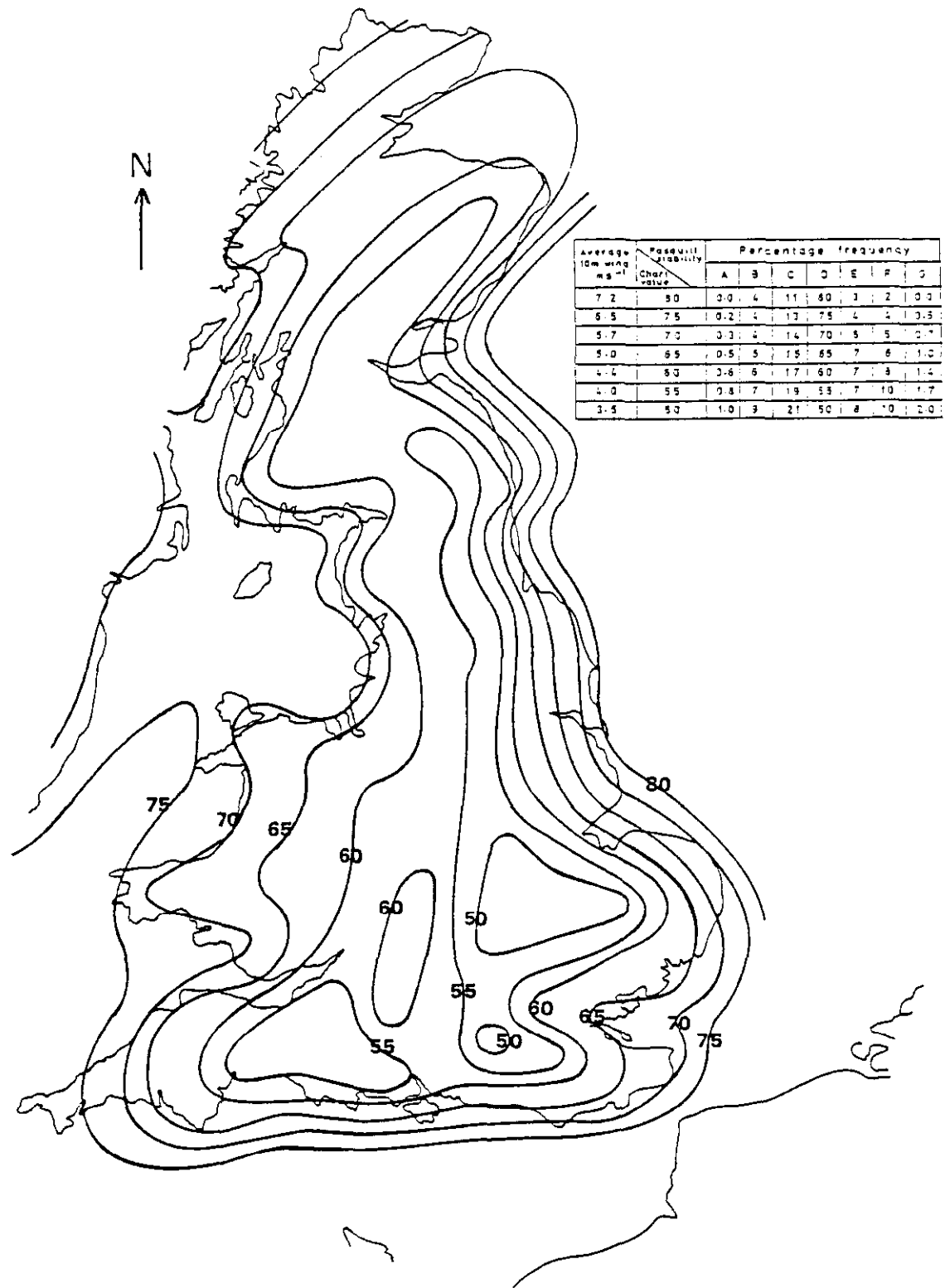


Figure 11. Frequency of occurrence of the Pasquill stability categories over Great Britain



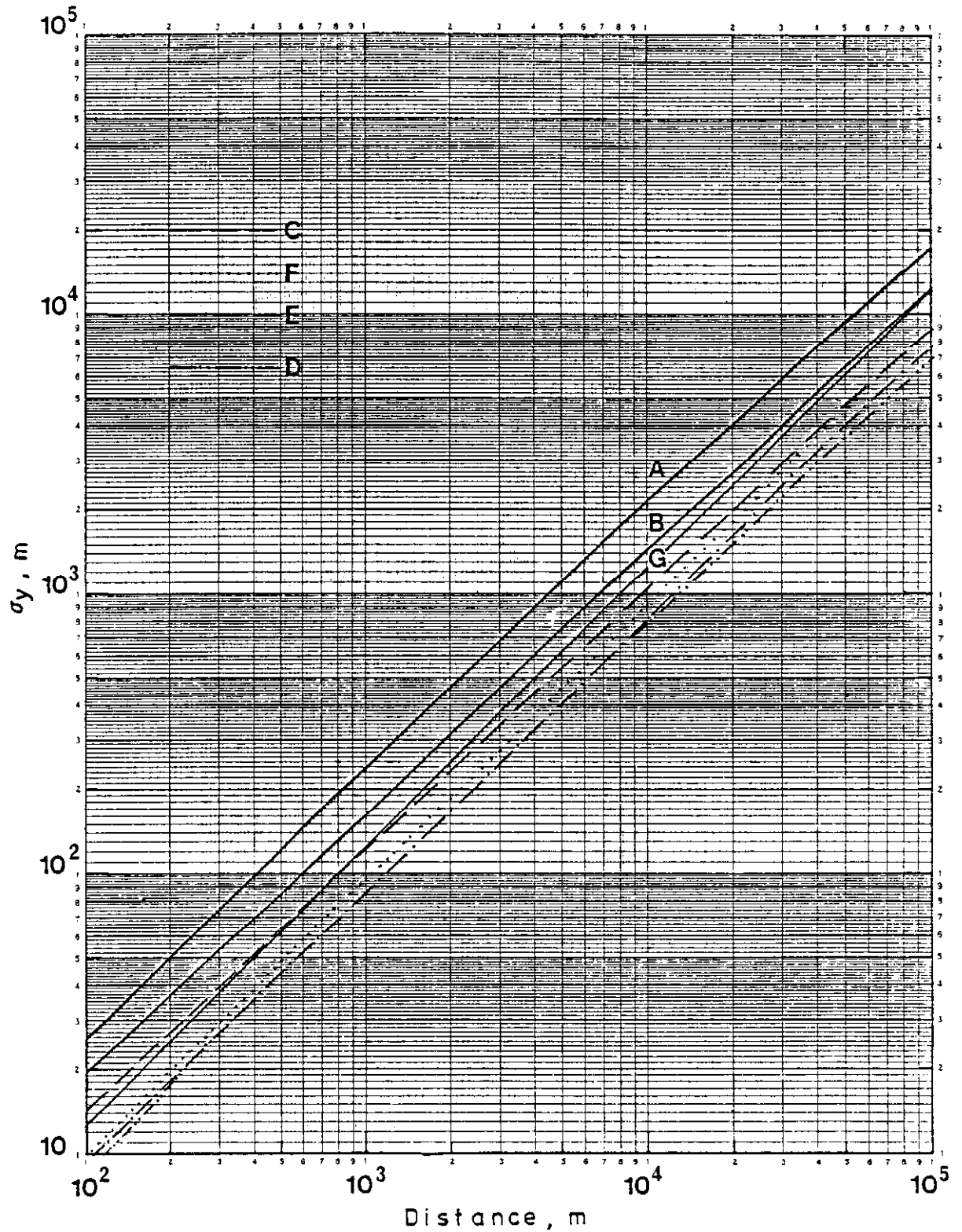


Figure 12. Horizontal standard deviation,  $\sigma_y$ , for a release of 30 min duration in each Pasquill stability category

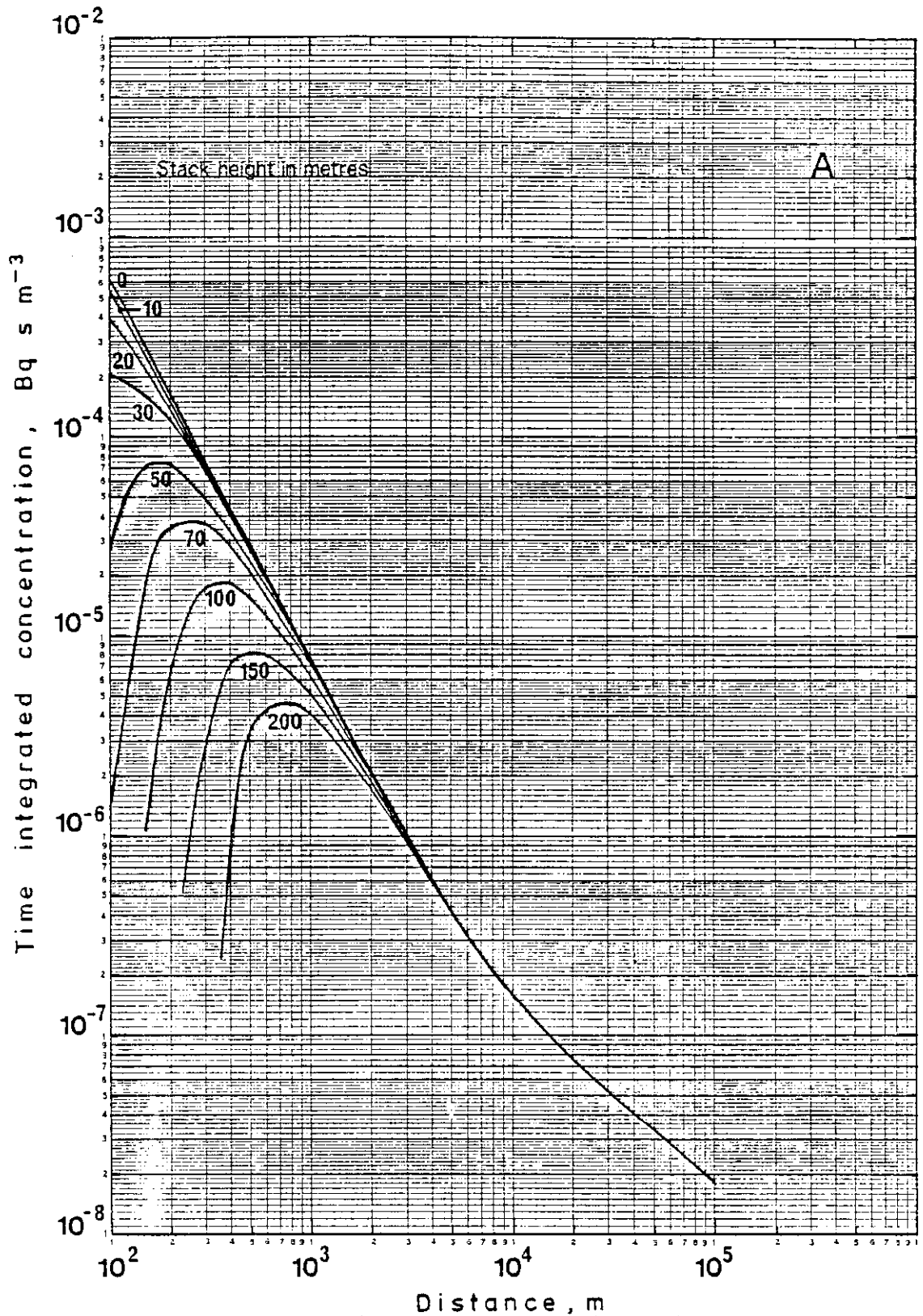


Figure 13. On-axis ground level time integrated concentrations as a function of effective release height for a short (30 min) release of unit activity in Category A conditions

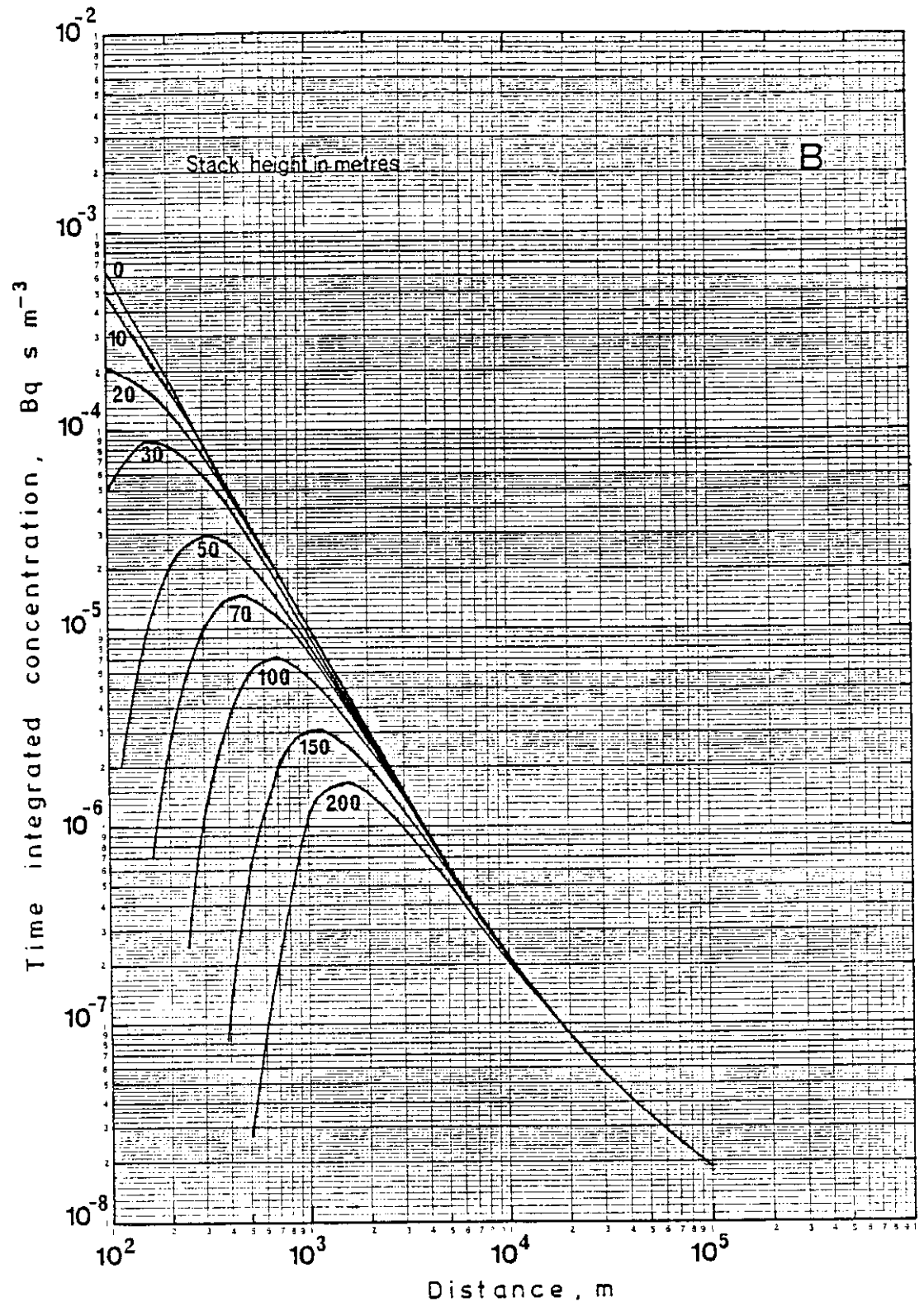


Figure 14. On-axis ground level time integrated concentrations as a function of effective release height for a short (30 min) release of unit activity in Category B conditions

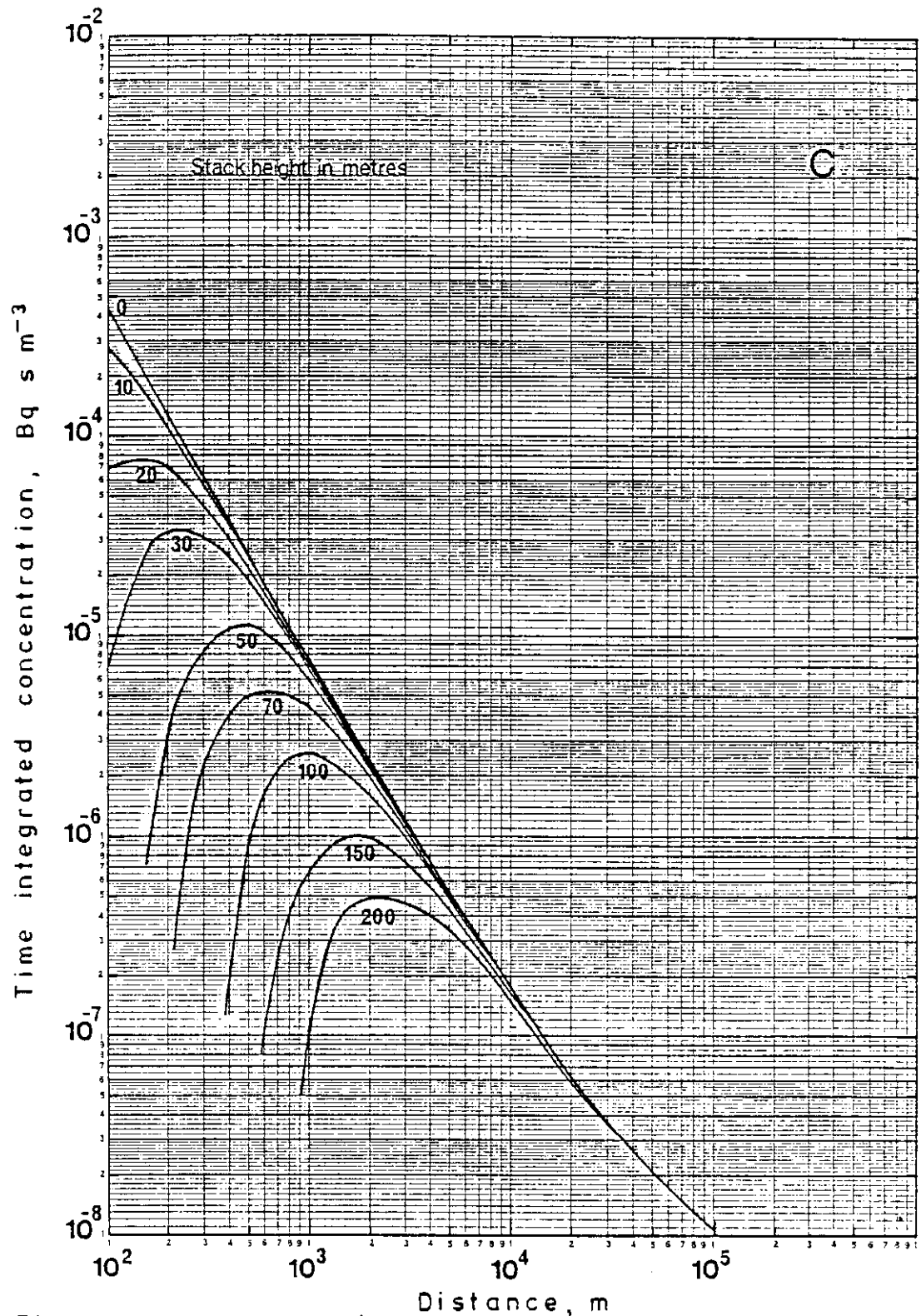


Figure 15. On-axis ground level time integrated concentrations as a function of effective release height for a short (30 min) release of unit activity in Category C conditions

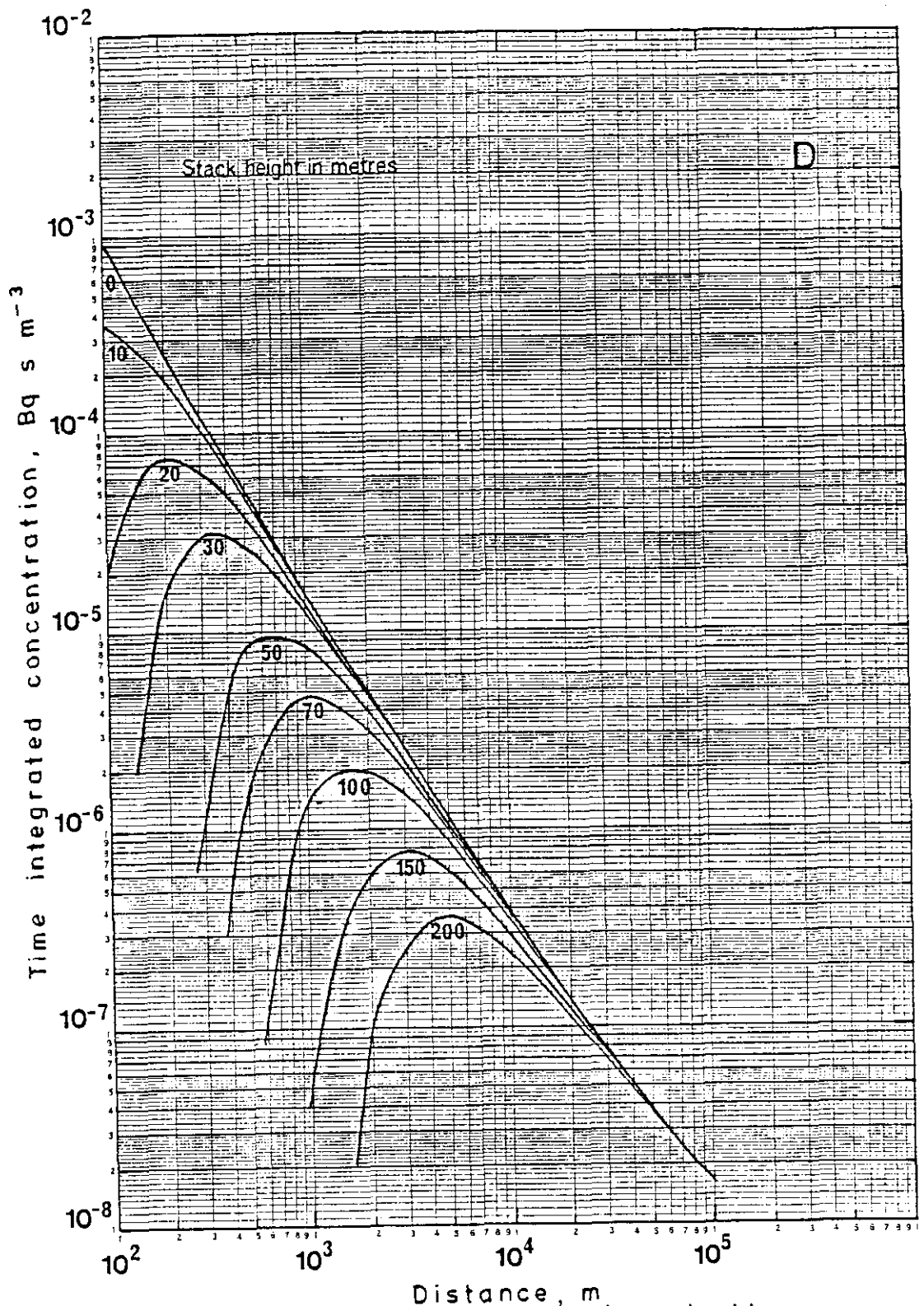


Figure 16. On-axis ground level time integrated concentrations as a function of effective release height for a short (30 min) release of unit activity in Category D conditions

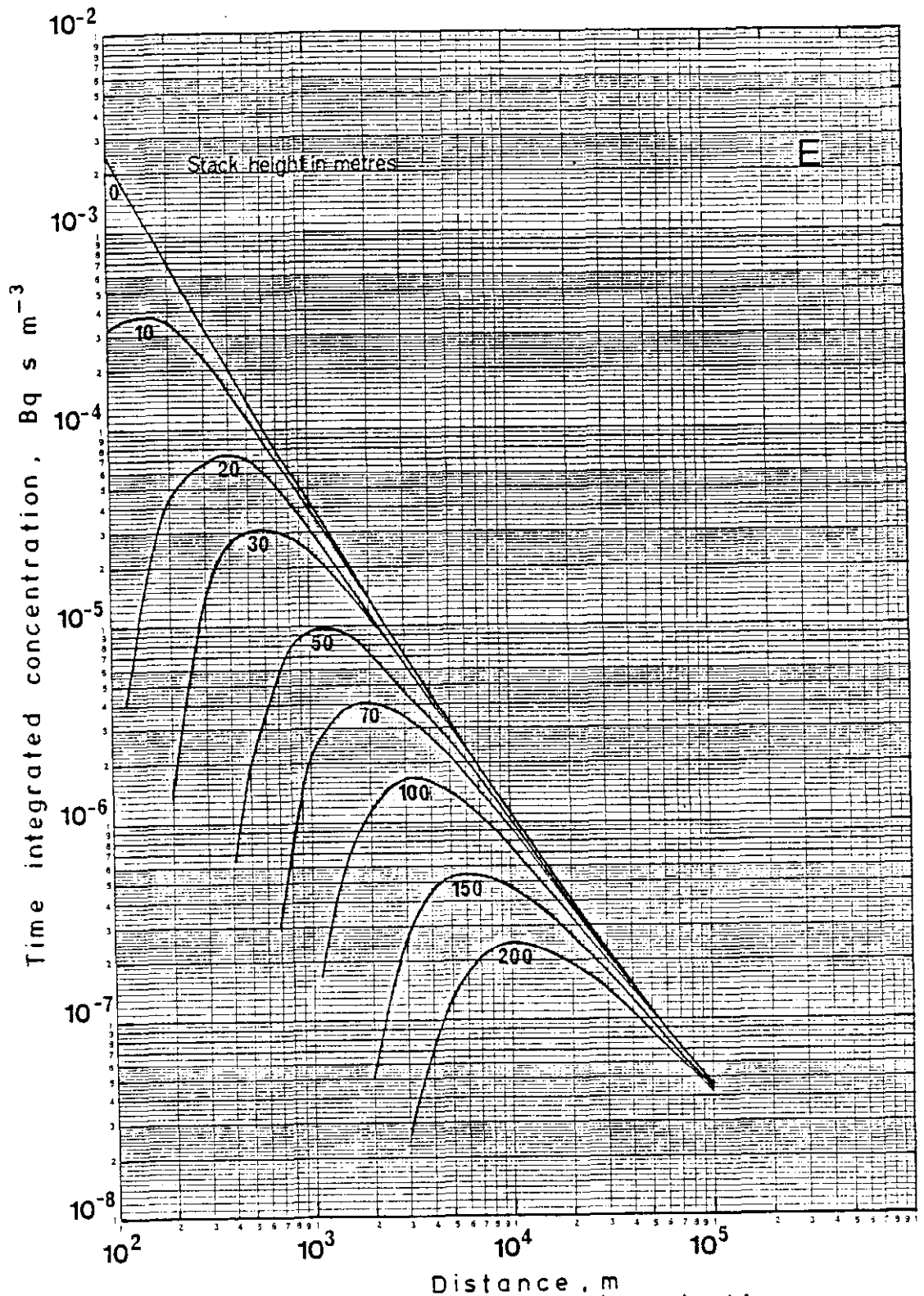


Figure 17. On-axis ground level time integrated concentrations as a function of effective release height for a short (30 min) release of unit activity in Category E conditions

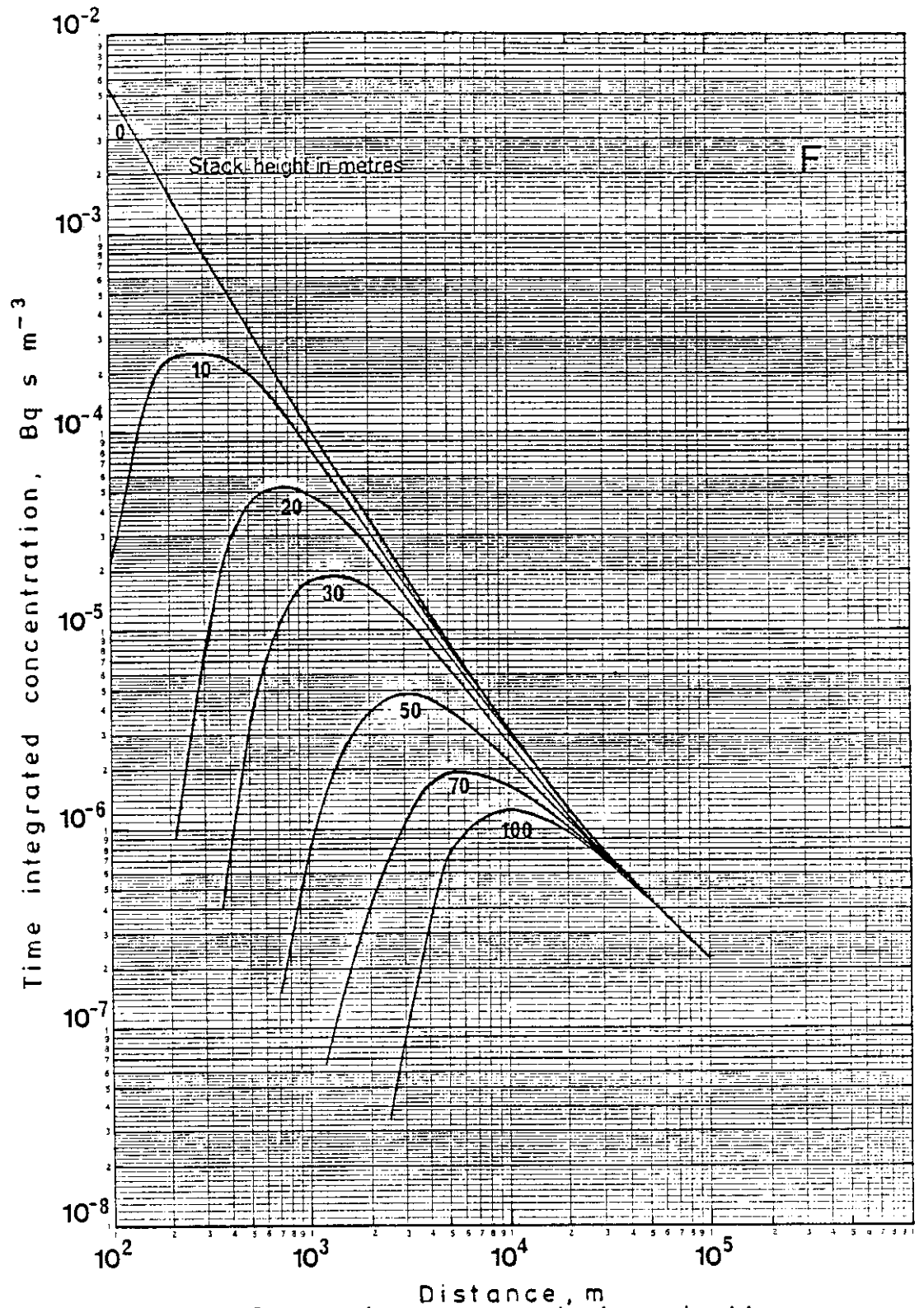


Figure 18. On-axis ground level time integrated concentrations as a function of effective release height for a short (30 min) release of unit activity in Category F conditions

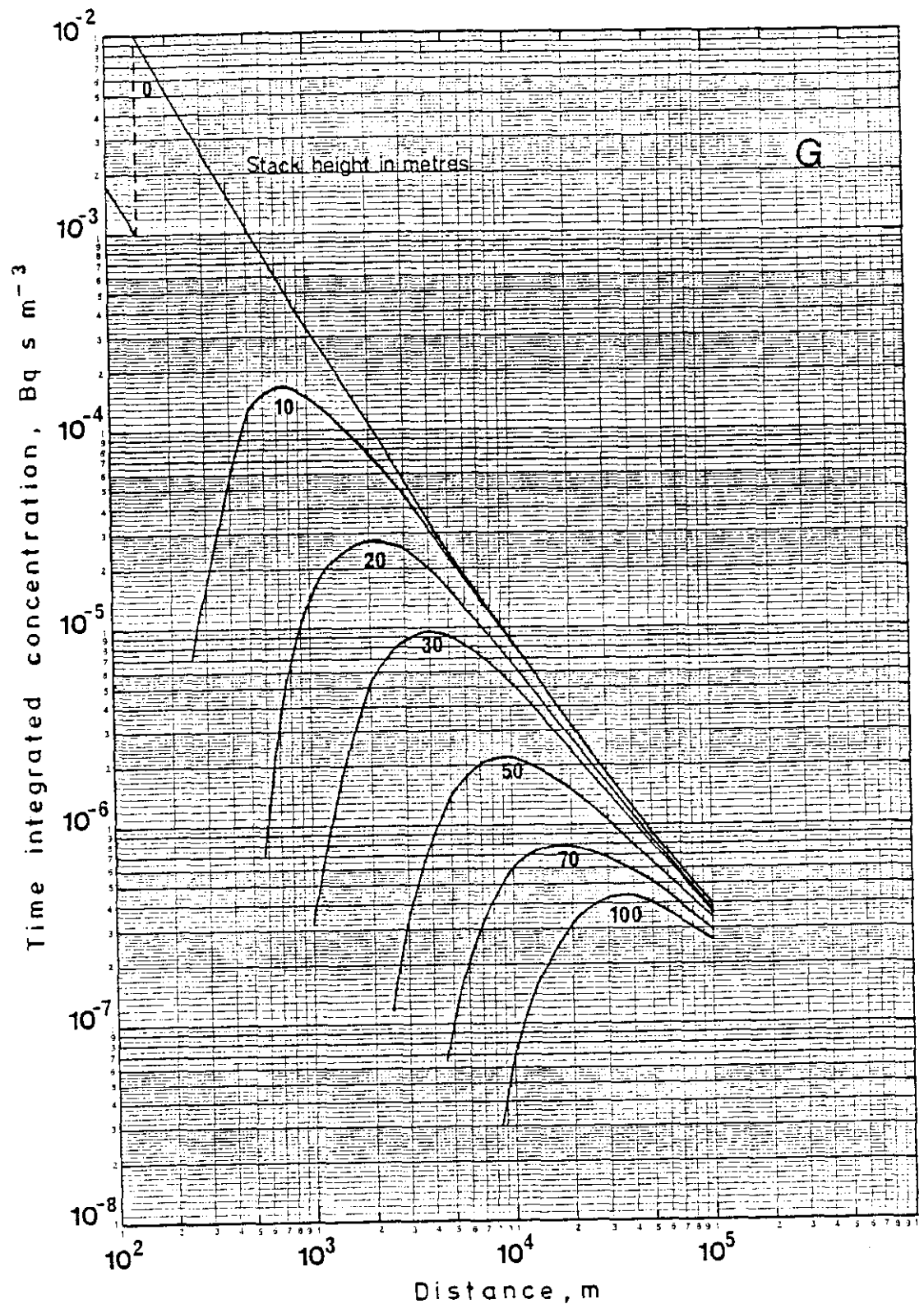


Figure 19. On-axis ground level time integrated concentrations as a function of effective release height for a short (30 min) release of unit activity in Category G conditions



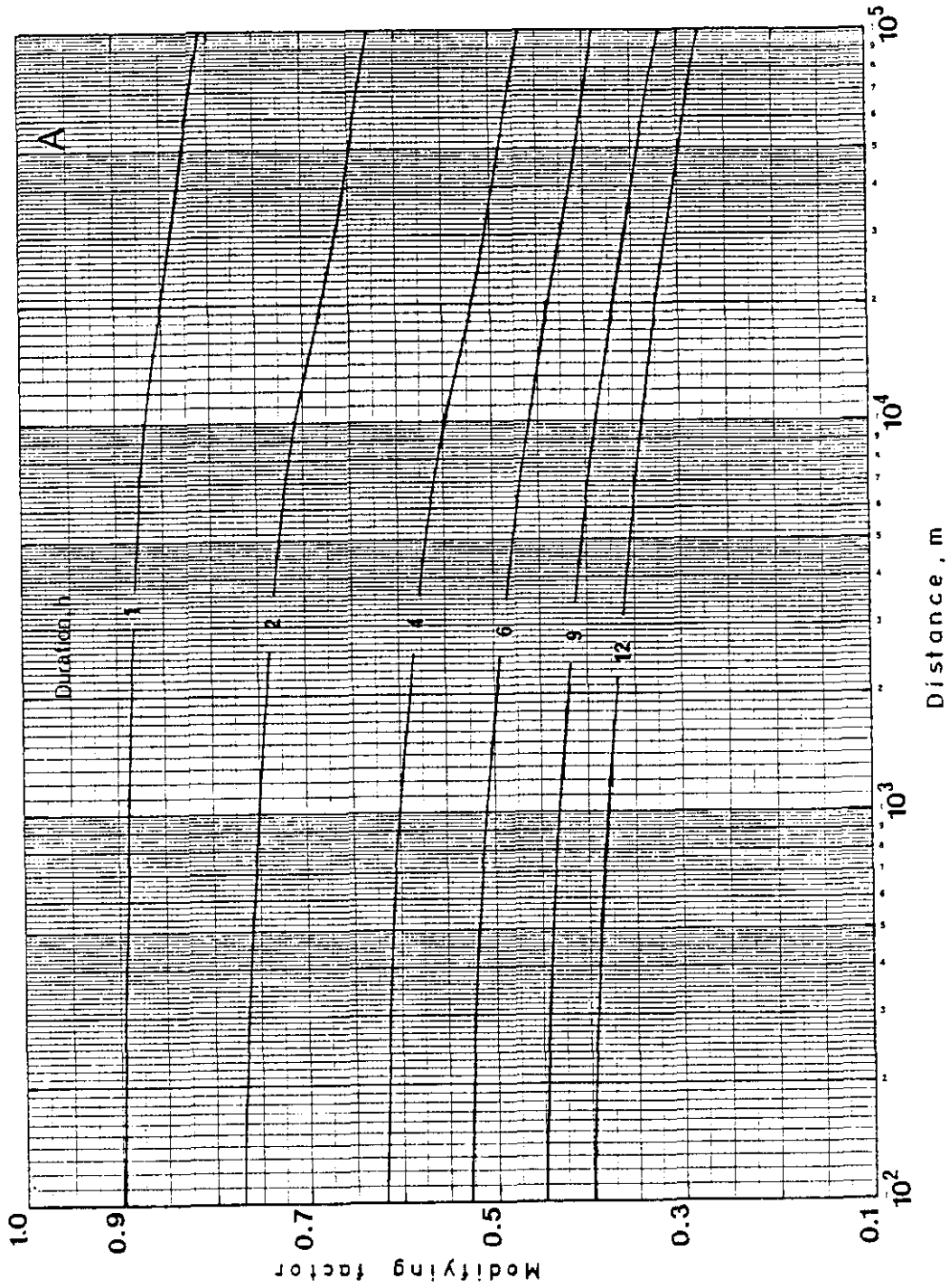


Figure 20. Modifying factor for the on-axis ground level concentration as a function of release duration in Category A conditions

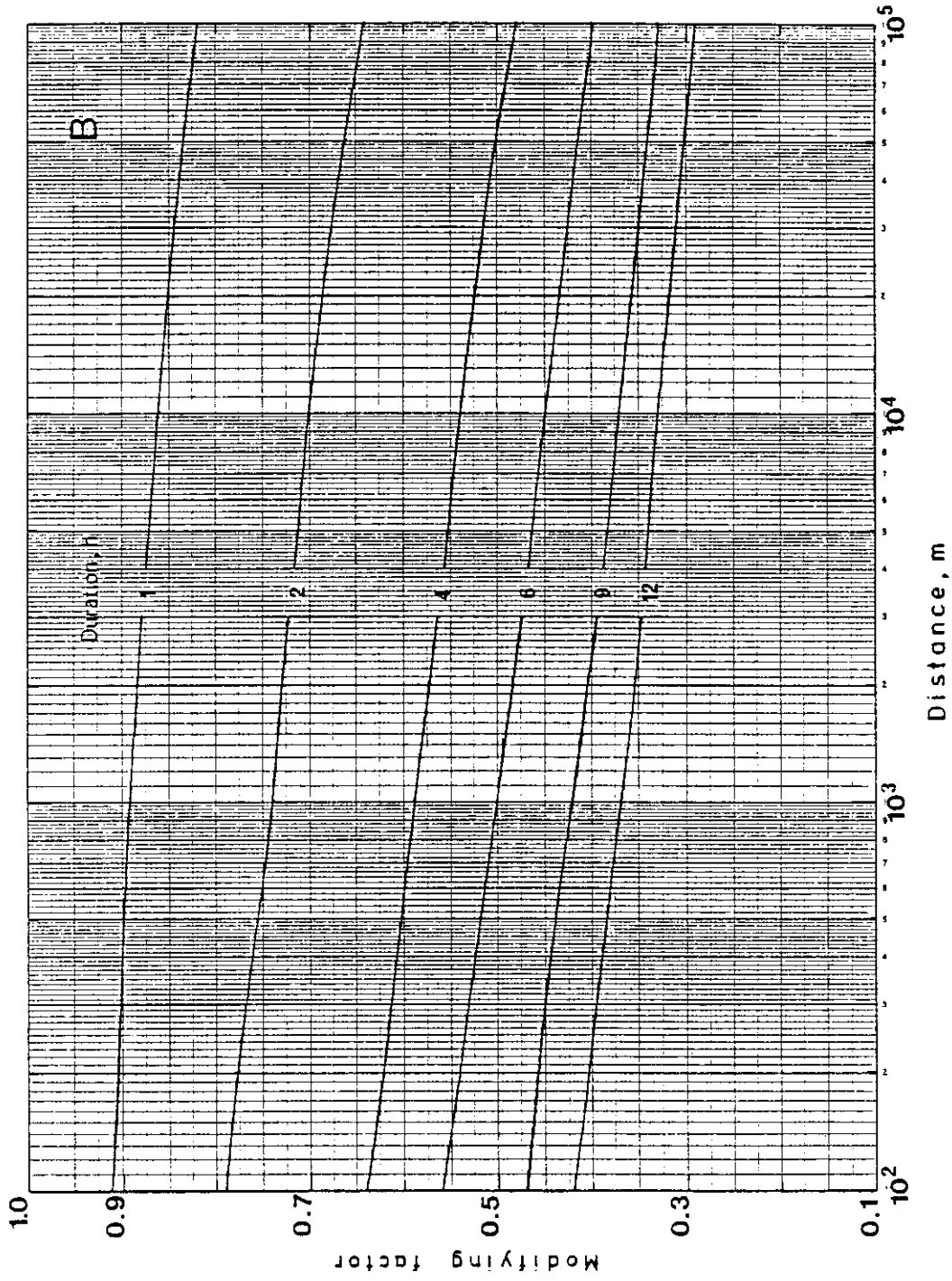


Figure 21. Modifying factor for the on-axis ground level concentration as a function of release duration in Category B conditions

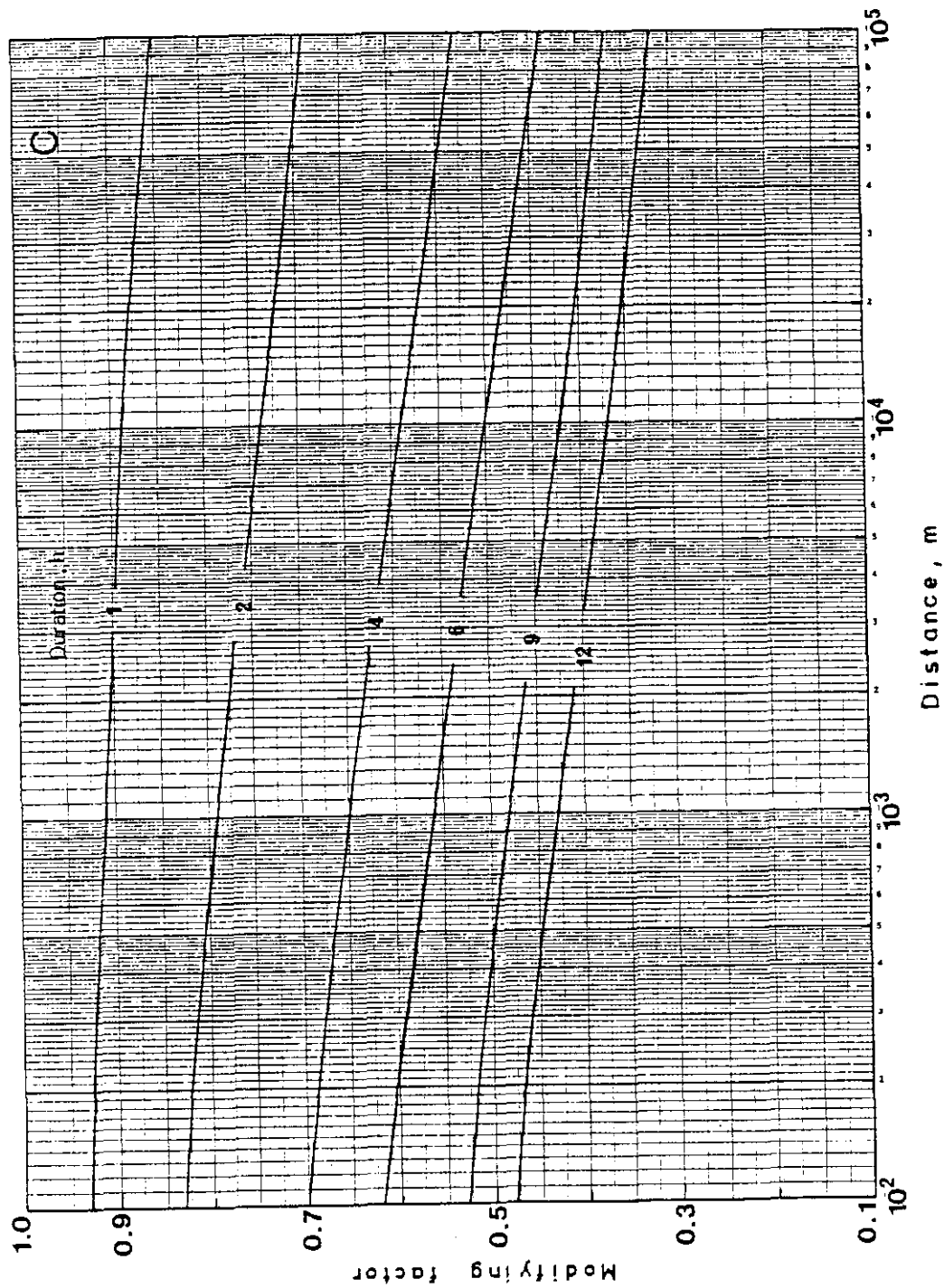


Figure 22. Modifying factor for the on-axis ground level concentration as a function of release duration in Category C conditions

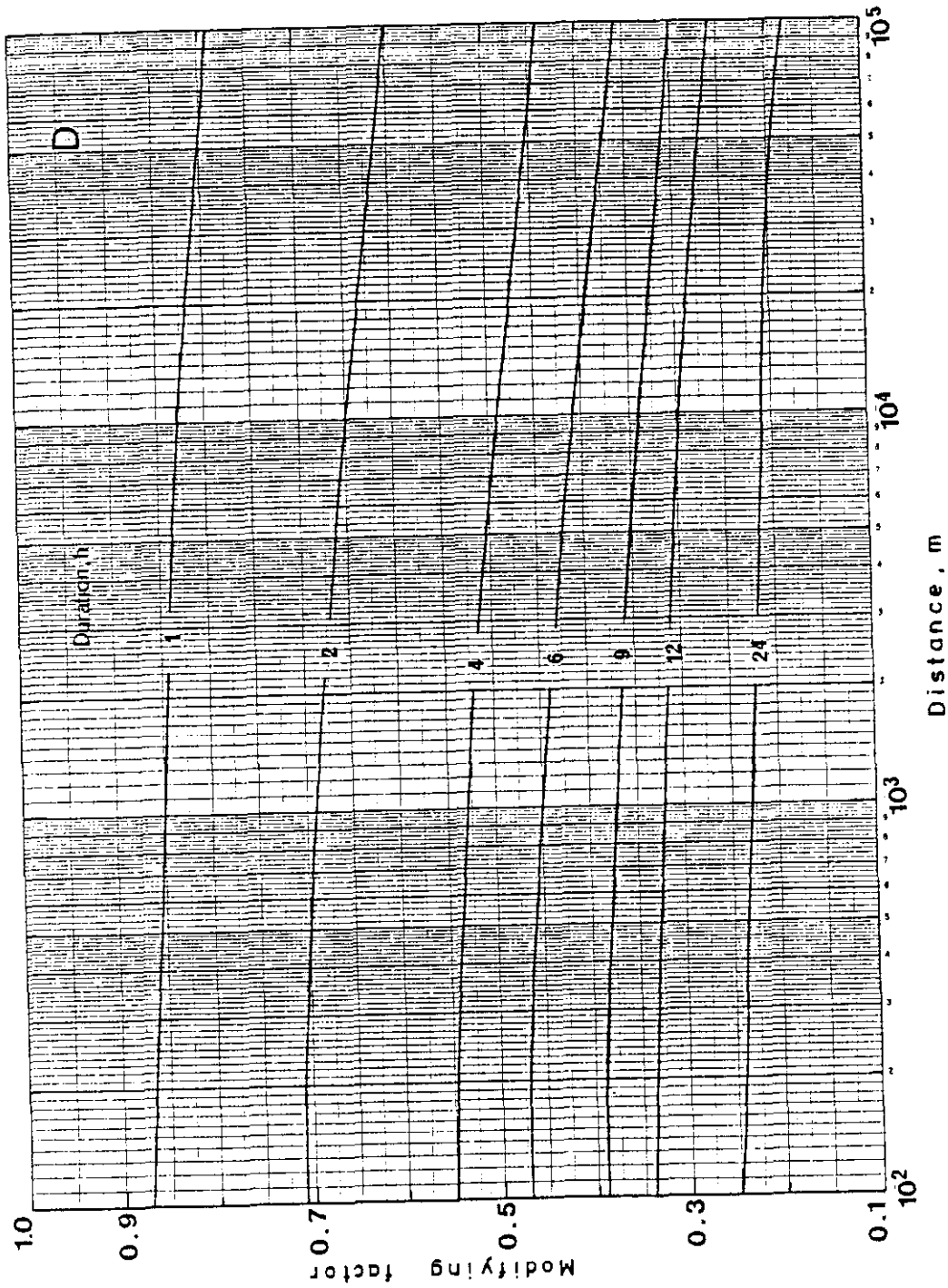


Figure 23. Modifying factor for the on-axis ground level concentration as a function of release duration in Category D conditions

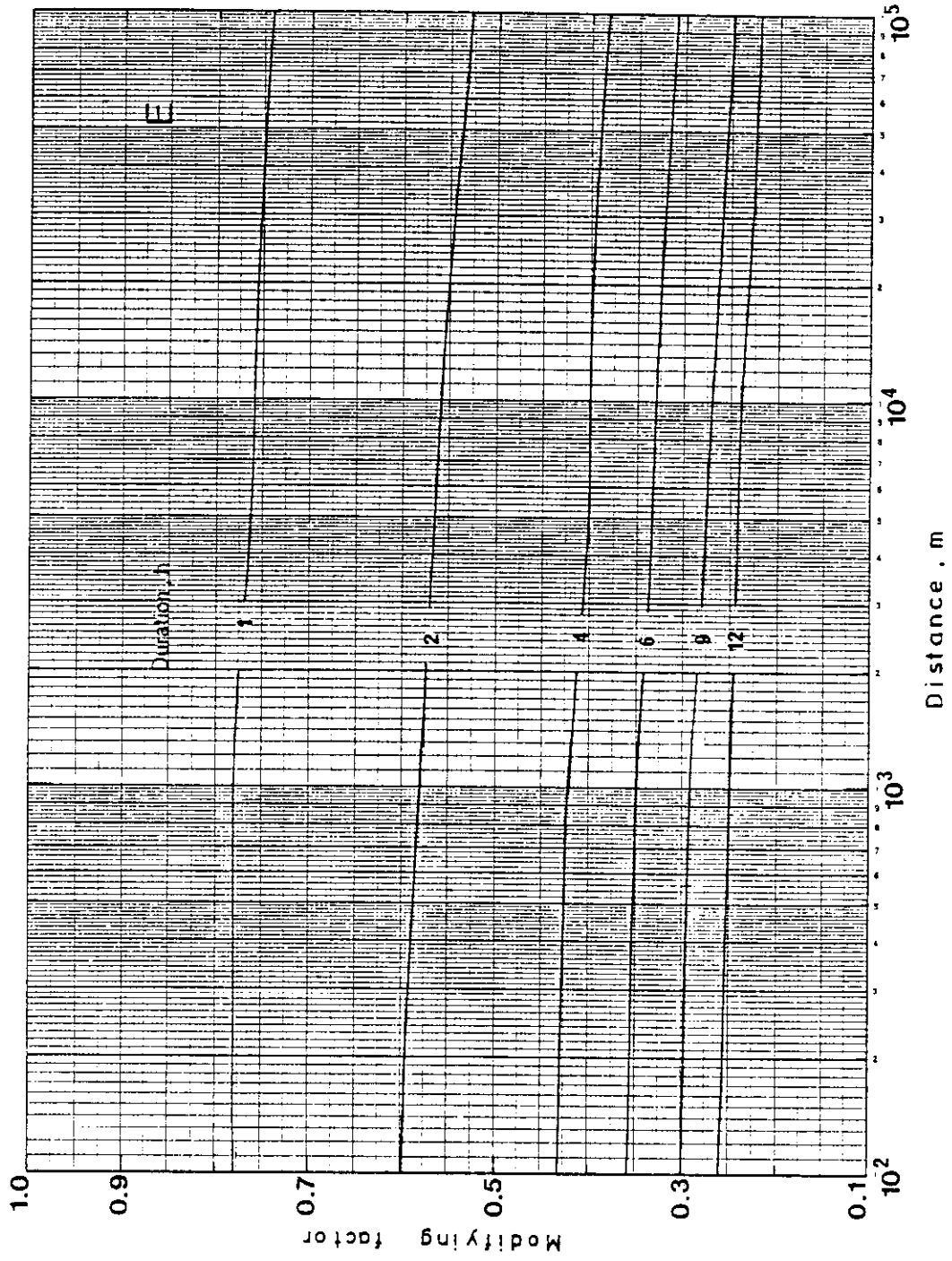


Figure 24. Modifying factor for the on-axis ground level concentration as a function of release duration in Category E conditions

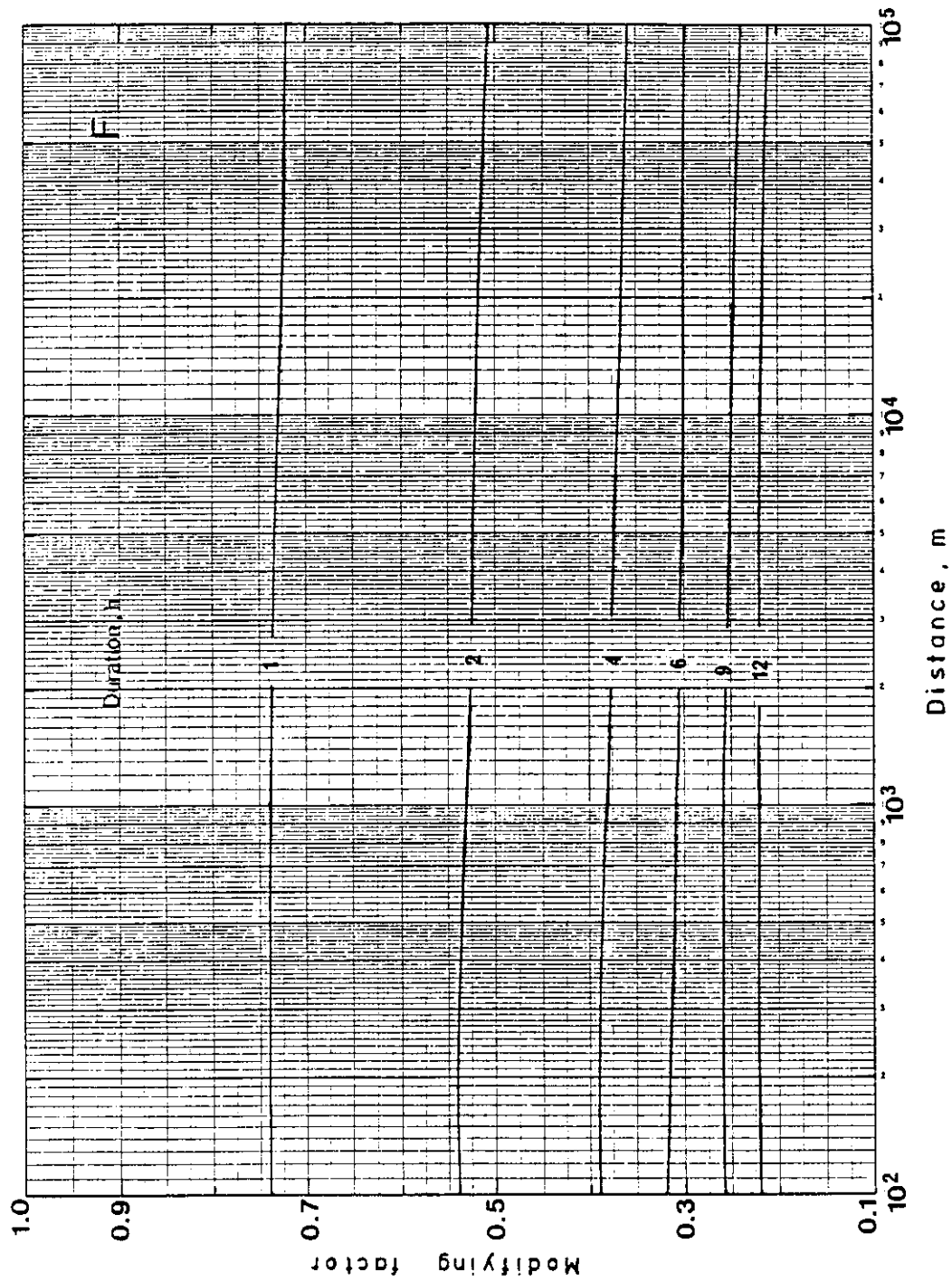


Figure 25. Modifying factor for the on-axis ground level concentration as a function of release duration in Category F conditions

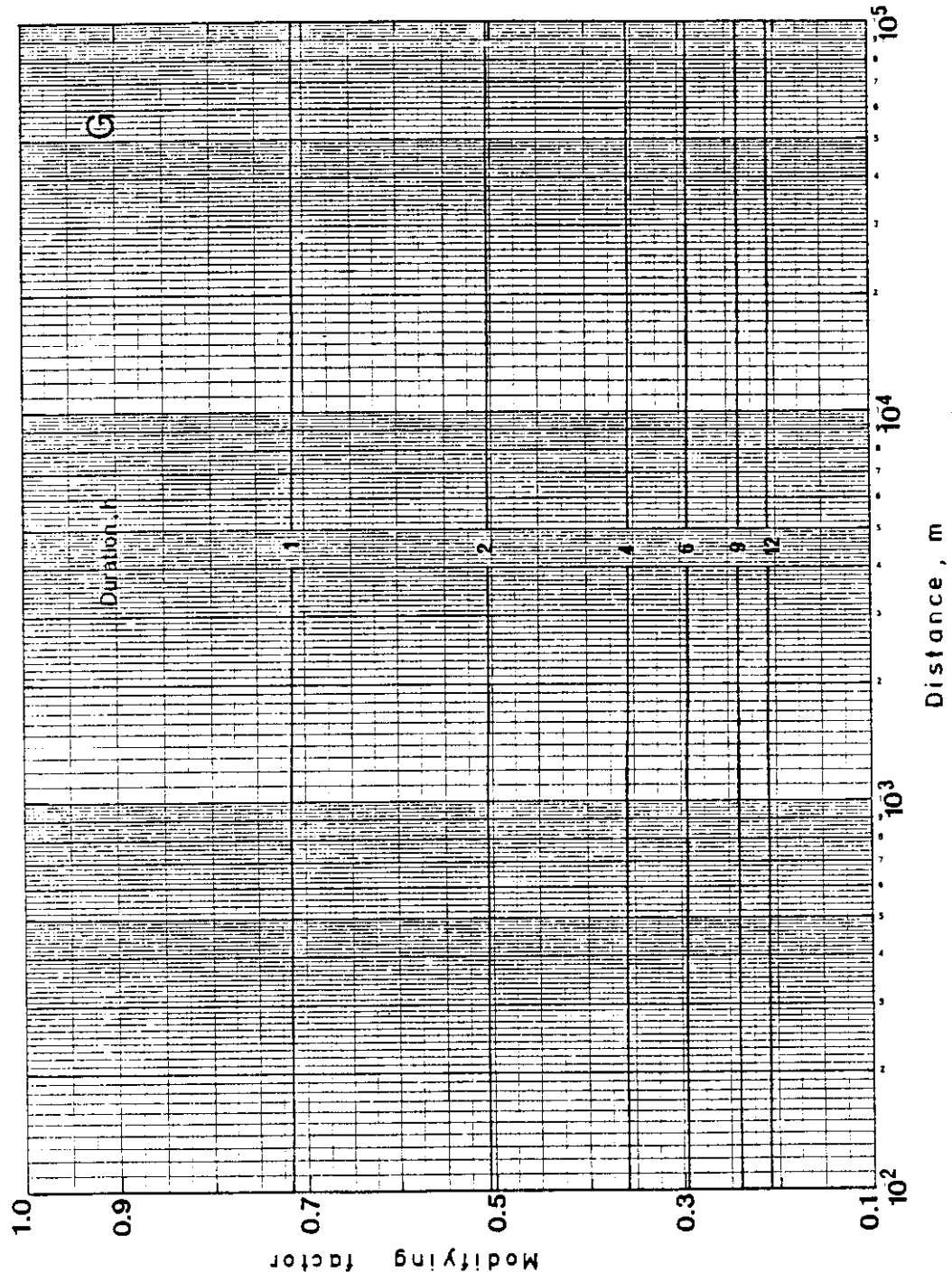


Figure 26. Modifying factor for the on-axis ground level concentration as a function of release duration in Category G conditions

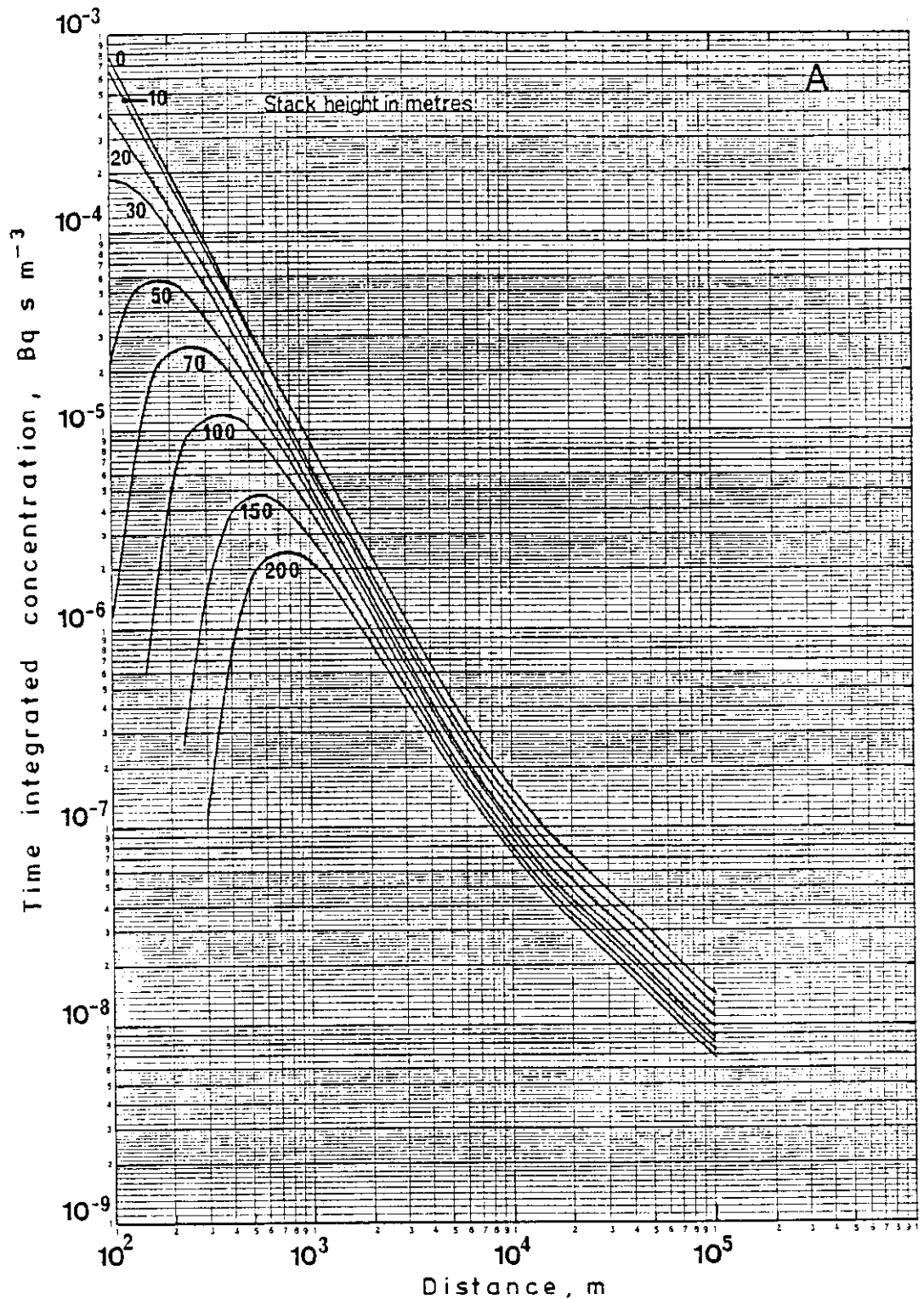


Figure 27. On-axis ground level time integrated concentrations for unit releases as a function of effective height of release for uniform horizontal dispersion into a sector of angular width  $\pi/6$  ( $30^\circ$ ) in Category A conditions



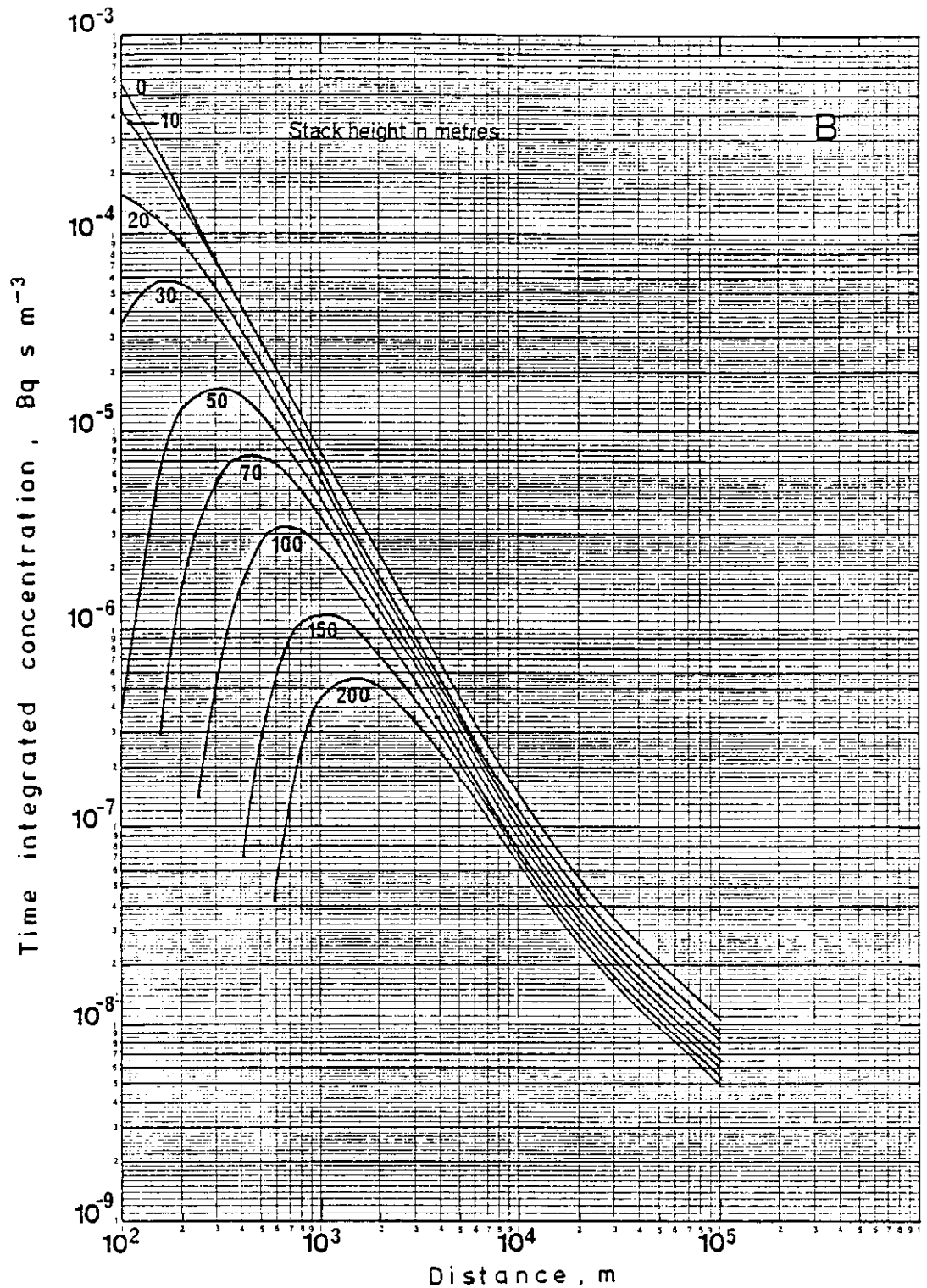


Figure 28. On-axis ground level time integrated concentrations for unit releases as a function of effective height of release for uniform horizontal dispersion into a sector of angular width  $\pi/6$  ( $30^\circ$ ) in Category B conditions

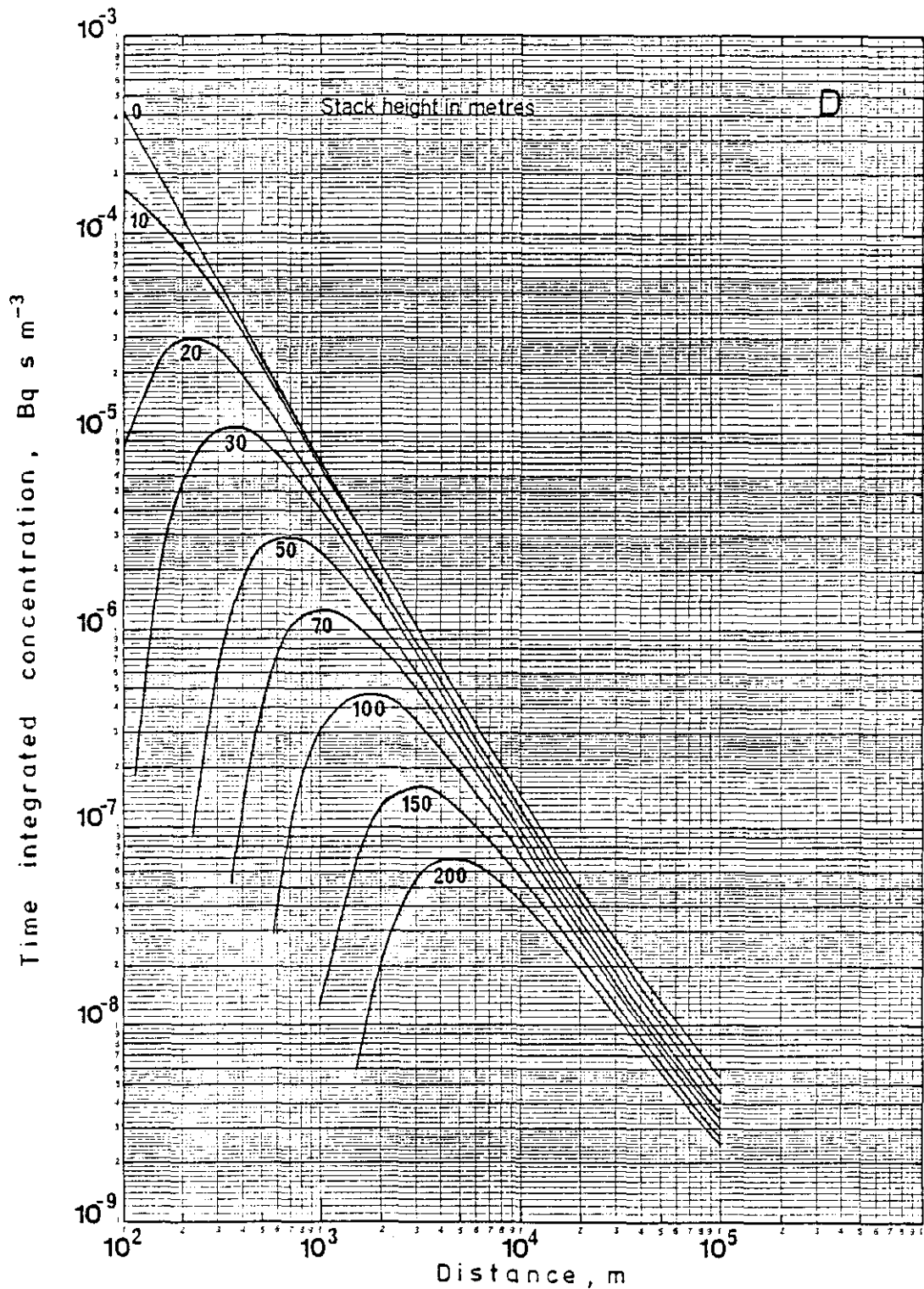


Figure 30. On-axis ground level time integrated concentrations for unit releases as a function of effective height of release for uniform horizontal dispersion into a sector of angular width  $\pi/6$  ( $30^\circ$ ) in Category D conditions

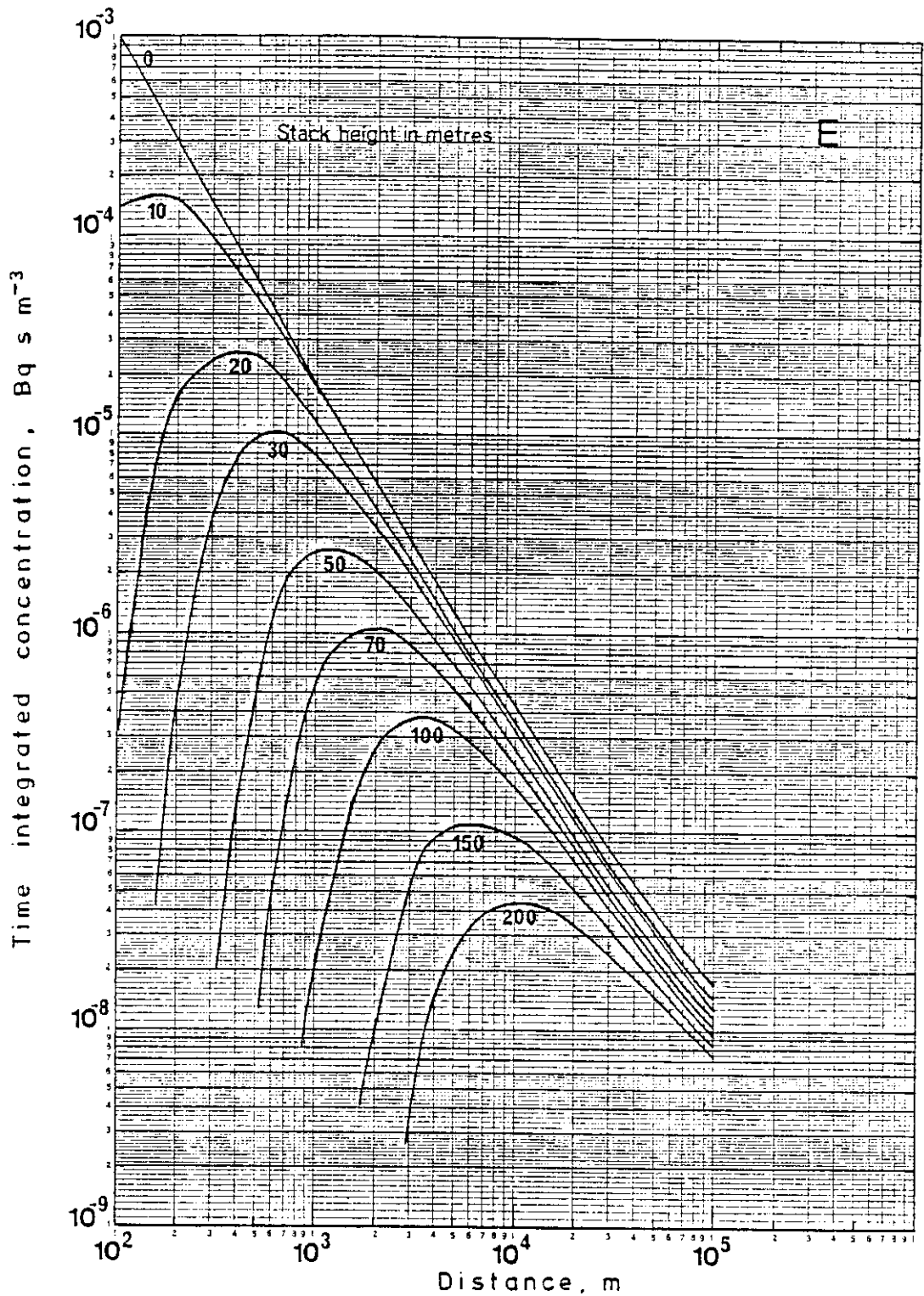


Figure 31. On-axis ground level time integrated concentrations for unit releases as a function of effective height of release for uniform horizontal dispersion into a sector of angular width  $\pi/6$  ( $30^\circ$ ) in Category E conditions

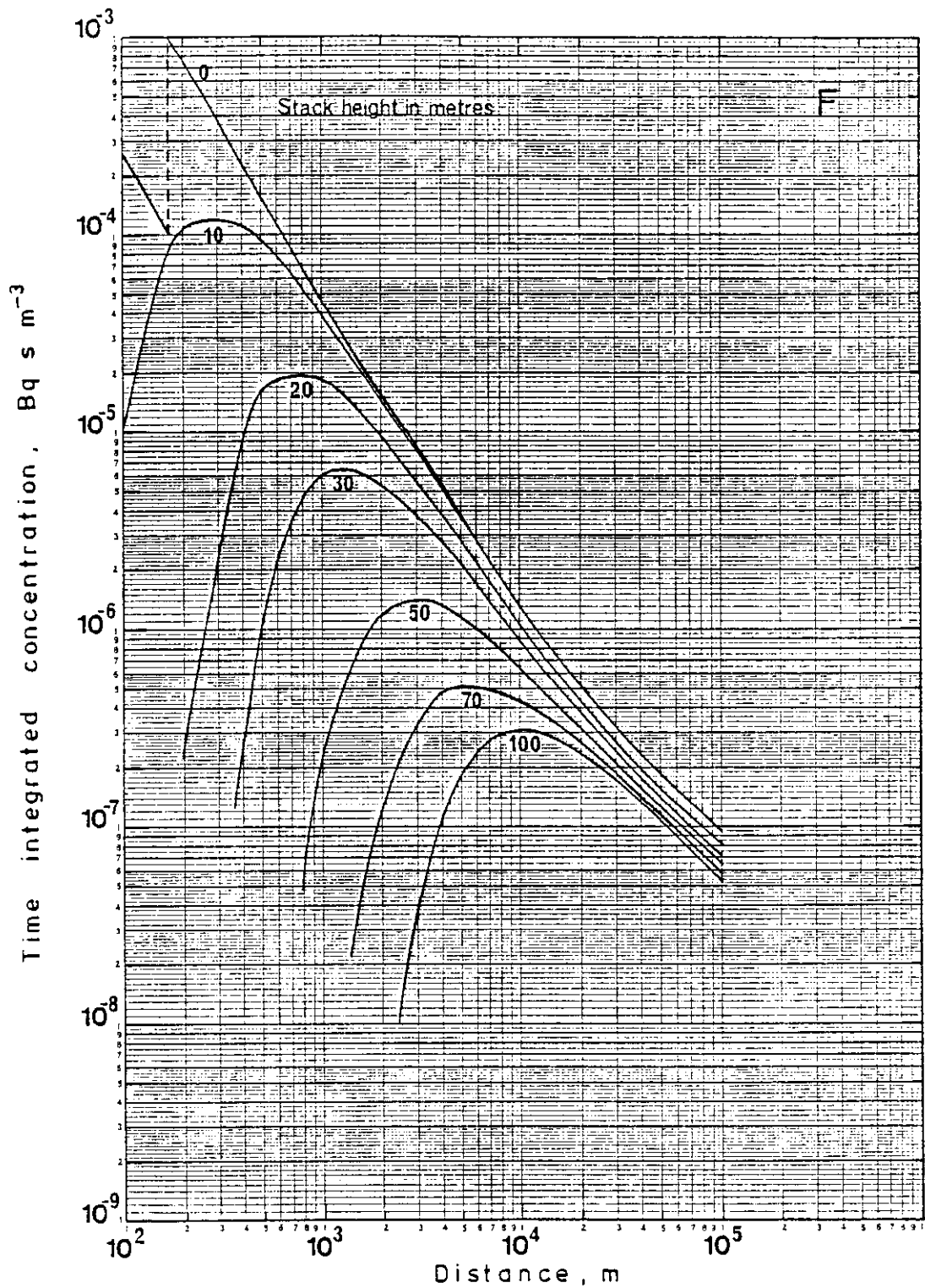


Figure 32. On-axis ground level time integrated concentrations for unit releases as a function of effective height of release for uniform horizontal dispersion into a sector of angular width  $\pi/6$  ( $30^\circ$ ) in Category F conditions

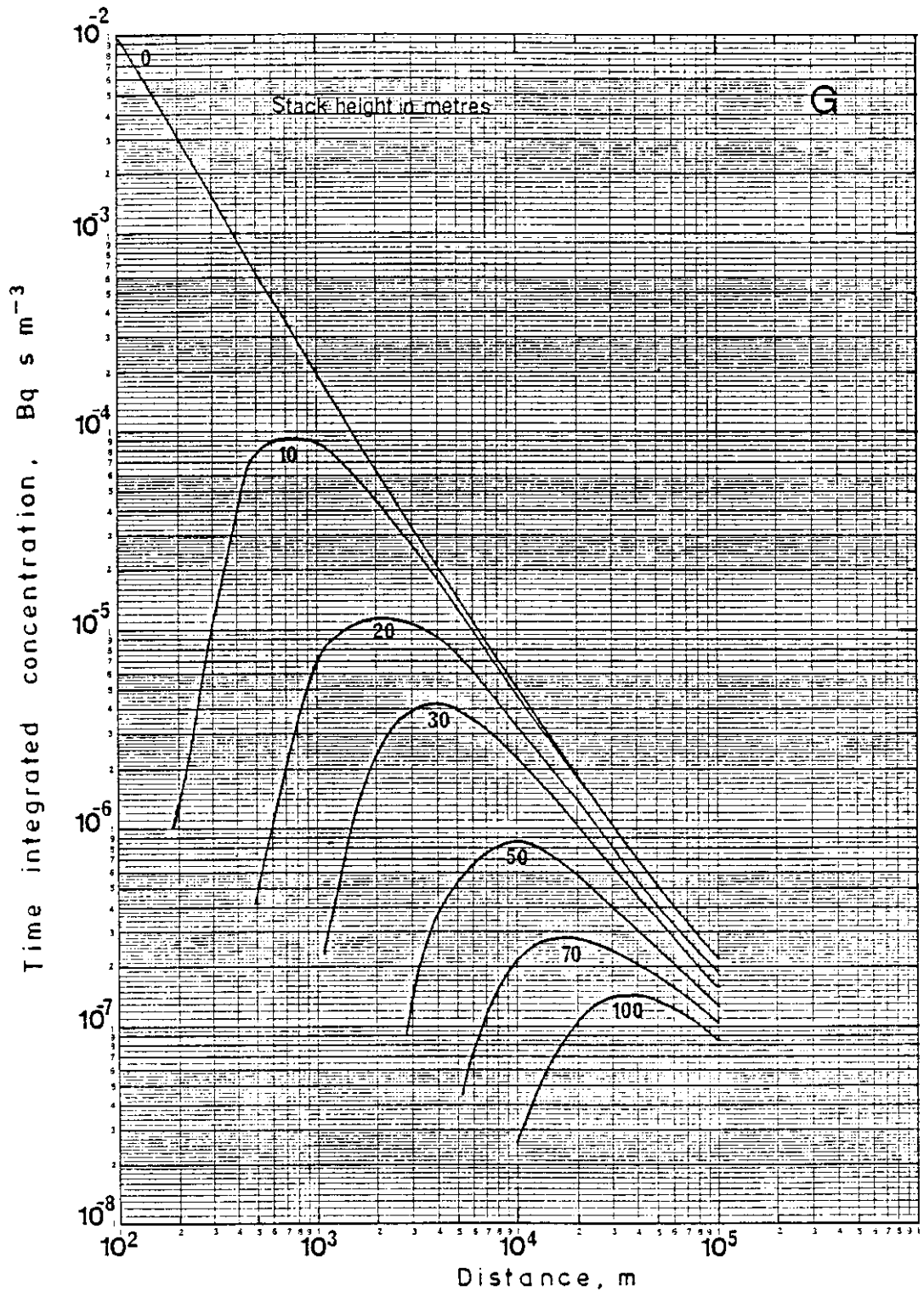


Figure 33. On-axis ground level time integrated concentrations for unit releases as a function of effective height of release for uniform horizontal dispersion into a sector of angular width  $\pi/6$  ( $30^\circ$ ) in Category G conditions

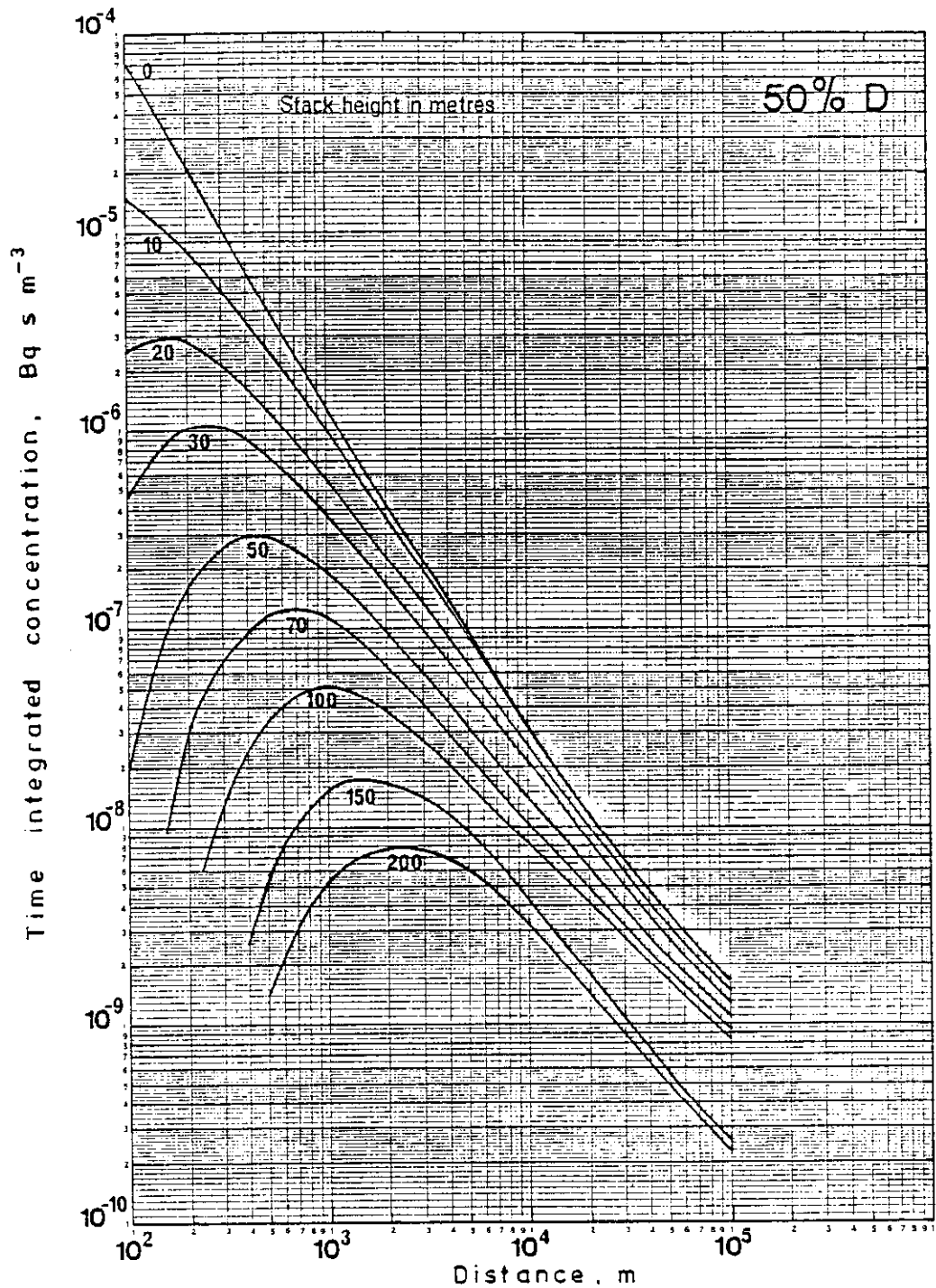


Figure 34. Continuous release results for ground level concentration as a function of distance and effective stack height for unit release. A uniform windrose is assumed and the frequency distribution of Pasquill categories corresponds to the 50% 'D' contour of the UK Pasquill stability map (see Figure 11)

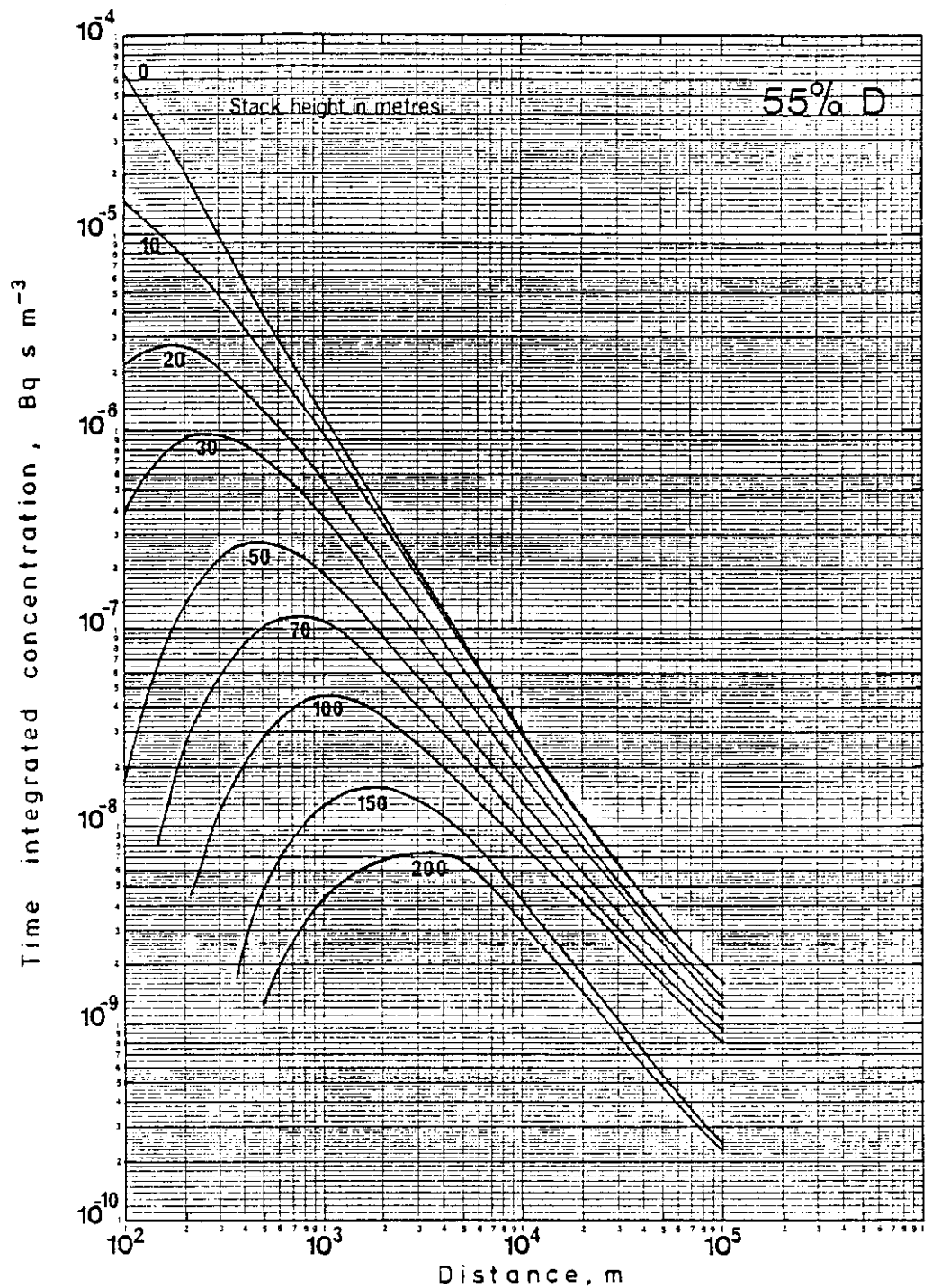


Figure 35. Continuous release results for ground level concentration as a function of distance and effective stack height for unit release. A uniform windrose is assumed and the frequency distribution of Pasquill categories corresponds to the 55 % 'D' contour of the UK Pasquill stability map (see Figure 11)

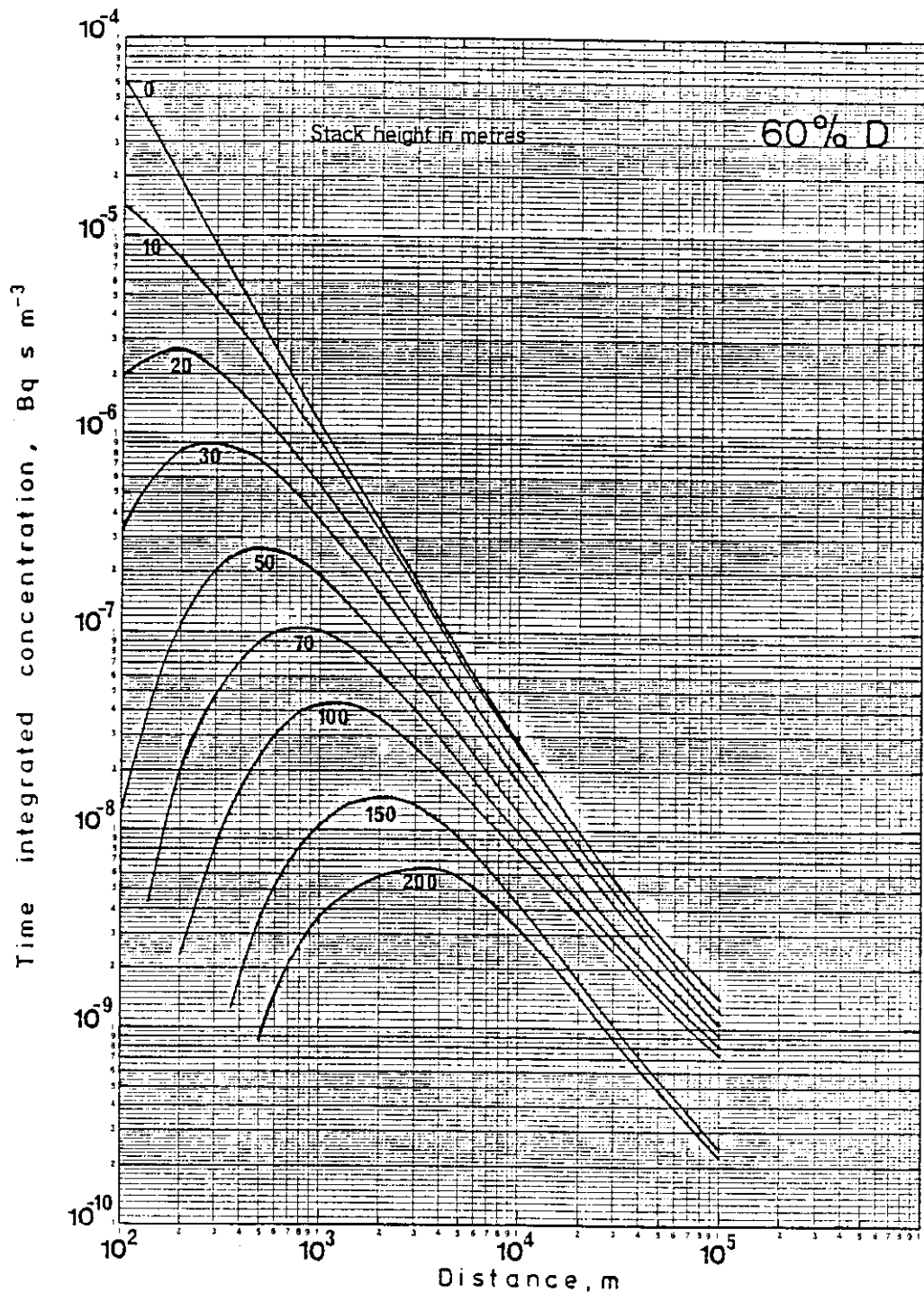


Figure 36. Continuous release results for ground level concentration as a function of distance and effective stack height for unit release. A uniform windrose is assumed and the frequency distribution of Pasquill categories corresponds to the 60 % 'D' contour of the UK Pasquill stability map (see Figure 11)



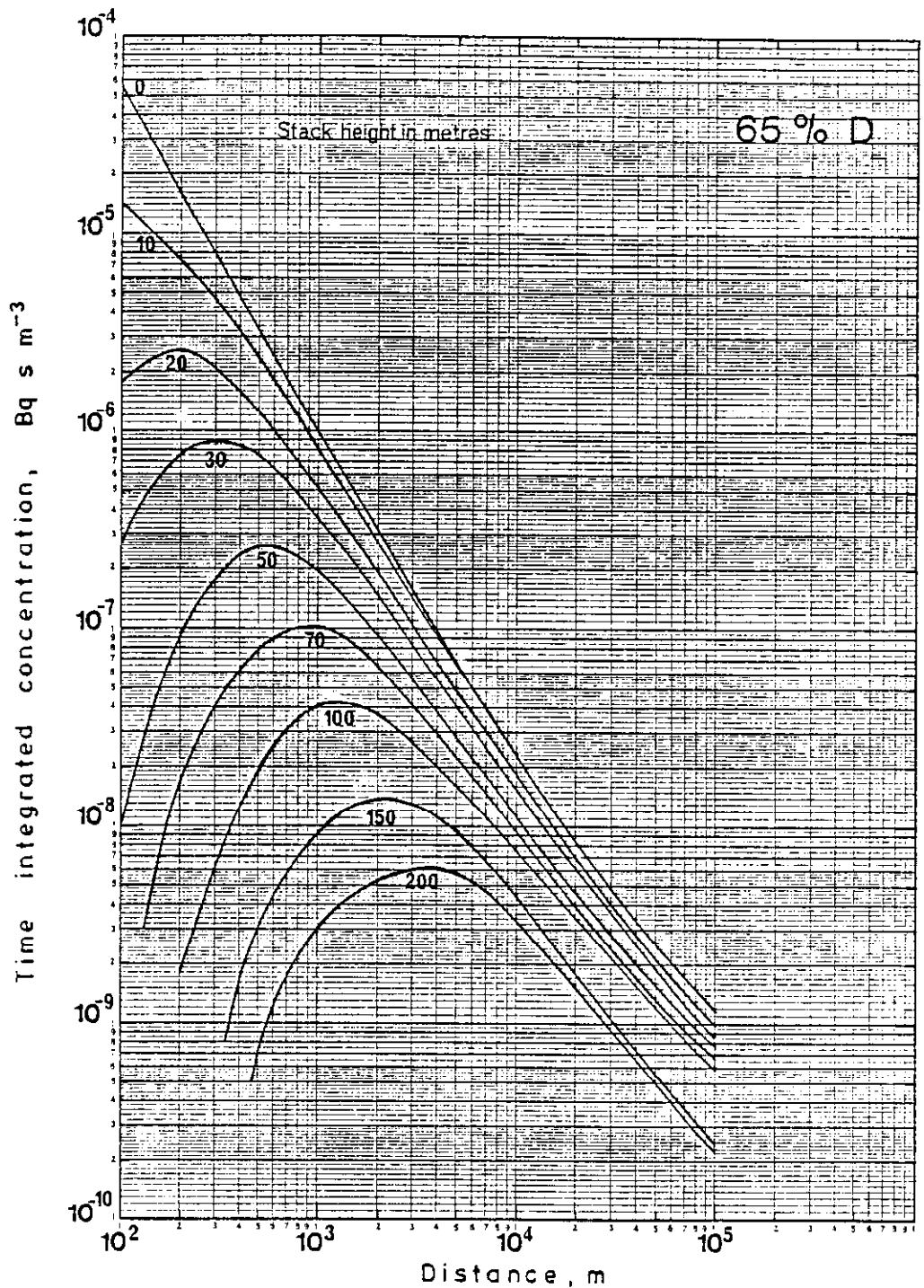


Figure 37. Continuous release results for ground level concentration as a function of distance and effective stack height for unit release. A uniform windrose is assumed and the frequency distribution of Pasquill categories corresponds to the 65 % 'D' contour of the UK Pasquill stability map (see Figure 11)

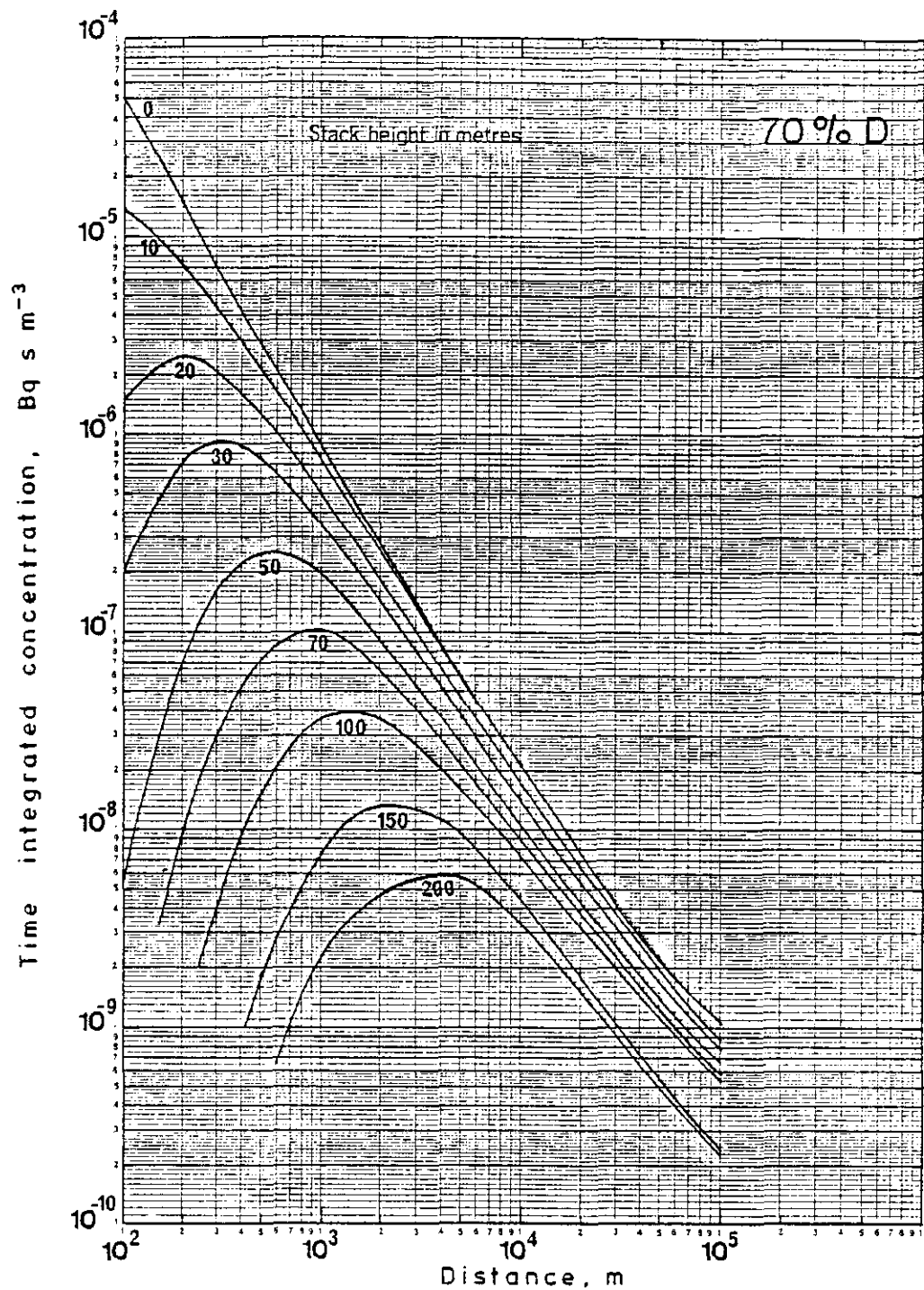


Figure 38. Continuous release results for ground level concentration as a function of distance and effective stack height for unit release. A uniform windrose is assumed and the frequency distribution of Pasquill categories corresponds to the 70 % 'D' contour of the UK Pasquill stability map (see Figure 11)

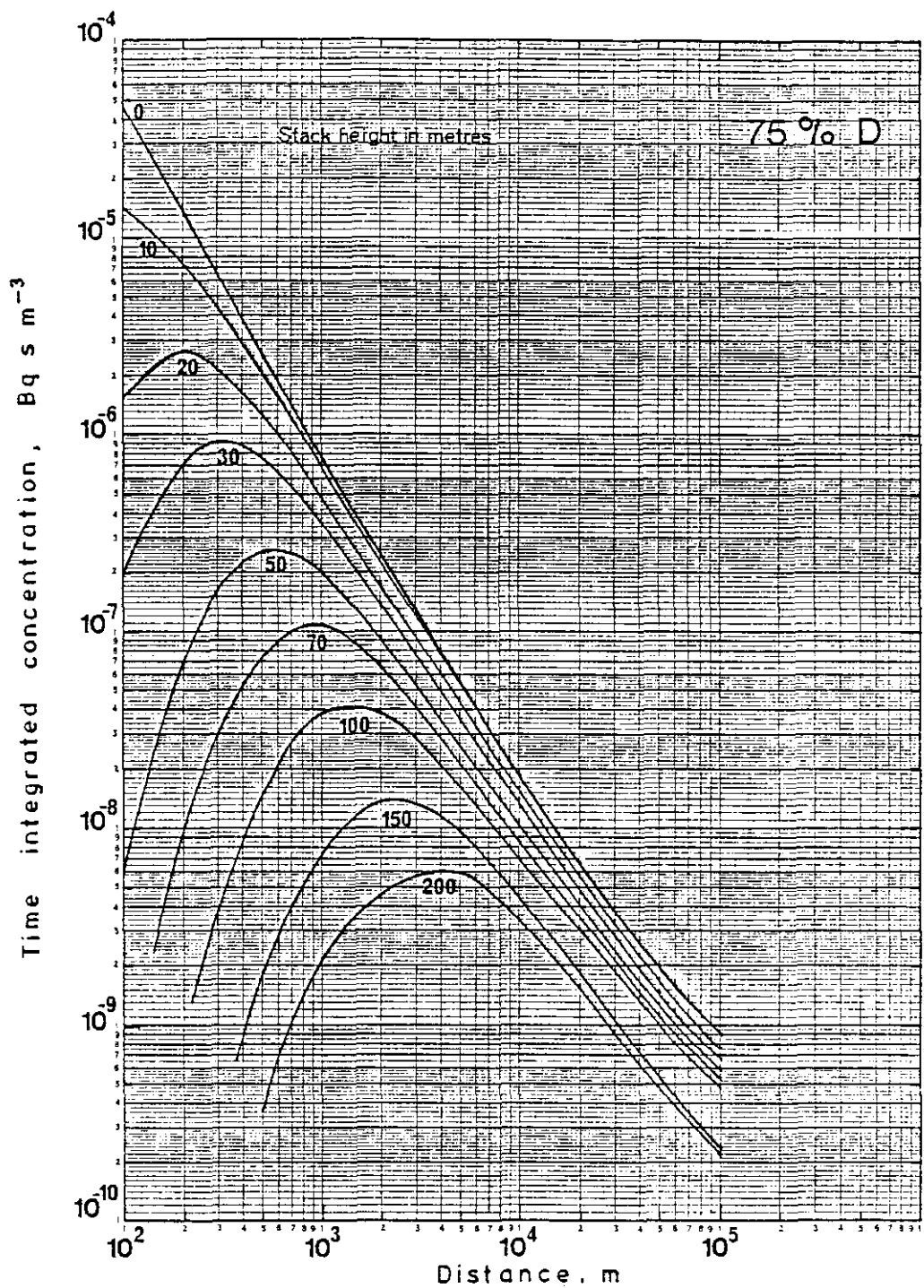


Figure 39. Continuous release results for ground level concentration as a function of distance and effective stack height for unit release. A uniform windrose is assumed and the frequency distribution of Pasquill categories corresponds to the 75 % 'D' contour of the UK Pasquill stability map (see Figure 11)

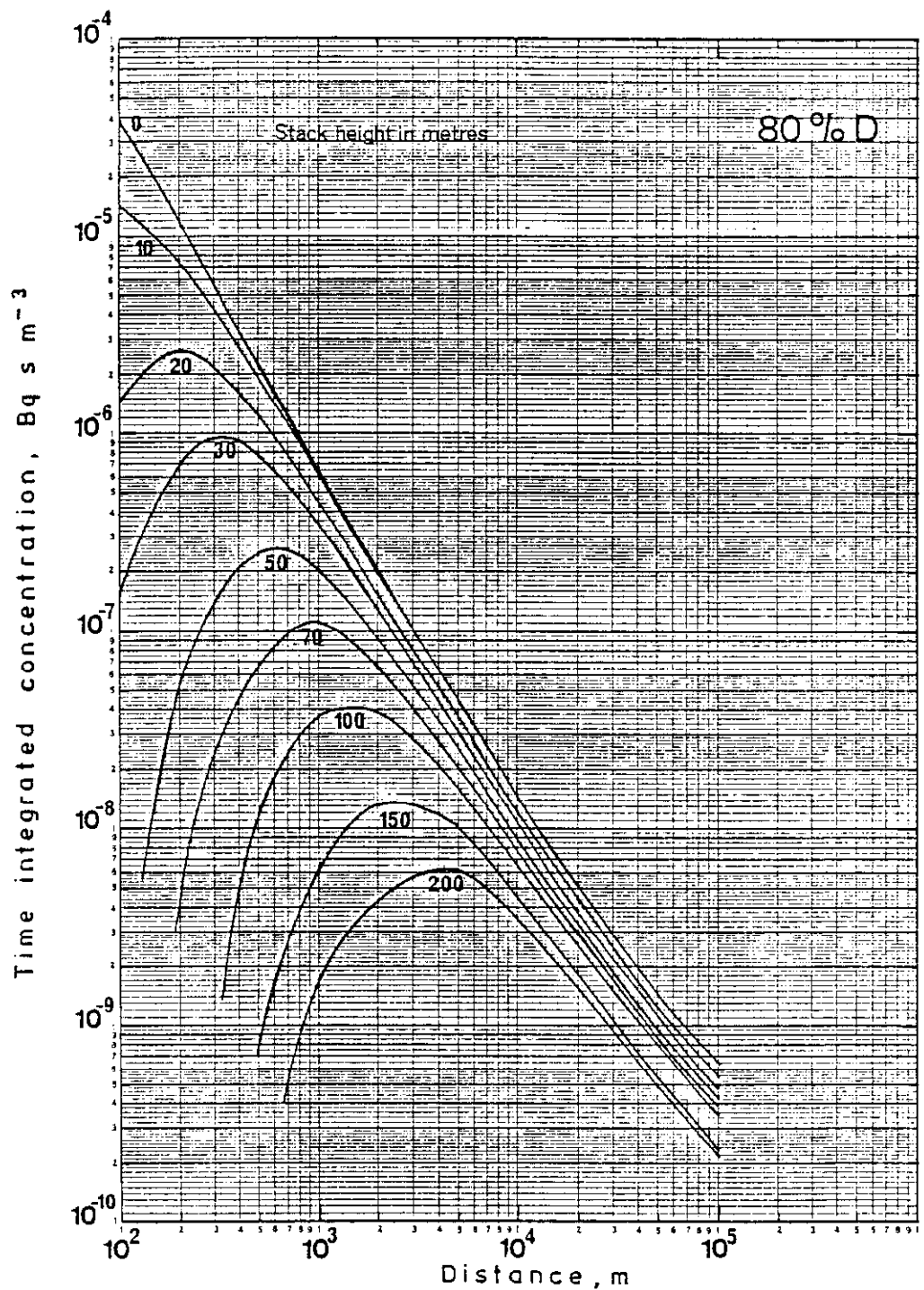


Figure 40. Continuous release results for ground level concentration as a function of distance and effective stack height for unit release. A uniform windrose is assumed and the frequency distribution of Pasquill categories corresponds to the 80 % 'D' contour of the UK Pasquill stability map (see Figure 11)



## APPENDIX A

### Diffusion in the lower layers of the atmosphere

F B Smith

Meteorological Office, Bracknell, Berks

Vertical diffusion of pollutant within the atmosphere is a consequence of turbulent motions or eddies superimposed on the mean airflow. The more intense these eddies are, and the larger they are, the more rapid is the dispersion. Ground level concentrations are at first enhanced by rapid dispersion if the source is elevated but are later diminished. For ground level sources, the surface concentrations are always reduced by rapid vertical dispersion.

There are two normal sources of turbulent energy. The first is dynamic in nature and arises from the breaking action of a rough underlying surface on the airflow. This results in momentum and energy being transferred from the mean motion into the "tumbling" eddies. The eddies in turn help to bring down mean-motion momentum from aloft to balance the losses in the surface layers. The intensity of turbulence increases both with wind speed and with roughness  $z_0$  of the underlying surface. One measure of the intensity is the friction velocity  $u_*$ , defined as:

$$u_* = \sqrt{\frac{\tau}{\rho}}$$

where  $\tau$  is the surface drag per unit surface area;

$\rho$  is the air density.

Typically the ratio of  $u_*$  to the wind at 10 m lies between 0.05 for a smooth open surface and 0.20 for a very rough surface. Over typical countryside  $u_* \approx 0.1 u_{10}$ . In neutral stability conditions the intensity of the vertical motions, represented by the root-mean-square vertical velocity  $\sigma_w$ , is directly related to  $u_*$  in the first few tens of metres above ground.

$$\sigma_w \approx 1.3 u_* \quad \text{generally, and}$$

$$\approx 0.13 u_{10} \quad \text{over typical British countryside.}$$

The second major source (or sink) of turbulent energy is the buoyancy generated by internal density or temperature differences. These differences arise from the air and the underlying ground surface having different temperatures and water vapour pressures. Unlike the situation over the sea, the buoyancy effects arising from water vapour over land can normally be neglected and attention can be concentrated on the consequential flux of sensible heat either from the ground into the air

(when the former is hotter than the latter as it often is during the day) or the reverse (as often happens at night).

During the day incoming solar radiation tends to heat the ground and some fraction of this may be advected into the overlying airflow as sensible heat. The elevation of the sun, the amount and type of cloud and the dampness and character of the ground surface are obvious factors determining the upward heat flux  $H$ . At night the ground usually cools as a result of an imbalance between outgoing and incoming long-wave radiation. The incoming radiation component is largely governed by the amount of cloud, and is therefore probably the principal variable determining the thermal influence of the ground on the air at night.

When the sensible heat flux  $H$  is upwards (from the ground to the air) the air temperature tends to increase rapidly in a downward direction and, in consequence, any fluid element perturbed upwards, say, soon finds itself hotter than its environment and buoyancy accelerates it upwards. The motion is unstable, turbulent motions tend to be intense, and pollution dispersion is rapid. At night when the heat flux is downwards, the temperature decreases downwards and perturbed fluid elements are soon restored back to their original levels. Turbulence tends therefore to be suppressed and dispersion is slow. Turbulence may be entirely quenched in time, especially in clear sky conditions when surface cooling is rapid and in light winds when the dynamic generation is small.

In 1959 Pasquill<sup>(12)</sup>, recognising these basic physical principles, tried to relate what experimental data on vertical dispersion was available at that time to meteorological factors related to these basic parameters. It was clearly sensible to select factors which could be rapidly observed or assessed without sophisticated instrumentation. The scheme developed was in this sense based soundly on good physical and practical concepts, but the details of the relationships were empirical. Pasquill defined six stability categories, A to F, in which A represents the most unstable conditions, B and C less unstable, D neutral, E and F stable conditions. Later a very stable category G was added to the list. The details of the scheme are elaborated in Pasquill<sup>(12,16)</sup>. Figure A1 and Table A1 set out the essentials of his scheme.

Smith<sup>(15)</sup> (see also Pasquill<sup>(16)</sup>) later generalised the original scheme in the following ways:

- (i) by helping the user to obtain a more objective estimate of the incoming solar radiation as a function of time of day, month and cloud;
- (ii) by making specific allowance for surface roughness  $z_0$ ;
- (iii) by replacing the seven classes by a continuous numerical scale from 0 to 7.

To achieve this generalisation, Smith used measurements of radiation made at Cambridge to help with (i) above, and an improved understanding of the turbulent structure of the boundary layer to specify the eddy diffusivity profile  $K(z)$  as a function of wind speed, stability and roughness, and to thereby derive numerical solutions to the eddy diffusivity equation:

$$u \frac{\partial C}{\partial x} = \frac{\partial}{\partial z} \left[ K(z) \frac{\partial C}{\partial z} \right]$$

These solutions were added to the experimental data to provide an extended and improved scheme (see Figures 2,3,5-7) which are described in more detail by Pasquill<sup>(16)</sup>.

Nevertheless, Figure 2 itself contains little more essential physics than Table A1 on which it is based. Recently Smith has revised the curves on the unstable side without implying the original Table A1 needs significant alteration. The cause of the changes to the figure comes from recognising that the vertical dispersion of a pollutant must depend on the thermodynamic stability of the mixing layer, that is on the parameters discussed earlier in this appendix. Thus for a given distance downwind from a ground level source, the vertical spread of the plume (represented by the root-mean-square height of the pollutant particles  $\sigma_z$ ) must depend on the basic parameters as follows:

$$\sigma_z = \sigma_z(u_*, H, z_0)$$

The question arises as to the form of this dependence. It may be anticipated that, for a given  $z_0$ , the other two parameters should be combined in a way that expresses "stability". The only such combination which is independent of height is in terms of

$$\mu = \frac{ku_*}{fL}$$

where  $L$  is the Monin-Obukhov length scale =  $-\frac{\rho c_p T u_*^3}{kgH}$

$f$  is the coriolis parameter ( $= 1.12 \times 10^{-4}$  at latitude  $51^\circ N$ )

$k$  is von Karman's constant ( $\approx 0.4$ ).

Thus  $\mu$  is proportional to  $H/u_*^2$  and, for the UK, the constant of proportionality is  $-0.038$  and it would be reasonable to postulate that

$$\sigma_z = \sigma_z(\mu, z_0)$$

The best fit between  $P$  and  $\mu$  implied by Figure 2 is given by

$$P = \frac{3.6}{1+X(\mu_*)}$$

where  $X(\mu_*) = 0.53\mu_* + 4.9\mu_*^2 - 2\mu_*^3$

$$\mu_* = \frac{1\mu}{100} = 3.8 \times 10^{-4} H/u_*^2$$

$\mu_*$  is in  $m s^{-1}$ ,  $H$  is in  $W m^{-2}$ .



The wind profile relationship for unstable conditions quoted in Table 1 can be used to relate  $u_*$  to  $u_{10}$  and  $H$ .

Very approximately for  $z_0 = 0.1$  m

$$u_* \approx \frac{1}{12} \left[ u_{10} + \frac{0.8H}{H+100} \right]$$

Figure 11 shows the geographical distribution of Pasquill stabilities (as defined originally by Pasquill) within the UK. This is a version of an earlier map, refined by the addition of more statistics. As the map implies there is a fairly good correlation between the average mean wind speed and the percentage frequency of the neutral category, and this has been used to extend the contours into areas with no P-statistics. Observations are very sparse in mountainous areas and it may be that the D category frequencies are underestimated in these exposed windy areas.

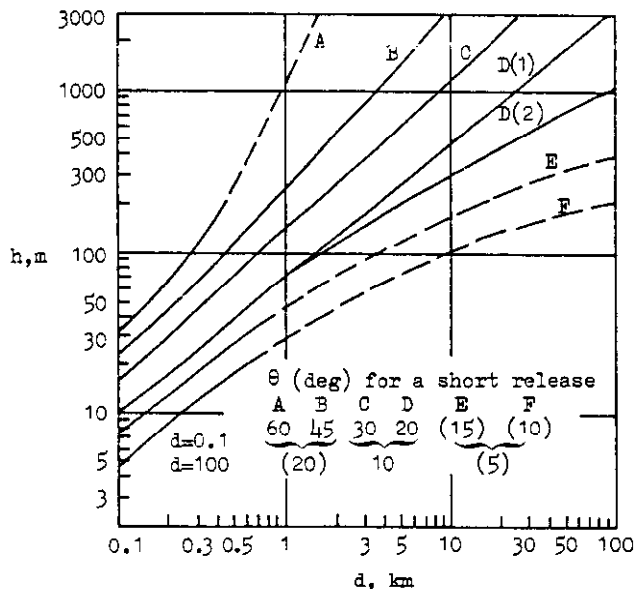


Figure A1 Tentative estimates of vertical spread ( $h=2.15\sigma_z$ ) and angular lateral spread ( $\theta=4.3\sigma_y/x$ ) for a source in open country

Table A1

Surface wind speed ( $m s^{-1}$ )	Insolation			Night	
	Strong	Moderate	Slight	Thinly overcast or $\leq 4/8$ low cloud	$\leq 3/8$ cloud
<2	A	A-B	B	-	-
2-3	A-B	B	C	E	F
3-5	B	B-C	C	D	E
5-6	C	C-D	D	D	D
>6	C	D	D	D	D

(for A-B take average of values for A and B etc)

Strong insolation corresponds to sunny midday in midsummer in England, slight insolation to similar conditions in midwinter. Night refers to the period from 1 h before sunset to 1 h after dawn. The neutral category D should also be used, regardless of wind speed, for overcast conditions during day or night, and for any sky conditions during the hour preceding or following night as defined above. The D(1) curve should be followed to the top of the dry-adiabatic layer; thereafter, in sub-adiabatic conditions, D(2) or a curve parallel to D(2) should be followed. (Pasquill 1961. from The Meteorological Magazine, February 1961, HMSO, Crown Copyright Reserved)

Table A2

Meteorological parameters as a function of stability class

Pasquill stability P	Category	% frequency	Mean wind $u_{10}$ ( $m s^{-1}$ )	Mean heat flux H ( $W m^{-2}$ )	Friction <sup>†</sup> velocity $u_*$ ( $m s^{-1}$ )	$z_i$ <sup>†</sup> (m)
0.5	A	0.125	0.625	250	0.11	1300
1	A-B	1.25	1.25	180	0.17	1080
1.5	B	3.8	2.0	150	0.24	920
2	B-C	2.6	3.37	125	0.33	880
2.5	C	15.0	4.12	90	0.38	840
3.6	D	62.4	4.12	0	0.36	800
4.5	E	6.7	3.4	?	?	~400
6	F-G	8.4	1.2	?	?	~100

<sup>†</sup> Estimates of  $z_i$  are based on the work of Carson<sup>(21)</sup> and Smith<sup>(17)</sup>

<sup>†</sup> A surface roughness  $z_0 = 0.1$  m is assumed.

The standard deviation of  $z_i$  about the mean is expected to be about 250 m for each P-category ( $P \leq 4$ ).

## APPENDIX B

### The determination of the crosswind spread $\sigma_y$

B E A Fisher and D J Moore

CEGB Research Division, Central Electricity  
Research Laboratories, Leatherhead, Surrey

The modelling guidelines are intended to apply out to a nominal travel distance of 100 km from the source. However, the measurements to which reference is made only involve travel distances up to about 10 km. Hence the extrapolation of these techniques to longer distances should be treated with caution. The upper limit on what is a valid travel distance for the model should only be regarded as an approximate criterion of the distance at which other important effects (to be discussed in later reports) cannot be ignored. Even out to travel distances of 10 km there may be special effects disturbing the flow. The dispersion is assumed to occur over open level country, not strongly influenced by buildings or topographical features, for example. If special effects are thought to influence the flow, separate additional calculation or wind tunnel modelling, at the discretion of the user, is required. It is also assumed that the effect of relative motion on the dispersion is not important.

In the following discussion the conditions of release of the airborne material are not discussed and will, in many cases, lead to a modification of  $\sigma_y$ . An intelligent application of the methods is left to the user's discretion. In the first section of this discussion we consider the crosswind spread of pollution from a continuous source. The application of similar equations to a source with a finite release time can often be made, but the terms must be interpreted differently (see equation (B6)). However, these arguments definitely do not apply to the concentration distribution of an instantaneously released cloud or puff of pollutant, the spread of which depends on relative diffusion.

$\sigma_y$ , the standard deviation of the concentration distribution in the horizontal direction, is dependent on horizontal turbulent fluctuations over various time scales (ie, on microscale, mesoscale and large scale eddies and on the interaction between vertical turbulent fluctuations and the shear in the mean horizontal wind velocity). In the nearfield when a plume has not spread deeply through the atmospheric boundary layer this last term is not very important and it will not be considered explicitly in the following. However it may be the reason that measurements of  $\sigma_y$  against distance indicate a distance dependence which is not a power law of distance with a simple exponent.

The way in which  $\sigma_y$  depends on eddy sizes and on averaging time and travel time can be seen from Taylor's theory of diffusion in stationary, homogeneous conditions.  $\sigma_y$  is then given by

$$\sigma_y^2 = 2\sigma_v^2 \int_0^t \int_0^{t_1} R(t_2) dt_2 dt_1 \dots\dots\dots(B1)$$

where  $\sigma_y$  is standard deviation of horizontal wind fluctuations and  $R(t)$  is the Lagrangian autocorrelation of the horizontal wind velocity fluctuations.  $R(t) \approx 1$  for small  $t$  ( $t/t_L \ll 1$ ) and zero for large  $t$  ( $t/t_L \gg 1$ ) where the Lagrangian time scale,  $t_L$ , is defined by  $\int_0^\infty R(t) dt$ .

Though equation (B1) does not apply to atmospheric turbulence which is neither homogeneous nor stationary it illustrates a number of points which are true even in the simplest situations. Equation (B1) only applies to the "ensemble" average of a large number of realisations of the flow. Thus all estimates of concentration based on theory are of "ensemble average" concentrations for stated dispersion conditions and are not estimates of the concentration for specific occasions. Secondly, the wide range of scales of horizontal turbulence shows that the limit  $t/t_L \gg 1$  in the autocorrelation function is never reached and the assumption of an effective horizontal eddy diffusivity is not appropriate.

The usual assumption made is that a major contribution to the crosswind spread is from eddies with a Lagrangian time scale long compared with travel time, so that

$$\sigma_y^2 = \sigma_v^2 t^2 b^2 + \sigma_{y_t}^2 \dots\dots\dots(B2)$$

where  $\sigma_{y_t}$  is the turbulence-induced term and  $b^2$  is an empirical correction hopefully close to one, since  $\sigma_v$  can be measured directly, and the second term is the contribution from microscale turbulence.  $\sigma_v$  depends on the sampling time,  $T$ , over which fluctuations are measured and also on height above ground. The averaging time for these measurements should be long enough to smooth out the effects of microscale turbulence. For sampling times between one and twenty-four hours large scale wind fluctuations cause plume meanderings which produce additional lateral spread, which should be incorporated in the expression for  $\sigma_v$ . It was decided to approximate  $\sigma_v^2 b^2$  in the following way.

For sampling time  $T = 1$  h, the average crosswind spread from measurements of dispersion around tall stacks out to 15 km<sup>(22)</sup> was represented by the simple expression  $\sigma_y = .08x$ . There was a tendency for a larger spread in light winds and a smaller spread in strong winds. Measurements made about 100 m above ground on an adjacent meteorological tower, suggested that  $\sigma_\theta$  ( $= \sigma_v/u$ ) varied from 0.16 for light winds ( $u = 1 \text{ m s}^{-1}$ ) to 0.05 in strong winds<sup>(23)</sup> ( $u > 16 \text{ m s}^{-1}$ ). Hence  $\sigma_y$

could be approximated by

$$\sigma_y = 0.08 \left( \frac{z}{u} \right)^{\frac{1}{2}} x \dots\dots\dots(B3)$$

The first term of equation (B2) can be written  $b^2 (\sigma_v/u)^2 (ut)^2 = b^2 \sigma_\theta^2 x^2$ , where the wind speed is measured at some suitable height. The crosswind spread is therefore a function of both travel time and wind speed or travel distance and wind speed. It only depends on travel distance alone if  $b^2 (\sigma_v/u)^2$  is independent of velocity and either the same restriction applies to the microscale term or the microscale term is small. Equation (B3) suggests that  $b(\sigma_v/u)$  is only weakly dependent on wind speed.

$\sigma_y$  and  $u$  are clearly dependent on height above ground at which they are measured. However, since they occur in the combination  $u\sigma_y$  in the expression for the concentration and  $u\sigma_y$  is approximately equal to  $\sigma_y x$ , which is roughly independent of height, this is not a problem. As long as  $\sigma_y$  and  $u$  are referred to the same height above ground it is not too important to fix their height dependence.

For a low level source (<70 m above ground) a standard height of 10 m is convenient being the normal height at which wind speeds are measured near the ground in meteorological applications. For high level emission (>70 m above ground) it is more convenient to refer  $u$  and  $\sigma_y$  to the mean effective height of the plume on emission. Some error is included in most practical applications as usually  $\sigma_y$  is referred to near ground level, but this is regarded as acceptable (see Section 2.2 of main report). This may also be the reason why the analysis of experimental data leads to a power law dependence on distance in  $\sigma_y$  ( $\propto x^{0.8-0.9}$ ) which is close to, but less than one.

The argument above does not apply to the calculation of the long-term average concentration, the formula for which does not include  $\sigma_y$  explicitly. For this situation it was agreed that either the wind speed at the effective stack height or the average wind speed over the depth of the plume should be used.

Moore<sup>(19)</sup> extended equation (B3) to longer sampling times of between 1 to 24 hours by generalising the expression for  $\sigma_y$  to

$$\sigma_y = 0.08 \left( \frac{Tt}{u} \right)^{\frac{1}{2}} x \dots\dots\dots(B4)$$

where  $T$  is the sampling time in hours. This reduces to expression (B3) for a sampling time of one hour. For a sampling time of one day when the mean wind speed is  $7 \text{ m s}^{-1}$ ,  $\sigma_y/x \approx 22 \frac{1}{2}^\circ$ . Thus wind direction fluctuations averaged over a

day are confined to a sector of angular width

$$2\sqrt{3} \times 22\frac{1}{2}^\circ = 60^\circ$$

defining the sector in terms of an equivalent plume with rectangular cross-section. This is in broad agreement with measured variations of wind direction over one day. Equation (B4) is based on measurements of wind direction fluctuations on tall towers and agrees with the large number of routine daily measurements of sulphur dioxide at ground level around power stations. It is not valid for days when a sea breeze reverses the wind direction or a feature such as a depression centre or front crosses the area.

For sampling times of less than one hour and especially for short-term sampling, such as over three min, there is an important contribution to the crosswind dispersions from microscale turbulence. In order to include this,  $\sigma_y^2$ , given by Gifford's standard curves which refer to a three min sampling time  $y^t(24)$ , has been added explicitly in equation (B2). Gifford's suggestion for including the effect of sampling time<sup>(25)</sup> has not been adopted. This is because of the essentially different nature of the turbulent contributions in different sampling time ranges. Since the microscale contribution has been implicitly included in the original formulation, equation (B3), Moore<sup>(19)</sup> suggests an alternative value for the empirical constant, leading to a final form for  $\sigma_y$ , of

$$\sigma_y^2 = (0.065x)^2 \left(\frac{7}{u}\right) T + \sigma_z^2$$

.....(B5)

The new value of the empirical constant (0.065) in this expression was chosen because the microscale turbulence accounted for about one third of the variance at a distance of 5 km in a 7 m s<sup>-1</sup> wind and  $0.065 = \sqrt{2/3} \times 0.08$ . In equation (B5) the microscale turbulence term has been written as  $\sigma_z^2$  since it is expected to be comparable with the variance in the vertical concentration distribution. Alternatively, the expression from Gifford<sup>(24)</sup> for the standard deviation of the horizontal concentration distribution referred to a sampling time of three min;  $\sigma_y$  (Gifford, three min), could be used if this is greater. Barker<sup>(3)</sup> confirms that this expression for  $\sigma_y$  together with the method for estimating vertical dispersion recommended by this Working Group gives a reasonable fit to a data set of measurements of dispersion from sources with effective heights up to 200 m. For this reason Gifford's  $\sigma_y$  values are used in equation (B5) and the modified equation (B5) is thought to be a reasonable compromise between producing a simple usable expression and the complicated physical processes which determine the crosswind spread out to distances of 100 km.

For many applications it is necessary to know the crosswind spread of a cluster of particles, ie, a cloud or puff of airborne material. The concentration distribution in a horizontal plane (assuming the vertical concentration distribution is a steady function of travel time) is then, to a reasonable approximation,

$$\frac{Q(t_0)}{2\pi \sigma_{yI} \sigma_{xI}} \exp \left[ -\frac{(y - \bar{y})^2}{2(\sigma_{yI})^2} - \frac{(x - \bar{x})^2}{2(\sigma_{xI})^2} \right]$$

.....(B6)

where  $\sigma_{yI}(t-t_0)$  and  $\sigma_{xI}(t-t_0)$  are the spreads of the puff, or cloud at time  $t$ ,  $Q(t_0)$  is the quantity of material emitted at time  $t_0$ , and  $\bar{x}(t, t_0)$  and  $\bar{y}(t, t_0)$  are the centroids of the cloud. In general the puff standard deviation,  $\sigma_{yI}$ , will differ from the corresponding plume standard deviation,  $\sigma_y$ . (See Gifford<sup>(24)</sup> for a simple account of relative diffusion.) In nuclear applications one usually requires the time-integrated dose and so integrates equation (B6) with respect to  $t$ , for the time it takes for the cloud to pass over the receptor point  $(x, y)$ . Since it is a reasonable approximation to write  $\bar{x} = \bar{u}(t-t_0)$  equation (B6) reduces on integration, to

$$\frac{1}{\sqrt{2\pi}} \frac{Q(t_0)}{\bar{u} \sigma_{yI}} \exp - \frac{(y - \bar{y})^2}{2(\sigma_{yI})^2}$$

.....(B7)

which has the same form as the expression for the concentration from a continuous source except that now  $Q(t_0)$  is the total emission and not the rate of emission, and  $\sigma_{yI}$  is the crosswind spread of the cloud and not that of the plume. It has been assumed that the time for the passage of the cloud over the receptor is sufficiently short for  $\sigma_{yI}(t-t_0) = \sigma_{yI}(x/u)$  and  $\bar{y}(t, t_0) = \bar{y}(t_0 + x/u, t_0)$ .

Equation (B7) applies to an effectively instantaneous period of release at time  $t_0$ . If the period of the release is finite one must integrate equation (B7) with respect to  $t_0$  over the period of the release  $T'$ . If the period of release  $T'$  is much longer than the travel time  $x/\bar{u}$ , the resulting dose is the sum of a large number of individual puffs. One then may reasonably expect the distribution of puff centres  $\bar{y}(t_0 + x/u, t_0)$  to be Gaussian with a standard deviation  $\sigma_{yT'}(x/u)$ . The dose becomes

$$\frac{QT'}{\sqrt{2\pi} \bar{u} \left( (\sigma_{yI})^2 + (\sigma_{yT'})^2 \right)} \exp - \left[ \frac{y^2}{2 \left( (\sigma_{yI})^2 + (\sigma_{yT'})^2 \right)} \right]$$

.....(B8)



This is just another way of writing Gifford's<sup>(26)</sup> fluctuating plume model. Both  $\sigma_{yI}^2$  and  $\sigma_{yT}^2$  depend on two-particle statistics which are difficult to evaluate. For example, as only eddies of size less than and equal to the cloud width contribute to the relative diffusion, the initial source configuration affects the spread of a puff in a complicated way. However, if the dose can be considered to be the sum of contributions from a large number of individual puffs, the crosswind spread  $\sigma_{yI}^2 + \sigma_{yT}^2$  in equation (B8) can be identified with the crosswind spread from a continuous source, as given by equation (B5), provided T the sampling time in equation (B5) is now taken to be the duration of release T'. If the release duration is so short that the emission must be treated as a puff other methods may be more applicable (see Pasquill<sup>(16)</sup> and Smith and Hay<sup>(27)</sup>).

The recommended method for specifying  $\sigma_y$  is related to other methods. The first term on the right hand side of equation (B5) can be related to Hay and Pasquill's expression for  $\sigma_y$ <sup>(28)</sup>, namely

$$\sigma_y^2 = \left[ \sigma_\theta^2 \right]_{T, x/\beta\bar{u}} x^2 \dots\dots\dots(B9)$$

where  $\left[ \sigma_\theta^2 \right]_{T, x/\beta\bar{u}}$  is the standard deviation of the wind direction from a record averaging over elementary intervals  $x/\beta\bar{u}$  (where  $\beta$  is the ratio of Lagrangian and Eulerian time-scales) and extending over either the period of release or the period of sampling. The method depends directly on wind fluctuation measurements, which are to be recommended, though not usually available in practice.

Similarity theory cannot be applied to horizontal dispersion because other velocity and length scales associated with larger scale flow features, apart from  $z_0$  and  $u_*$ , must affect the concentration.

## APPENDIX C

### Accuracy of the prediction of ensemble means and the spread about the mean

B E A Fisher and D J Moore

CEGB Research Division, Central Electricity  
Research Laboratories, Leatherhead, Surrey

Any calculation based on a model implies the assumption of an idealised boundary layer structure. The structure is based on some broad classification of meteorological conditions. There will always be considerable variations in concentrations for periods described by the same dispersion category. These variations can be due to variations in source strength, or fluctuations within dispersion categories, but are more likely to be because of departures from idealised boundary layer behaviour. For example, the plume from elevated sources may escape from the turbulent layer for various fractions of the sampling period, or there may be a change in surface roughness, or variations in the surface heat flux.

In order to estimate the variations to be expected within a given wind speed/stability category results from Moore<sup>(29)</sup> may be used on the variability of the maximum ground level concentration from elevated sources. Typically the ratio of the standard deviation of concentrations about the mean, for a given dispersion category, to the ensemble mean lay in the range 0.5 to 0.7 with the larger scatter, in conditions dominated by convection, and with the smaller scatter, in conditions dominated by mechanical turbulence. The ratio of the standard deviation of fluctuations in source strength to the mean source was about 0.3. Roughly speaking, in convective conditions the concentration may vary between 0 and 3 times the ensemble average for that wind speed/stability category with the probability of finding zero concentrations being highest. In conditions dominated by mechanical turbulence concentrations are distributed more equally about the ensemble mean concentration with infrequent occurrences of zero concentrations and concentrations twice the ensemble mean. (For more information see Table C1 and Figure C1.)

These numbers give some idea of the spread in observed concentration values around the mean concentration. The main error in calculations of the ensemble mean concentration for a given occasion is likely to come from an incorrect choice of the wind speed/stability conditions. Hence a simple measure of the spread in values of the ensemble average is obtained by considering the concentration in adjacent stability categories.

Table C1

Ratio of mean observed/calculated maximum ground level concentration for individual hour's data

Wind speed (m s <sup>-1</sup> )	1	3	5	7	9	11	13	15	>16	All
Time of year										
Jan-Feb				1.0 (0.1)	0.9 (0.4)	0.8 (0.4)	0.9 (0.4)	0.8 (0.3)	0.8 (0.3)	0.9 (0.4)
Mar-Apr	1.0 (1.0)	1.1 (0.6)	1.1 (0.6)	1.1 (0.6)	1.2 (0.7)	1.1 (0.5)	0.9 (0.3)	0.9 (0.2)	0.9 (0.0)	1.1 (0.6)
May-Jun	0.9 (0.7)	1.1 (0.9)	1.0 (0.6)	1.1 (0.7)	1.0 (0.5)	1.1 (0.5)	1.1 (0.5)	1.0 (0.3)	0.7 (0.1)	1.0 (0.6)
Jul-Aug	0.5 (0.1)	0.7 (0.3)	0.9 (0.5)	1.0 (0.5)	1.0 (0.5)	1.1 (0.5)	1.1 (0.6)	1.5 (0.0)		1.0 (0.5)
Sep-Oct	1.0 (0.4)	1.5 (0.8)	0.8 (0.3)	1.0 (0.3)	0.8 (0.4)	1.0 (0.1)	0.9 (0.1)		0.9 (0.3)	1.0 (0.5)
Nov-Dec	0.6 (0.1)	1.0 (0.4)	0.9 (0.7)	1.0 (0.4)	1.0 (0.5)	0.9 (0.4)	1.2 (0.9)	0.8 (0.4)	0.9 (0.3)	1.0 (0.6)
Time of day										
01-04	0.8 (0.5)	1.1 (0.6)	0.9 (0.4)	1.2 (0.8)	1.1 (0.5)	1.0 (0.5)	1.4 (1.0)	0.5 (1.0)	0.9 (0.4)	1.1 (0.7)
05-08	0.7 (0.4)	0.9 (0.7)	1.0 (0.6)	1.2 (0.6)	1.0 (0.6)	1.1 (0.5)	1.0 (0.4)	1.0 (0.2)	0.8 (0.2)	1.0 (0.6)
09-12	1.3 (0.9)	1.4 (0.9)	1.2 (0.8)	1.2 (0.5)	1.2 (0.6)	1.2 (0.4)	1.1 (0.6)	1.1 (0.4)	1.1 (0.3)	1.2 (0.6)
13-18	0.9 (0.4)	1.4 (0.7)	1.0 (0.6)	1.0 (0.4)	1.0 (0.5)	1.1 (0.4)	1.0 (0.5)	0.9 (0.3)	0.6 (0.1)	1.0 (0.5)
19-20	0.5 (0.0)	1.2 (0.9)	1.0 (0.7)	0.9 (0.3)	1.0 (0.5)	0.9 (0.4)	0.9 (0.3)	0.8 (0.3)	0.9 (0.2)	0.9 (0.5)
21-24	0.6 (0.1)	0.6 (0.3)	0.9 (0.4)	1.0 (0.4)	0.9 (0.4)	0.9 (0.4)	0.7 (0.2)	0.7 (0.2)	0.8 (0.3)	0.9 (0.4)
All times	0.9 (0.7)	1.1 (0.8)	1.0 (0.6)	1.1 (0.5)	1.0 (0.5)	1.0 (0.5)	1.0 (0.6)	0.9 (0.3)	0.9 (0.3)	1.0 (0.6)
Hours of data	61	90	258	406	427	290	179	54	51	1816
Estimate of plume rise error		(0.56)	(0.48)	(0.35)	(0.3)	(0.3)	(0.36)		(0.27)	(0.4)

Note:

Standard deviations are given in brackets. The data is divided according to time of day, year and wind speed. The lowest row gives an estimate of the minimum standard deviation due to differences between individual hourly and ensemble averages of plume rise (D J Moore, 1978, Large point sources and observed concentrations, ADMWG paper 16).

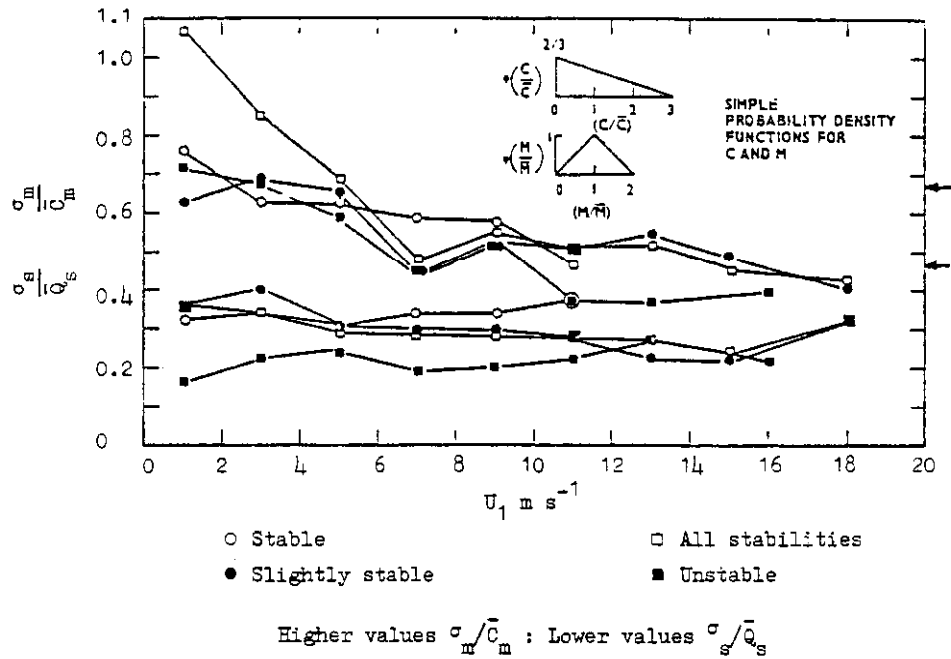


Figure C1 Standard deviation of observed maximum ground level concentration divided by mean maximum ground level concentration ( $\sigma_m/\bar{C}_m$ ) and standard deviation of sulphur dioxide emission divided mean emission strength ( $\sigma_s/\bar{Q}_s$ ) as a function of windspeed for various stability groups (Northfleet plume)